MINERAL ELEMENTS TRANSPORT ACROSS MINERAL–PEAT LANDFORMS UNDER OIL PALM PLANTATION IN INDONESIA

WAHYU ISKANDAR

2021

MINERAL ELEMENTS TRANSPORT ACROSS MINERAL–PEAT LANDFORMS UNDER OIL PALM PLANTATION IN INDONESIA

by

Wahyu Iskandar

A dissertation presented to the Kyoto University
in fulfillment of the thesis requirement for degree of Ph.D.
of Environmental Science and Technology
in
Agricultural Science

Kyoto, Japan, 2021

AUTHOR’S DECLARATION

I hereby declare that I am the sole author of this dissertation. This is a true copy of the dissertation, including any required final revisions, as accepted by the examiners.

ABSTRACT

Background and goal

A dramatic agriculture expansion in recent decades in Indonesia has led to the use of marginal land regardless of land suitability. Although extensive monoculture crop such as oil palm has contributed to the GDP, unwise land management drives environmental degradation such as accelerated erosion, nutrient loss, gas emission, and even catastrophic events such as land fire and flooding. In mineral upland, where terrains are evident, accelerated erosion under monoculture crops led to the loss of mineral nutrients hence mineral nutrients depletion. While in peatland, lack of mineral nutrients triggers land manager to apply fertilizer to offset nutrients, which in turn, causes eutrophication and accelerated gas emission due to enhanced decomposition of peat materials.

Although mineral nutrients can be added by artificial intervention, nature has its mechanism to regain its balance. The nutrient loss in upland can be compensated by biomass input from the above ground vegetation. In peatland, a lack of mineral nutrients can be obtained from the surrounding landform via a hydrological network at a catchment scale. However, the integration of these two land ecosystems is poorly understood. In this study, I reported; 1) mineral nutrient budget in peatland as the downstream enriched by uplands; 2) mineral element loss and its controlling factors in upland, and 3) distribution of mineral nutrients in peat soil under oil palm plantation.

First, I clarified the mineral nutrient budget in a complex peat-mineral catchment. In this study, I monitored mineral input from mineral uplands with similar geology, soil, and climatic conditions under oil palm plantation. Then, I evaluated the mineral elements budget in the two peatlands having similar characteristics but the size under oil palm plantation. The peatland was managed by canalization and multiple water gates. The result showed that under similar land management, peatland size was important to trapped mineral nutrient input. The larger the peatland, the longer watercourse that captured mineral elements; hence, the more mineral elements deposition was found in the larger peatland. When more eroded mineral soil occurred in the upland during intensive rainfall, peatlands with a gentle slope associated water gate slowly distributed the watercourse—the more extended time water in the peatland allows mineral element deposition. The mineral input in the bigger peatland could compensate for mineral element loss, preventing mineral element deficit.

Then, I clarified the mechanism of mineral elements transportation in the upland under the late stage of oil palm plantation. Erosion by quantifying mineral nutrient loss was measured in the outlets of four small sub-catchments (later called as “uplands”) with similar geologic, soil type, and climatic conditions but different sizes, network density, slope gradient, and shape. The strong correlations between mineral elements and DOC indicated that transportation of mineral elements such as Al, Fe, Ca, and Mg would be in mineral-OM complexes. Mineral element concentrations were higher in the small upland. However, when considering the amount of loss, uplands with a higher water discharge rate had greater mineral element loss, regardless of the size of the uplands. Compared to estimated erosion by Revised Universal Soil Loss Equation, RUSLE, the total transported soil estimated by mineral elements was lower, indicating that some portion did not reach the outlets. The result reveals that it is important to consider water discharge rate, size, and shape of catchment when considering mineral nutrient loss from upland or input to the downstream ecosystem.

I also investigated the mineral nutrient distribution in the solid phase (peat soil) in the peatland adjacent to the mineral upland. Systematic sampling collected 32 points; each point consisted of three surface samples 0–15, 15–30, and 30–50 cm. I also investigated mineral nutrient distribution in the profile: 1) Along mineral upland (transect-1); and 2) along the riverbank (transect-2); 3) elongating from mineral upland–peatland–riverbank (transect-3). The surface layer shows higher mineral nutrients near the upland compared to the near riverbank. The profiles in transect-1 support the findings that enrichment occurred not only on the surface but also on the profile. The ash content and mineral content in the profile near the upland were higher than those near the riverbank. The result strengthens the two previous findings above that landforms affect the distribution of mineral nutrients to the peatland.

This dissertation provides new insight into the integration of mineral land and peatland that erosion and mineral nutrients loss in upland can be beneficial for adjacent peatland. The nutrients loss from upland compensates for those of a nutrient-lacking ecosystem of peatland. This scheme is valuable when considering land for agriculture, which is affected by the surrounding environmental condition.

ACKNOWLEDGMENT

I would like to express my gratitude to the special people both in Japan and Indonesia. Special mention goes to my supervisor, Prof. Shinya Funakawa and Assciate Prof. Tetsuhiro Watanabe. Their warm guidance is not only for sharpening my academic skill but also for widening my horizon to the update of global perspective of agriculture, soil, and peat issues. The author was zero in this topic, but since Prof. Funakawa had introduced research in peatland in my home country, I gained amazing experience and countless knowledge during the survey. I am thankful to Associate Prof. Watanabe wholeheartedly, not only for his tremendous academic support but also for giving me so many comments on how to have critical thinking in writing an academic paper. It also goes to Associate Prof. Hitoshi Shinjo and Assistant Prof. Makoto Shibata for their constructive feedbacks on my study.

To IPB staff: Prof. Supiandi Sabiham, Dr. Syaiful Anwar, Dr. Heru B. Pulunggono for the mutual collaboration.

To PT. Kimia Tirta Utama Staffs: Mr. Zulfikar, Mr. Nizam, Mr, Muis, Mr, Husni Mubarok, Mr, Hermawan, and field assistants for their kind support during field works.

Big appreciation also goes to Mr. Setiari Marwanto, who has been a truly dedicated mentor. He is a partner and an elder brother with humbleness supporting me in every way.

Gratitude also goes to my basement mates, Araki Sensei, Furutani-san, Okuoka-san, Mr. Obike, Ajay, Lyu, Athuman, Nishigaki-san, and Jinsen-senpai! for the togetherness, fun, and great talks beyond academic. And not to forget for all members of the Laboratory of Soil Science, thank you all. We are such a great team!

MEXT and LPDP Scholarships gave me the opportunity to have such an amazing journey to Japan to pursue my path to get higher education. My awardee teams and PPI, who have already colorized my life in Japan without missing Indonesia.

Ultimately, to my Sikipi, my big family Dad, Mom, brothers, sisters, and my niece and nephew! I highly dedicate this for you.

CONTENT

Table of Contents

LIST OF TABLES

LIST OF FIGURES

1.1 Main Figures

1.2 Supplementary Figures

CHAPTER 1
INTRODUCTION

1.1 General introduction

Indonesia faces a dilemma of providing land for agriculture expansion. Projection of additional land demand for palm oil production in 2020 was up to 28 Mha in Indonesia (Wicke et al. 2011). However, land available for such massive crop production no longer meets suitable land for oil palm. If no further deforestation is assumed, the additional land to meet the demand are upland and peatland. In addition to that, land-use change to agricultural land has also raised debate regarding further environmental and social implications such as soil erosion (Labrière et al. 2015; Borrelli et al. 2021), nutrient loss (Vijiandran et al. 2017a; Lal 1995), loss of biodiversity, greenhouse gasses emission from biomass and peatland, and land tenure and human conflicts (Colchester et al. 2006; Gibbs et al. 2008; Koh et al. 2008; Wicke et al. 2008; Davies 1995).

The scale of oil palm plantations is large, ranging from hundreds to thousands of hectares, which makes it difficult to measure soil erosion and mineral nutrient loss. In oil palm plantations, soil erosion studies generally apply field observations (Clarke and Walsh 2006; Lal 1994; Marten et al. 2016; Mohamad et al. 2020; Murtilaksono et al. 2018; Nainar et al. 2018). However, these methods are difficult to apply to large areas such as catchment scales because such measurements are laborious and expensive. Considering these difficulties, soil erosion and nutrient loss can be measured at the outlet of a catchment scale. Yet, such empirical validation of actual mineral loss by monitoring at an outlet on a catchment scale is absent.

A small upland catchment (<10 km^2) (Singh 1994; Singh 2018) is often part of a bigger catchment consisting of different ecosystems. For example, in Siak Sumatra Indonesia, where the current research is underway, the upland oil palm concession grows on tertiary sedimentary rocks (Kementerian ESDM the Republic of Indonesia, 2010) and Ultisols (USDA 2005) while the downstream is a peatland. The upland and the peatland are connected by stream networks.

Ecologists have long been aware that there is a flux of energy and nutrients from a terrestrial ecosystem to the surrounding aquatic ecosystem and vice versa (Ballinger and Lake 2006). The report reveals that ecosystems provide permeable boundaries that enable nutrients to be transferred among adjacent ecosystems, such as at a catchment scale. The transfer of nutrients from one ecosystem to another is referred to as a "subsidy" or "donation" (Polis et al. 1997), compensating nutrient-poor ecosystems indicated by vegetation patterns. In Sumatra of

Indonesia, the tropical peatlands lie on lower elevations (Anderson 1978; Ritung et al. 2011), in which mineral elements loss from upstream mineral upland would be utilized in downstream peatland. Nevertheless, it is unclear how mineral nutrient loss from mineral land can be deposited and beneficial for compensating oligotrophic peatland and preventing further environmental problems such as sedimentation in and eutrophication of a water body downstream.

Seasonal change in the flow of mineral elements from upland and their possible deposition in peatland would be affected by various factors. In the upland, surface runoff increases surface erosion that releases mineral elements during intense rainfall. In the peatland area, the size of peatland is important as the seasonal elemental flow would also be influenced by the water discharge from peatland responding to rainfall. Generally, a larger peatland has a slower responding time. In order to maintain water level, peatland under oil palm plantation also has a drainage system equipped with multiple watergates. Gentle slope gradients in peatland having watergates would retard its straightforward drainage and distribute water across the plantation along canals, possibly depositing mineral elements.

Clarifying the seasonal change of mineral element flow from upland and deposition in peatland is essential to conceptualize mineral element transfer across a catchment. We hypothesized that peatland size and canal length are vital features for the deposition and retention of mineral elements. The finding in this study can optimize the use of peatland under oil palm plantations managed by the current drainage system with wiser mineral nutrient management.

Spatial distribution of mineral nutrients in peat soil is also rarely studied. Previous reports attempt to describe mineral nutrient distribution based on the shape of a peatland dome. A tropical peatland is typically shallow at its river-bounded fringes and thicker interior (Anderson 1983), creating a dome. Anderson's model has often been used to structure nutrient distribution evaluations (Cameron et al. 1989; Page et al. 2006). Nutrient contents are generally low in the central part of the dome because the surface peat is laterally and vertically far from mineral soil sources. This low mineral nutrient status is supported by research showing that the distance from the coastal levee affects soil solution composition (Funakawa et al. 1996). Haraguchi et al. (2000) found that peat in the surface and the mid-depth sections of peat profiles has lower Ca^{2+} and Mg^{2+} than the peat near the bottom because salt retention from underground water flows high elemental concentrations. A detailed study on the relationship between

mineral nutrient distributions and distance to mineral bed (peat thickness) in Riau was carried out by Watanabe et al. (2013), which suggested that nutrient availability is better in the fringe bordering riverbank with a thickness of less than 3 m. These reports suggest that peatland fringes bordering riverbank are richer in mineral nutrients.

A peatland fringe is a transitional zone between a peat area and the surrounding landforms. Transitional zones may function differently in terms of the mineral nutrients based on the location. In the temperate peatlands, the type of mineral land and the transitional zone has been introduced as a conceptual framework describing vegetational and hydro-chemical gradients (Whitfield et al. 2009; Howie et al. 2009). Based on long-term studies, the studies categorize transitional zones between raised peat area and a) mineral upland, b) river levee (riverbank), c) beach, and d) flat delta (floodplain). Only type a) receives water flow, and probably mineral nutrients, from raised peat areas and mineral upland sources. It was evident that a confined transitional zone found in a topographic depression between a raised peatbog area and a mineral upland of greater than 1% has a higher pH (4.8±0.9) than an unconfined transitional zone (pH 4.2±0.4) bordering a flat or receding mineral land (Langlois et al. 2015).

In contrast to the state of knowledge for temperate peatlands, the interactions between tropical peat and its surrounding landforms, particularly mineral upland, are rarely studied. Studies of peatland as an individual ecosystem are abundant, yet the crucial questions of how mineral nutrients are distributed and which types of surrounding landform enrich peatland remain. Surrounding landforms such as mineral uplands can be important mineral nutrient sources because they are often at higher elevations than peat. Runoff from the mineral uplands can drive mineral nutrients downward.

1.2 Study objectives and dissertation organization

The ultimate goal of this study was to conceptualize mineral element transports across integral peat–mineral landform that can subsidy mineral nutrients to the oil palm plantation and prevent further environmental effects downstream. To achieve the goal, multiple field works were carried out to:

1. clarify the mineral element budget in peat-mineral landform at catchment scale.
   I measured the inflow (from mineral upland) and outflow (from peatland) of mineral elements and investigated their temporal changes and retention in a peatland. I hypothesized that peatland size and canal length are vital features for the deposition and

retention of mineral elements. The finding in this study can optimize the use of peatland under oil palm plantations managed by the current drainage system with wiser mineral nutrient management.

2. clarify erosion (mineral element loss) and its controlling factors in mineral upland under oil palm plantation.

   Seasonal change in eroded soil reaching outlet was also observed and correlated with the morphology and hydrological characteristics of the catchment and possible factors which might control erosion rate.

3. clarify the effect of landform on the distribution of mineral nutrients in tropical peat that borders a mineral upland.

   I hypothesized that the mineral nutrient content is higher in tropical peat that borders mineral upland than in riverbank peat. It is also possible that enrichment occurs continuously across the fringe and into the interior peatland as a result of topographic gradients between mineral upland and peatland, compensating for nutrients lost due to vegetation uptake and leaching. Understanding how mineral nutrients are distributed in a tropical peatland bordering on other landforms will contribute to the wise use of the peatland as well as informing strategies for the restoration of integrated tropical peatland ecosystems.

The dissertation organization is as follows. After this chapter, Chapter 2 describes the study area, site characteristics, installation of monitoring point, and sampling of soil and water. Chapter 3 clarifies the seasonal and total mineral element budget in the peatland downstream, which received mineral input from the corresponding mineral upland. Chapter 4 clarifies the mineral element element loss in upland and its controlling factors. Chapter 5 clarifies the spatial distribution of mineral nutrients in the soil phase in the peatland area. Based on findings in Chapter 3–5, Chapter 6 provides a general discussion and the concluding remarks.

CHAPTER 2
DESCRIPTION OF STUDY SITES, SAMPLING DESIGN, AND FIELD MONITORING

2.1 Study area

The study area lay about 60 km from the nearest coastline, within the watershed of the Siak River, Riau Province, Indonesia, and had a mean elevation of approximately 21 m above sea level (Fig. 2-1). Peatland had formed in a local depression, which bordered mineral upland and the Siak River. River meandered around the study site and formed more than half its perimeter. The remaining part of the study site borders the mineral upland, which was approximately 7 km from the Siak River at its closest approach. The mineral upland was the edge of mineral upland elongating from Sumatran backbone. The climate in this region was a typically humid ecosystem with high precipitation (2082 mm) and daily temperature (23°C–27°C) throughout year (Marwanto et al. 2018). The study site generally experienced bimodal pattern of rainy seasons during the period of October to December and March to May with dry season during July to September. The study area had been cultivated for oil palm since 2002 and is managed using farm road with a pair of intersecting canals (from 3 m to 5 m in width,~2 m deep) running south-north and east-west in the peatland area. The canals were constructed at approximate intervals of 0.3 km (south to north) and 1 km (east to west), which made the farm blocks. The dig out materials during canal construction were put onto the road.

2.2 Site characteristics

2.2.1 Mineral upland

The study was conducted in two adjacent peat-mineral upland landforms, namely catchment-1 (4662 ha) and catchment-2 (2302 ha) situated in the Siak watershed, Riau (Table 2-1). The study area in mineral upland in the for Chapter 3 and 4 consisted of four small adjacent sub-catchments namely upland-1, upland-2a, upland-2b, and upland-2c which had similar soil, geology, and climatic conditions but different size. The soil type of study area was Ultisol (USDA 2005) and the geology was tertiary sedimentary rock (Kementerian ESDM The Republic of Indonesia, 2010). Each upland had a stream that drained water to peatland located in the downstream. The details of study site characteristics are presented in Table 2-1.

2.2.2 Peatland

Study in Chapter 4 and Chapter 5 was conducted in the peatland area as downstream of upland-1 and upland-2 (2a, 2b, and 2c). The areas were identified as part of two different catchments, namely peatland-1 and peatland-2. Because of the proximity, peatland-1 and peatland-2 were similar, except for their sizes (Table 2-1). Peatland-1 accounts for 3632 ha, while peatland-2 accounts for 1478 ha. The peat depth in the two peatlands was similar, ranging from 0.5–7 m (Iskandar et al. 2020). The study sites were dominated by sapric peat at the surface and fabric and hemic peat in the deeper layers. Peatland-1 and peatland-2 received streamflow from corresponding uplands via inlets and drained water via a single outlet, namely outlet-1 and outlet-2,). The study in the Chapter 5 was only conducted in peatland-1.

2.3 Monitoring and sampling: an integrated mineral element transport between mineral upland and peatland

Fig. 2-2 presents the conceptual framework, field monitoring, and sampling of the study. An automatic weather recorder (Vantage Pro 2, Davis, California, USA) was set at the center of study area (see "weather station" in Fig. 2-1 and Fig. 2-2) and recorded rainfall data every 30 minutes. To estimate mineral nutrient flow, I monitored water discharges at the inlet and the outlet of each site. I set discharge monitoring stations equipped with an absolute pressure water level data logger (HOBO U21-001-04, ONSET, Massachusetts, USA) with an accuracy of 1 mm at entry and exit points: inlet-1, inlet-2 (a, b, and c), outlet-1 (before November 26, 2020), and outlet-2 (on December 12, 2020) (Fig. 2-1). Water level (h, m) at each outlet was monitored every 30-minutes, and the cross-section of each inlet and outlet was measured. The flow rate was periodically measured on stable water flow using a current water meter (UC-300, Tamaya Inc., Tokyo, Japan), and discharge rating curves were calculated to obtain water discharge (Q, m s^{-1}) at a 30-minute basis.

The entire study site had been cultivated for oil palm since 2002, and was managed into farming blocks (300 × 1000 m, each) bordered with intersecting roads running south-north and east-west. Only in the peatland area, the roads were constructed with canal. The dig out materials during canal construction were put onto the road. The canal water level during the sampling period ranged from 15 cm to 120 cm below soil surface level. The fertilizer application had an unclear effect on the chemical composition of the soil solution in this study site (Marwanto et al. 2018). However, to avoid any effect of fertilizer on the solid phase, sampling points were distanced about five meters from the trunks of the oil palms. I also

confirmed that fertilizer input to the mineral upland had very little influence on the streams because nutrients from fertilizer were much lower than nutrient demand oil palm and quickly absorbed (Tarmizi and Tayeb 2006) after the application.

Peat samples were collected at the center of the farm blocks from the surface layer at three depths (0–15 cm, 15–30 cm and 30–50 cm) on the grid at ~1 km intervals (total 32 grid points) using peat sampler (volume = 530 ml, length = 50 cm) (Royal Eijkelkamp, The Netherlands) for chemical analysis. Further samples were taken at 50 cm depth intervals thereafter until the mineral bed was reached. To enable investigation of the effects of the mineral upland on the chemical properties of the surface layers, the minimum distance from the mineral upland was measured at all sampling points. Profile samplings were also obtained along transects comprised of the grid points beside the upland (T1), the riverbank (T2), and elongating from mineral upland to riverbank (T3) (Fig. 2-1 and Fig. 2-2).

2.4 List of Tables and Figures

Table 2-1 Study site characteristics

	Catchment-1	Catchment-2		
Total Area (ha)	4662 [1] + [2]	2302 [1] + [2]		
Precipitation (mm)	2080	2080		
Streamflow entry point name	Inlet 1	Inlet 2a	Inlet 2b	Inlet 2c
Catchment characteristics				
[1] Mineral upland	Upland-1	Upland-2a	Upland-2b	Upland-2c
Area (ha)	1030	301	437	86
Soil type	Ultisol†	Ultisol†		
Geology	Tertiary sedimentary rock‡	Tertiary sedimentary rock‡		
Elevation (m a.s.l)	10–59	5–39	4–59	8–47
Land use	Oil palm (> 20 years)	Oil palm (> 20 years)		
[2] Peatland				
Area (ha)	3632	1478		
Soil type	Peat soil	Peat soil		
Elevation (m asl)	0–8.4	0–9.0		
Relief	Flat	Flat		
Land use	Oil palm (10–20 years)	Oil palm (10–20 years)		
Main canal length (km)	195	48		

†: obtained from Global Soil Map Regions, USDA, NRCS (2005) (https://www.nrcs.usda.gov/Internet/FSE_MEDIA/nrcs142p2_050722.jpg)
‡: obtained from Geological map of Indonesia, Ministry of Energy and Mineral Resources, the Republic of Indonesia (2010) (https://psg.bgl.esdm.go.id/pameran/index.php?kategori=indeks-peta&halaman=peta-geologi-indonesia&title=Peta%20Geologi%20Indonesia

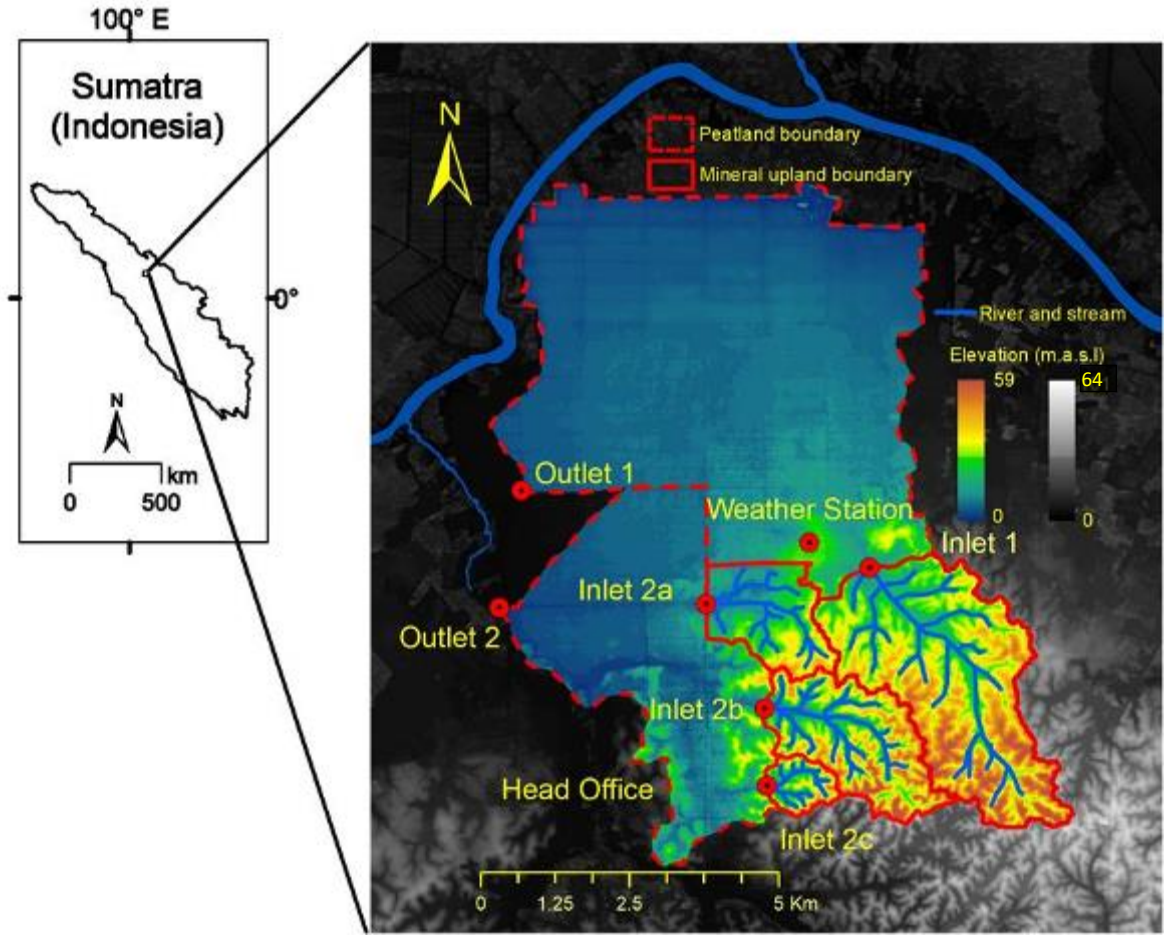

Fig. 2-1 Study site characteristics. The study site is located between mineral terrain and Siak River (thick blue line elongating from west to east). Dashed-red line indicating the hydrological border between peatland and surrounding area. Redline indicates hydrological border between mineral upland catchment and surrounding area. Peatlands are located at lower elevations indicated by green to blue color. A small stream (thin-blue line) runs from mineral upland to the peatland. Fade-thick rectangular line in the peatland indicating canal system. The background map of the study location is derived from a digital elevation model (DEMNAS, http://tides.big.go.id/DEMNAS/), resolution 8.3 m × 8.3 m and vertical accuracy of 3.7 m

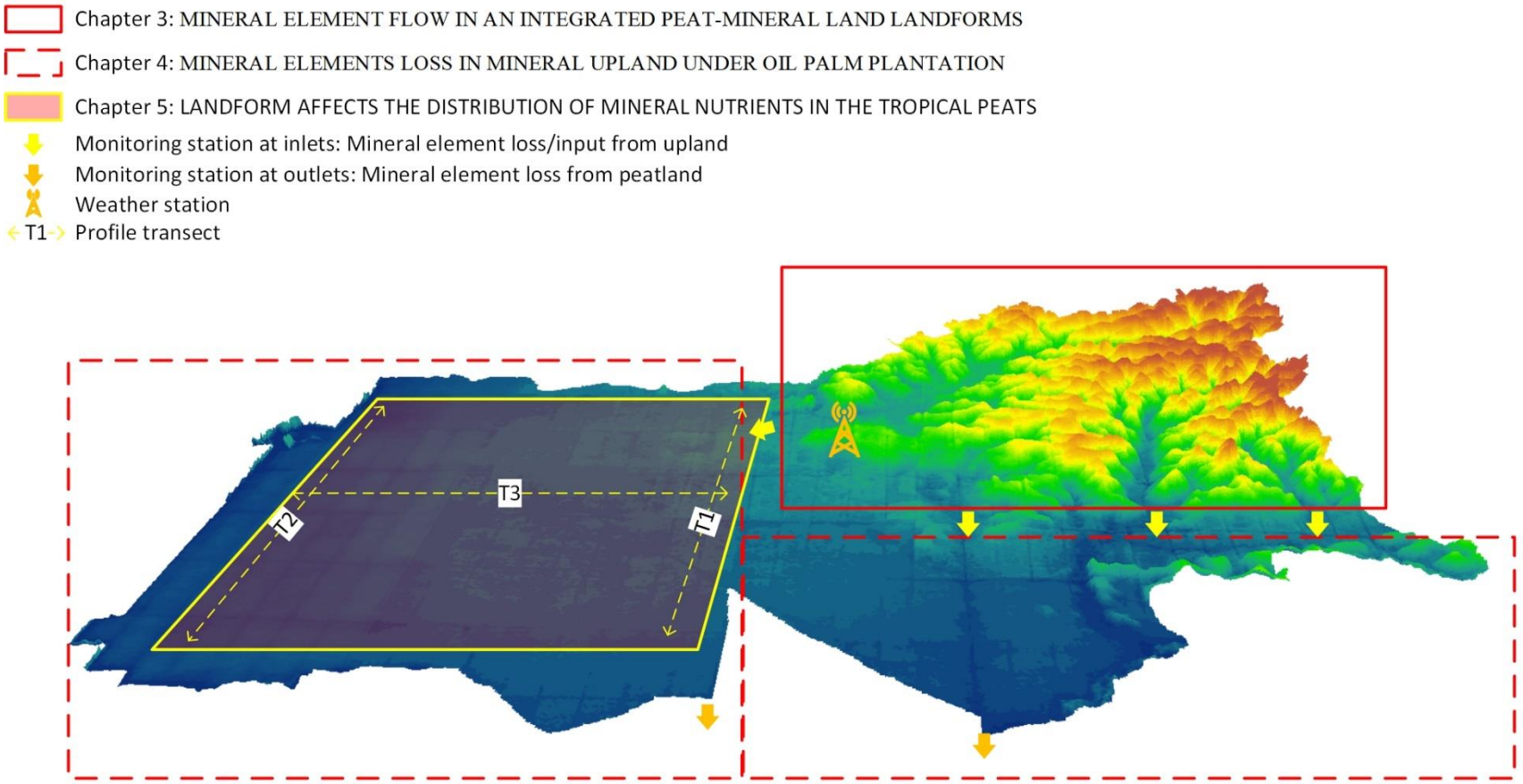

Fig. 2-2 Conceptual frame work of thesis organization.

CHAPTER 3
MINERAL ELEMENT FLOW IN AN INTEGRATED PEAT-MINERAL LAND LANDFORMS

3.1 Introduction

Most studies examining mineral nutrients status in tropical peatland are exclusively considered a single-peatland ecosystem. Tropical peatland is highly acidic (Anderson et al. 1983) and low mineral nutrient status (Watanabe et al. 2013; Funakawa et al. 1996; Page et al. 2006). Therefore, tropical peatland is less favorable for crop production (Agus and Subiksa 2008; Haraguchi et al. 2000; Driessen 1978). The low mineral nutrient status in most tropical peatlands is caused by a lack of inputs due to 1) a long distance from the sea (Funakawa et al. 1996), 2) far distance from the underlying mineral bed (Funakawa et al. 1996; Watanabe et al. 2013), and 3) an absence of biomass input (Funakawa et al. 1996; Page et al. 2006; Lampela et al. 2014). Erosion is pronounced in humid tropical regions (Labrière et al. 2015; Sumiahadi and Acar 2019) with intensive rainfall, particularly from agricultural fields. However, an ecosystem elsewhere is a part of another more extensive ecosystem connected by a hydrological system, and mineral nutrient input from the adjacent lands can be substantial to compensate the mineral nutrient loss and prevent environmental degradation. Unfortunately, studies on mineral nutrient input from the adjacent land are surprisingly scarce in the tropical peatlands receiving intensive rainfall.

Ecologists have long been aware that there is a flux of energy and nutrients from a terrestrial ecosystem to the surrounding aquatic ecosystem and vice versa (Ballinger and Lake 2006). The report reveals that ecosystems provide permeable boundaries that enable nutrients to be transferred among adjacent ecosystems, such as at a catchment scale. The transfer of nutrients from one ecosystem to another is referred to as a "subsidy" or "donation" (Polis et al. 1997), compensating nutrient-poor ecosystems indicated by vegetation patterns. For instance, in temperate peatland ecosystems, change in vegetation pattern is evident at a transitional zone where minerotrophic water meets the nutrient demand of poor-nutrient and acidic water of oligotrophic peatland (Howie et al. 2009; Langlois et al. 2015). A richer-nutrient ecosystem in terms of Ca, K, Mg, Na, Fe, and Mn consists of tree species, while the poor nutrient part consists of shrub, grasses, and sphagnums (Paradis et al. 2015; Langlois et al. (2015) reported that a confined transitional, a depression zone between peatland and mineral land, was wetter and supported higher pH (4.8±0.9) and EC (105±52 μS cm^{-1}) than in the bog: pH (3.7±0.3) and EC (32±24 μS cm^{-1}). That report is also congruent with Paradis, Rochefort, and Langlois

(2015) that revealed that topography is the primary factor for the formation and function of the transitional zone, which determines water flow direction and possibly nutrient transport.

In the tropical region of Southeast Asia, soil and environmental degradation under agriculture have been major issues (Tarigan et al. 2016; Ziegler et al. 2009). Monoculture with intensive cultivation in mineral land decreases infiltration rate (Marten et al. 2016), accelerate surface runoff (Murtilaksono et al. 2019), soil erosion (Clarke and Walsh. 2006; Nainar et al. 2018), and mineral nutrient loss (Maene et al. 1979; Malaysian Oil Palm Board 1994; Chew et al. 1999). Furthermore, dissolved mineral nutrient (<0.45 um) loss in runoff water was reported higher than in sediment (Vijiandran et al. 2017), indicating that higher mineral nutrients in dissolved form moved further. Nevertheless, it is unclear how mineral nutrient loss from mineral land can be deposited and beneficial for compensating oligotrophic peatland and preventing further environmental problems such as sedimentation and eutrophication of a water body downstream. Given that most of the tropical peatlands in Indonesia lay on lower elevations (Anderson 1978; Ritung et al. 2011), lost nutrients from upstream mineral upland would be utilized in downstream peatland.

Seasonal change in flow of mineral elements from upland and their possible deposition in peatland would be affected by various factors. In the upland, surface runoff increases surface erosion that releases mineral elements during intense rainfall. In the peatland area, the size of peatland is important as seasonal elemental flow would also be influenced by water discharge response of peatland. Generally, the larger the peatland, the slower the responding time. In order to maintain water level, peatland under oil palm plantation also has a drainage system equipped with multiple watergates. Gentle slope gradients in peatland having watergates would retard its straightforward drainage and distribute water across the plantation along canals, possibly depositing mineral elements.

Clarifying the seasonal change in mineral element flow in upland and deposition in peatland is essential to conceptualize mineral element transfer across a catchment. This study aimed to investigate the mineral element budget in peatland. I measured the inflow (from mineral upland) and outflow (from mineral–peat landform) of mineral elements and investigated their temporal changes and retention in a peatland. I hypothesized that peatland size and canal length are vital features for the deposition and retention of mineral elements. The finding in this study can optimize the use of peatland under oil palm plantations managed by the current drainage system with wiser mineral nutrient management.

3.2 Materials and methods

3.2.1 Characteristics of study site

The study was conducted in two adjacent peat-mineral upland landforms, namely catchment-1 (4662 ha) and catchment-2 (2302 ha) situated in the Siak watershed, Riau (Fig. 3-1). The climate in this region was a typical humid climate with high precipitation (above 2000 mm) and high temperatures ranging from 23–27°C throughout the year (Marwanto et al. 2018). The study area generally experiences a bimodal pattern of rainy seasons during October to January and March to August, with a short dry spell in February and August. Because of the proximity, peatland-1 and peatland-2, were similar conditions, except for their sizes (Table 3-1). Peatland-1 accounts for 3632 ha, while peatland-2 accounts for 1478 ha. The peat depth in the two peatlands was similar, ranging from 0.5–7 m. (Iskandar et al. 2020). The study area was dominated by sapric peat at the surface and fabric and hemic peat in the deeper layers. Peatland-1 and peatland-2 drained water via a single outlet, namely outlet-1 and outlet-2, respectively (Fig. 3-1).

Each peatland was connected to mineral upland lying at the higher elevations of the hydrological system. Mineral upland-1 was connected to peatland-1 by a single stream draining water via a single inlet (inlet-1). In comparison, mineral upland-2 was connected to peatland-2 by three streams draining via separated inlets (inlet-2a, 2b, and 2c) (Fig. 3-1). Due to the proximity, both mineral upland characteristics such as size, soil type, land use, and elevation are similar. The detailed information regarding their characteristics is presented in Table 3-1.

3.2.2 Land use management, effect of fertilizer, and nutrient inflow from the mineral upland

Both peatland and mineral upland at the two catchments had been cultivated for oil palm plantation since 2002. The plantation was managed in farming blocks (300 × 1000 m each), which were bordered by roads for farm management. Each peatland area was drained at each farm block with intersecting canals (from 3 m to 5 m in width, ~2 m deep) running south-north and east-west and equipped with multiple water gates at every intersection to maintain water table inside the farm block. The crops were planted in rows at planting distances of 8–9 m. The average density of oil palm was 133 trees ha^{-1} (Marwanto et al. 2018). The peat soil under oil palm was not plowed for the entire growing period, and weeds were regularly eradicated using herbicide or mechanical equipment. Old fronds were regularly pruned and remained in the sites.

To estimate the effect of fertilizer input on the increase in mineral elements in the water body from the mineral upland, I calculated mineral nutrient demand by oil palm and supply from fertilizer input. I confirmed that fertilizer input to the mineral upland had very little influence on the streams because nutrients from fertilizer were much lower than nutrient demand oil palm and quickly absorbed after the application (Tarmizi and Tayeb 2006).

3.2.3 Catchment characteristics and boundary between upland and peatland

The catchment characteristics both in mineral uplands and peatlands such as boundary, slope distribution, and stream networks were determined based on a DEM map (DEMNAS, 2018 resolution 8.3 m × 8.3 m) using special tools of hydrology, in Spatial Analyst Tools of Arc GIS 10.7 (ESRI, California, USA). Hydrological boundary, watercourse direction, and stream links in the mineral upland were evident in the topographical map (Fig. 3-1). In contrast, local topography in the peatlands was relatively gentle; hence I defined the catchment boundary and elevation gradient by a real-time kinematic GPS (GRS-1 GG, TOPCON, Tokyo, Japan), which has an accuracy of ± 4 mm, and computer software (GNSS-Pro, TOPCON, Tokyo, Japan) coupled with ground validation of watercourse direction. Separated by the Siak River levee, ground elevation and water level in the peatland area were still above the mean water level of the Siak River (Fig. 3-1). Therefore, I assumed that there was little groundwater leakage from the river to the peatland.

3.2.4 Monitoring of hydrology

An automatic weather recorder (Vantage Pro 2, Davis, California, USA) and multiples absolute pressure water level data logger (HOBO U21-001-04, ONSET, Massachusetts, USA with an accuracy of 1 mm) were set to record rainfall and water discharge every 30 minutes (see "weather station, inlets and outlets" in Fig. 3-1). To estimate nutrient flow, I monitored water discharges at the inlet and the outlet of each site. Water level (h, m) at each outlet was monitored every 30-minutes, and the cross-section of each inlet and outlet was measured. The flow rate was periodically measured on stable water flow using a current water meter (UC-300, Tamaya Inc., Tokyo, Japan), and discharge rating curves were calculated to obtain water discharge (Q, m s^{-1}) at a 30-minute basis (Table 3-2). Due to the proximity to the Siak River tributary, the flow rate at outlet-2 was occasionally affected by high tide, where the high-water level was not followed by normal discharge. However, I confirmed that there was no water intrusion to the peatland-2 (catchment-2) by visual observation. To estimate the water

discharge at outlet-2, I adjusted high water level during tide to the high of previous normal flow. I also ensured that flow rate measurement was undertaken during normal flow.

3.2.5 Sampling and laboratory analyses

Pre-mixed multiple water samples were collected biweekly from mid and near both sides of the watercourse at a depth of 0–20 cm below the water surface at inlets and outlets. Mixed water was placed in about 5 L containers, then pH and EC were determined *in situ* (Metler Toledo, Giessen, Germany). An aliquot of water sample was filtered with 0.45 μm syringe hydrophilic cellulose acetate membranes (Sartorius Stedim Biotec GmBH, Göttingen, Germany). Both filtered and non-filtered samples were kept in a 50 ml airless plastic bottle then preserved at 4 °C until the laboratory analyses. Decomposition of organic matter (OM) by microbial activity was inhibited by adding $CuBr_2$ solution (0.1–1 mg L^{-1}) to each sampling bottle (Fujii et al. 2009; Shibata et al. 2017).

Both filtered and non-filtered samples were analyzed to determine Al, Fe, Si, Ca, Mg, and K in the dissolved and suspended forms. Before analyses, the non-filtered sample was digested by HF and aqua regia (Hossner 1996), while the sample filtered by the 0.45 μm filter was directly analyzed. The concentrations of Si, Fe, Al were determined using an inductively coupled plasma atomic emission spectrometer (ICPE-9000, Shimadzu, Kyoto, Japan), Ca, Mg, K using flame emission spectroscopy (AAS AA-700, Shimadzu, Kyoto, Japan), and dissolved organic matter-DOM (dissolved organic carbon-DOC and dissolved nitrogen-DN) using TOC Analyzer (TOC-L, Shimadzu, Kyoto, Japan). The concentrations of elements in the suspended form were obtained by subtracting the concentration of filtered samples from non-filtered samples.

3.2.6 Calculating chemical flux and statistical analyses

I obtained the flow for each element, DOC, and DN in the sample by multiplying the concentrations by the corresponding water discharge at the time of sampling. The annual flow of each element (g yr^{-1}) at the inlets and outlets of both catchmens was calculated by multiplying the annual flow-weighted concentration (g m^{-3}) by annual water discharge (m^3 yr^{-1}), modified from the equation by Cook et al. (2018). The flow of inlet-2 was the sum of flow from inlet-2a, 2b, and 2c. The flow of sampling date during missing data due to the different installation dates and technical problems at outlet-1 was calculated based on manual water level measurement. To observe deposition (acquisition) and loss of mineral elements and DOC at

each site, I determined the net flow by subtracting the flow of those elements at outlet (whole catchment) from those at inlet (mineral land). The value above zero (positive) indicates the deposition occurring in the peatland, while the value below zero (negative) indicates the loss from the peatland.

Because most of the data were not normally distributed, even after being converted to logarithms, square roots, and reciprocal, a Spearman rank correlation was applied to investigate relationships between flow measured elements and water discharge. The significant differences in chemical concentrations and flow between catchment-1 and catchment-2 were tested using *t*-test for normally distributed data or *u-tes*t (Mann-Whitney Rank Sum test) for non-normally distributed data. Statistical significance was based on either $P < 0.01$ and $P < 0.05$. All statistical analyses were done using Sigma Plot 11.0 software (Systat Software, California, USA).

3.3 Results

3.3.1 Rainfall and water discharge

Both catchments experienced a relatively wetter year than the average of 20-years rainfall data (Fig. 3-2), and an intense rainy season occurred from March to August 2020 (Fig. 3-3). Cumulative water discharge at outlet-1 was about one-fifth (387 mm) of the cumulative rainfall (2082 mm) and that at outlet-2 was about a half (1012 mm) (Fig. 3-3a). The water discharge fluctuated following the rainfall amount. The rainy season during the monitoring period started in October 2019 to December 2019, and water discharge at both inlet and outlet increased in both catchments (Fig. 3-3b, 3c, 3d, 3e, and 3f). Later, both catchments experienced a short dry spell between January and February 2020, when water discharge decreased. The second rainy season started from early March 2020 to June 2020, followed by an increase in water drainage (Fig. 3-3b, 3-3c, 3-3d, 3-3e, and 3-3f). Further, the catchments experienced another short dry spell in the late August 2020, before the rainy season of the later year started in the mid-September 2020, which continued until the end of the study period. The average responding time of water discharge at outlet-1 was 26 hours, longer than that at outlet-2 (9 hours).

3.3.2 Seasonal variation of chemical properties in the two catchments

I identified three terms of seasonal changes in chemical properties of water at inlets and outlets: November 2019 to February 2020, March to August 2020, and September to November

2020. The terms corresponded to the seasonal change in rainfall and water discharge described above.

3.3.2.1 pH, EC, concentration of mineral elements, and DOM

The pH and EC at both inlets had similar patterns across the study period. The pH at both inlets tended to increase while EC tended to decrease, except for a high EC at inlet-2 in September 2020 (Fig. 3-4a). Both pH and EC values at inlet-1 and inlet-2 were also similar, ranging (4.37±0.28 and 50.6±14.3 µS cm^{-1}) and (4.43±0.31 and 72.1±24.3 µS cm^{-1}), respectively.

In comparison to the values observed at both inlets, the pH and EC at both outlets follow water discharge pattern. The pH sharply increased in February 2020 after showing low values from November 2019 to February 2020 (Fig. 3-4a). Afterward, pH remained relatively constant between March and September 2020 and decreased in October 2020. The EC showed a reverse pattern to pH: high between November 2019 and February 2020, low between March and September 2020, and back to high between October and November 2020 (Fig. 3-4a). Besides the pattern similarity, pH and EC at outlet-1 ranged narrower (3.5–4.1 and 61–151 µS cm^{-1}) than at outlet-2 (3.1–4.7 and 136–661 µS cm^{-1}) (Fig. 3-4a).

Both inlets and outlets had a similar seasonal trend of the mineral element concentrations in the three terms (Fig. 3-4 and Fig. 3-5). Except for dissolved Si, DOC, and DN which had unclear pattern both at inlets and outlets (Fig. 3-4b and 3-4e), the concentrations of dissolved Al, Fe, Ca, and K tended to be high between November 2019 and February 2020, low between March and August 2020, and again high between September and November 2020 (Fig. 3-4c, and 3-4d). The concentration of dissolved Mg was relatively compared to other mineral elements (Fig. 3-4d). Similarly, the concentrations of Si, Al, and Fe in the suspended form were generally high from the beginning of the sampling campaign in November 2019 until February 2020, low between March and August 2020, then again high from September 2020 to November 2020, being clearer at catchment-1 than catchment-2 (Fig. 3-5b and 3-5c). Suspended Ca, Mg, K did not show clear trend, Mg being low across the study period (Fig. 3-5d).

3.3.2.2 Comparison of elemental flows between inlet and outlet

The net flow of mineral elements in dissolved form had small variation in catchment-1 across the study period, except for Ca and K, while considerable variation was evident in catchment-2 (Fig. 3-6a, 3-6b, and 3-6c). In catchment-1 during November 2019 to February

2020, the net flow of Si, Al, Fe, Mg, and K was initially negative but then tended to close to zero line (Fig. 3-6a, 3-6b, and 3-6c). During this period, Ca tended to fluctuate (Fig. 3-6c). In the following two terms, from March 2020 to the end of the study period, the net flow of mineral elements tended to be close to zero line or above it in catchment-1 (Fig. 3-6a, 3-6b, and 3-6c). The net flow of DOC tended to fluctuate across the study period while DN tended to steady in peatland-1 (Fig. 3-6d). In comparison, the net flow of mineral elements in catchment-2 tended to be fluctuating below the zero line across the study period (Fig. 3-6a, 3-6b, and 3-6c), except for positive K in September 2020 (Fig. 3-6c). In catchment-2, the net flow of DOC showed noticeable negative values, particularly during intense rainfall between March and August 2020, while DN value was very low and steady across the study period (Fig. 3-6b).

The net flow of measured elements in suspended forms had considerable variations across the sampling period in the two catchments. During November 2019 to February 2020, the net flow of Si, Al, Fe, and Ca was negative, while Mg and K were around zero in both catchments. The loss of Si in catchment-1 was the highest that was up to (-)50 g s^{-1} at the beginning of sampling (Fig. 3-7a). The loss of Al and Fe were also markedly high below the average in catchment-1 (Fig. 3-7b). Then, the net flow of most mineral elements was nearly balanced between March 2020 and August 2020, fluctuating around zero line in catchment-1 (except a positive peak of Ca at outlet one in June 2020), while the loss of the elements was pronounced at catchment-2 (Fig. 3-7a, 3-7b, and 3-7c). Eventually, the net flow of mineral elements generally fluctuated around the zero line between September and November 2020. During this term, several positive net flow rates were noticeable in catchment-1 (Si, Al, K, Ca, and Mg) and in peatland-2 (Si, Al, Fe, Ca, and K) (Fig. 3-7a, 7b, and 7c). The original seasonal change of both inlet and outlet is shown in Fig. S 3-1 and Fig. S 3-2.

3.3.3 Comparison of mineral elements and DOM flows between inlet and outlet

The input of mineral elements and DOM at both inlets to the peatlands were similar. Fig. 3-8 shows that most of the elements, DOC, and DN flows in suspended and dissolved forms were not significantly different between inlet-1 and inlet-2. Only dissolved K was significantly higher 1.6±1.7 g s^{-1} (53.7 Mg yr^{-1}) at inlet-2 than at inlet-1 0.4±0.5 g s^{-1} (13.5 Mg yr^{-1}).

In comparison, the rate (Fig. 3-9) and total flow of mineral elements (summation of dissolved and suspended forms) at outlet-1 were lower than those at outlet-2 (Fig. 3-10). During

the study period, outlet-1 drained 1.46 Gg yr^{-1} of total mineral elements (excluding DOC and DN), which was lower than 1.98 Gg yr^{-1} at outlet-2. For example, outlet-1 drained Al (2.6±2.1 g s^{-1}; 96 Mg yr^{-1}), which was lower than outlet-2 (5.9±4.3 g s^{-1}; 206 Mg yr^{-1}). Also, outlet-1 drained total Ca, 2.9±1.1 g s^{-1} (96 Mg yr^{-1}) relatively lower than outlet-2, 4.6±4.8 g s^{-1} (161 Mg yr^{-1}). Concerning organic substances, outlet-1 drained DOC 43±18 g s^{-1} (1436 Mg yr^{-1}) higher than outlet-2, 39.0±25.0 g s^{-1} (1012 Mg yr^{-1}).

3.3.4 Correlation and statistical difference of two catchments

Spearman correlation test was performed to observe the relationship between the measured elements to indicate their associations. The correlation test was also done to observe the relationship between water discharge and mineral elements to check the diluting effect of rainfall in the peatland. In catchment-1, the elements correlated with each other (Table 3-3 and Table 3-4). For instance, in suspended forms, suspended Al was positively correlated with suspended Si and Ca. For dissolved forms, Al was positively correlated with dissolved Ca (rs = -0.44, P <0.05) and Mg (rs = -0.48, P <0.05). Correlations between the elements were also found for catchment-2 (Table 3-4). For instance, suspended Fe had a negative correlation with suspended K but had a positive correlation with dissolved Ca (rs = -0.79, P <0.01), Mg (rs = -0.60, P <0.01), and DOC (rs = -0.52, P <0.01). Despite of the significance, most of measure elements tended to correlate negatively with water discharge in outlet-1, while positively in outlet-2. Only suspended Si (rs = -0.42, P <0.05) and dissolved Fe (rs = -0.41, P <0.05) which had strong correlations.

Generally, outlet-1 had lower concentrations of the mineral elements (Fig. 3-11) than outlet-2. The concentration of suspended forms Fe and Mg at outlet-1 was significantly lower than that at outlet-2. Most of the concentrations of the mineral elements in the dissolved form were also significantly higher at outlet-2 except for dissolved Fe. On the contrary, DOC concentration at outlet-1 was significantly higher than that at outlet-2.

3.4 Discussion

3.4.1 Water discharge from the catchments

Both catchments experienced a relatively wetter year, and an intense rainy season occurred from March to August 2020 compared to the 20-years data (Fig. 3-2). However, the catchments had the water discharge less than half of the rainfall, indicating that evapotranspiration was higher than water discharge. The finding confirms the previous report

that in drained tropical peatland, evapotranspiration could be up to 67% of total rainfall (Hirano et al. 2015). Comparing the two peatlands, I found that the water discharge from outlet-1 was higher and less fluctuated than outlet-2 because of the larger area and long drainage system in peatland-1 (Fig. 3-3d and Table 3-1). Watercourse entering inlet-1 branches into canals before discharging from the catchment-1. In comparison, outlet-2 was more responsive because water from the mineral upland-2 run shorter canal length (Fig. 3-3f and Table 3-1). The longer responding time would give time and chances for the mineral nutrient to be deposited.

3.4.2 Seasonal changes in chemical properties and flow rate

3.4.2.1 Seasonal change in chemical properties

The increase in pH and decrease in EC (Fig. 3-4) was attributed to the seasonal dilution of the stream and canal by the rainfall. The low pH during November 2019 and February 2020 both at outlet-1 and outlet-2 (Fig. 3-4a) suggests that oxidation of organic matter generated organic acid after a long dry season in 2019 (Fig. S 3-3). The low pH in the current study was consistent with the previous report in the same location (Marwanto et al. 2018) that the rewetting process after the dry season resulted in acid transportation from the upper acidified peat layer. Acid was leached due to the high rainfall then drained to the canal. Compared to outlet-2, outlet-1 showed a longer time of low pH at outlet-1 (Fig. 3-4a) due to its larger area and longer drainage systems (Fig. 3-1 and Table 3-1). Also, the result suggests that low pH would persist despite of several rainfall events occurring during the initial sampling campaign. At the sampling period (March 2020 to August 2020), higher pH could be caused by diluting organic acid by rainwater and mineral element input such as Ca and K (Fig. 3-6c and Fig. 3-7c). Afterward, in the late September 2020, temporary low pH was evident at both outlets owning to organic acid transportation from the upper peat layer corresponding to the short dry spell in the late August 2020. The high and fluctuating EC at outlet-2 (Fig. 3-4a) between November 2019 and February 2020 might be attributed to the abundance of ionic species such as organic acid, NO_3^-, and SO_4^{2-} the decomposition of peat materials. The dilution of ionic species owing to intense rainfall would cause a gradual decrease in EC between March and August 2020 (Fig. 3-4a). Whereas the temporary high EC between late September to November 2020 was caused by the abundance of ionic species such as organic acid, NO_3^-, and SO_4^- due to the decomposition of peat materials in dry spell in the beginning September 2020 (Fig. 3-4a).

3.4.2.2 Seasonal flow

The effects of water discharge on seasonal mineral element flow were less in catchment-1 while more pronounced in catchment-2. Started slightly negative between November 2019 and February 2020, the net flow between input and output was balanced for the period of March and August 2020, and September and November 2020 in catchment-1 (Fig. 3-6 and Fig. 3-7). The result suggests that mineral element inflow from upland-1 could compensate for the loss in peatland-1 (Fig. 3-6 and Fig. 3-7) because of its larger area than peatland-2 (Table 3-1). The compensation in peatland-1 was indicated by the net flow of Al, Fe, Ca, and K in dissolved and suspended forms (Fig. 3-6b, 3-6c, 3-d, Fig. 3-7b, and 3-7c) which ranged from zero line to positive. Such compensation did not occur in peatland-2, indicated by the high loss of those elements (Fig. 3-6b, 3-6c, 3-d, Fig. 3-7b, and 3-7c) which particularly between march and August 2020. The high loss of mineral elements in peatland-2 was caused by the higher water discharge and shorter responding time between inlet-2 and outlet-2, which gives a lower chance of the mineral to deposit.

The higher flow of DOC at the outlet-1 (48.9±14.6 g s^{-1}) and outlet-2 (33.9±28.4 g s^{-1}) (Fig. 3-9) compared to their inlets 7.5±7.8 g s^{-1} and 6.5±3.1 g s^{-1} (Fig. 3-8) indicates an increase in organic matter leaching from the peatlands. The DOC and DN flow at outlet-1 was much higher than those at outlet-2 because of the larger contributing area and longer canal length of peatland-1 than peatland-2. The longer canal length implies more assessable area in the peatland that contributes to the more organic matter source.

In addition to the input from mineral land, the loss of mineral elements could also be attributed to the decomposition of the peat and the biomass input from oil palm. A strong and positive correlation between Al and Ca (Table 3-3) at outlet-1 suggests eroded soil from the mineral upland-1 contains Al and Ca. High outflow of Si, K, Ca, and DOC in peatland-2 (Fig. 3-6 and Fig. 3-7), would be attributed to the decomposition of surface peat and oil palm parts such as fronds were regularly pruned in the catchments and flush of water discharge. Oil palm parts decomposition released elements indicated by a high flow of Si, K, Ca, and DOC but lower Mg and Fe, particularly in peatland-2. The results confirmed the previous report that Si, Ca, and K contents are higher than Fe and Mg in the oil palm trunk and fronds (Saka et al. 2008).

3.4.3 Peatland as depositional zone

Peatland would function as the depositional zone of mineral elements. With similar mineral input rates (Fig. 3-8), outlet-1 (peatland-1) drained at lower rate (Fig. 3-9) and smaller cumulative amounts of total mineral elements (Fig. 3-10) than outlet-2 (peatland-2). The lower outflow of most mineral elements at outlet-1 than at outlet-2 (Fig. 3-9 and Fig. 3-10) indicates that more mineral elements deposit in peatland-1. The deposition was also supported by the correlation analysis between water discharge and flow of the mineral elements. The negative correlations between water discharge and mineral elements such as Al, Si, Ca, Mg, and K (Table 3-5) were found more for outlet-1, while the positive correlation for outlet-2 was found only for Fe and Si. The negative correlation suggests that the large amount of water draining from peatland-1 was not followed by the high outflow of mineral elements.

I suggest that the deposition process could occur by physical and chemical processes. Mineral elements in suspended forms would quickly deposit by gravitational force as water discharge was slower because of the gentle slope gradient and multiple water gates in the peatland. As dissolved forms are lighter to high-water discharge during intense rainfall, their transportation would be higher thus deposition could occur by association and flocculation with organic matters. The-nearly zero and stable net flow of Al, Fe, and Ca dissolved forms (Fig. 3-6b and 3-6c) implies their inflow from inlets could compensate the loss due to intense rainfall, particularly in catchment-1. Such elements in dissolved forms were distributed across the peatland via the canal network; thus, the high concentration of DOM could be the chelating agent that associates with them. The positive net flow of dissolved Al at catcment-1 was evident between March and November 2020 (Fig. 3-6b), which would come from the formation of Al–organic matters complexes as indicated by Funakawa et al. (1996). Association of dissolved mineral elements, such as divalent Ca and polyvalent Al, with DOM are more chemically active (Owens et al. 2005) than monovalen cations, which would bind and flocculate (Römkens et al. 1996)

The result suggests that peatland size and canal length are valuable to consider mineral nutrient deposition and retention in the tropical peatland with intense rainfall. Peatland-1 drained mineral elements at outlet-1 1.46 Gg yr^{-1} lower than peatland-2 at outlet-2 1.98 Gg yr^{-1} (Fig. 3-10) (Fig. 3-10), implying that peatland-1 retained more mineral elements. With the similar characteristics of mineral elements inflow from mineral upland, peatland-1 (3632 ha),

which was more than three times bigger than its mineral upland (1030 ha), was more effective in retaining mineral elements.

Since peatland-1 and peatland-2 still drained mineral elements temporarily, I recommend that making a longer watercourse would be beneficial to optimize sediment deposition and nutrient retention during the rainy season. Equipped by multiple water gates at every intersection, the watercourse could be distributed across the peatland; hence water-enriched mineral nutrients would intrude into farm block via smaller canal and be retained. Mineral elements enrichment can enhance peat soil's fertility (Wang et al. 2016), thus potentially support crop productivity. Association of mineral elements with DOC might also reduce organic carbon flow to under stream, preventing potential anoxia in Siak River (Rixen et al. 2008).

3.4.4 Effect of mineral enrichment on chemical properties of peatland waterbody: comparison with other studies

I compared the geochemical properties of the results with those in the previously published papers (Table 3-6). I classified the previous study sites based on landform as topogenous (e.g., fen, coastal) and ombrogenus peats (bog, mire, tropical deep peat). The pH values at outlet-1 and outlet-2 (3.76±0.24 and 3.86±0.34) were generally lower than that in topogeneous peat (5.71±0.19; 4.78±0.93; 4.22±0.48), but still relatively higher than bog (3.37±0.31). The EC value of outlet-1 was lower than topogenous peat (133±38 µS cm^{-1}) (Marwanto et al. 2018) but still higher than in coastal peat 80.2 µS cm^{-1} (Funakawa et al. 1996). The EC value at outlet-2 was higher than the same topogenous peat (Marwanto et al. 2018) and same coastal peat of Funakawa et al. (1996). Generally, the mineral elements were higher than ombrogenous peat but comparable with coastal peat. For instance, the concentrations of dissolved Fe in outlet-1 and outlet-2 were 1.34±0.44 and 1.50±0.56 mg L^{-1}, being higher than coastal peat (0.23 mg L^{-1}), while the concentrations of dissolved Ca in outlet-1 (1.88±1.01) and outlet-2 (1.06±0.48 mg L^{-1}) were also higher than that of the coastal peat (0.4 mg L^{-1}) (Table 3-6).

Most studies so far have reported mineral-enriched peatland in the temperate region (Table 3-6). To the best of my knowledge, no studies reported peat-mineral landform integration in a tropical peatland ecosystem. The mineral inflow to the current study could improve chemical conditions to more favorable for farmlands. The higher elements such as Al, Fe, and Si in the current study were evidence of continuous mineral inflow generated by

topographic gradient, which is different from those reported by Funakawa et al. (1996) located along coast where occasional tides induce enrichment of minerals such as Na, S, and Mg. Also, the continuous mineral element inflow from mineral upland to the peatland contribute to 1) higher Ca in outlet-1 compared to those reported in tropical ombrogenous peat (Funakawa et al. 1996) and ombrogenous bog of temperate region (Ulanowski and Branfireun 2013); 2) higher Mg in outlet-1 and outlet-2 compared to ombrogenous bog (Langlois et al. 2015); and 3) higher K in outlet-1 and outlet-2 compared to tropical topogenous and ombrogenous peat in Sarawak, Malaysia (Funakawa et al. 1996). These findings again suggest that integration of peatland with surrounding landform is beneficial when evaluating mineral nutrient source, transfer, and retention. To some extent, mineral element inflow such as Ca and Al would also associate with OM, potentially reducing labile OC hence potentially reduce CO_2 emission. On average, DOC in the current study was lower, especially in catchment-2 compared to those monitored on the farm (Marwanto et al. 2018) and in the others the previous study by Yupi et al. (2016) and Cook et al. (2018). The lower DOC than those previous studies would be partially caused by the association of OM with mineral elements and flocculation, as explained in the previous section. Association organic matters with mineral elements might form a bigger compound (>0.45 μm), which deposits as particulate organic matter on the canal bed.

3.4.5 Conclusion

Rainfall, peatland size, and canal length control the seasonal and total water discharge that carries mineral elements and DOM in suspended and dissolved forms. Seasonal changes in pH, EC, and mineral elements in the peatland were attributed to the seasonal change in rainfall which generated water discharge from the mineral upland. Seasonal change in mineral element flow found at the outlet of peatland was attributed to the high and continuous supply of water discharge and mineral element flow from the mineral upland. The-nearly and stable net flow of mineral elements in suspended and dissolved forms in cacthment-1 imply that inflow of those elements from inlets could prevent further loss due to intensive rainfall. The retention of the mineral element was indicated by positive net flow such as Si, Al, Fe, and Ca from September to November 2020. In the contrary, in catchment-2 showed the loss identified by negative net flow particularly from March and August 2020. Therefore, the total flow of elements in cacthment-1 (outlet-1) was significantly lower than cactment-2 (outlet-2). Size of peatland-1 (catchment-1), which was ca. two times bigger than peatland-2 (catchment-2) and had a longer canal, results in lower mineral elements (Al, Fe, Si, Ca, K and Mg) flow. Also, a comparison with previous studies without mineral upland association suggests that the current

study area had higher mineral elements and lower DOC. This study suggests that integrating mineral elements transfer across peat-mineral catchment is beneficial to compensate mineral elements lacking-peatland and prevent potential DOC release downstream.

3.5 List of Tables and Figures

Table 3-1 Study site characteristics

	Catchment-1	Catchment-2		
Total Area (ha)	4662 [1] + [2]	2302 [1] + [2]		
Precipitation (mm)	2080	2080		
Streamflow entry point name	Inlet 1	Inlet 2a	Inlet 2b	Inlet 2c
Catchment characteristics				
[1] Mineral upland	Upland-1	Upland-2a	Upland-2b	Upland-2c
Area (ha)	1030	301	437	86
Soil type	Ultisol†	Ultisol†		
Geology	Tertiary sedimentary rock‡	Tertiary sedimentary rock‡		
Elevation (m a.s.l)	10–59	5–39	4–59	8–47
Land use	Oil palm (>20 years)	Oil palm (>20 years)		
[2] Peatland	Peatland-1	Peatland-2		
Area (ha)	3632	1478		
Soil type	Peat soil	Peat soil		
Elevation (m asl)	0–8.4	0–9.0		
Relief	Flat	Flat		
Land use	Oil palm (10–20 years)	Oil palm (10–20 years)		
Main canal length (km)	195	48		

†: obtained from Global Soil Map Regions, USDA, NRCS (2005) (https://www.nrcs.usda.gov/Internet/FSE_MEDIA/nrcs142p2_050722.jpg)
‡: obtained from Geological map of Indonesia, Ministry of Energy and Mineral Resources, the Republic of Indonesia (2010) (https://psg.bgl.esdm.go.id/pameran/index.php?kategori=indeks-peta&halaman=peta-geologi-indonesia&title=Peta%20Geologi%20Indonesia

Table 3-2 Rating curve equation of each monitoring point. Q: water discharge (m s^{-1}); h: water level (m)

Location	Discharge rating equation (m s^{-1})	Water level range (m)	R^2
Catchment-1			
Inlet 1	$Q = e^{(5.5h\ -5.9)}$	$0 < h < 0.86$	$R^2 = 0.9011$
	$Q = 0.9h\ - 0.41$	$0.87 < h < 1.50$	$R^2 = 0.9489$
Outlet 1	$Q = \left(e^{(h-0.93)}\right)^{0.29}$	$0 < h < 0.74$	$R^2 = 0.9507$
	$Q = \frac{h}{2.02}$	$0.74 < h < 2.02$	$R^2 = 0.9856$
Catchment-2			
Inlet 2a	$Q = 0.882h\ - 0.017$	$0 < h < 0.46$	$R^2 = 0.9303$
Inlet 2b	$Q = e^{(9.6h\ -7.01)}$	$0 < h < 0.46$	$R^2 = 0.8474$
	$Q = 6.8h\ - 0.18$	$0.47 < h < 1.18$	$R^2 = 0.8890$
Inlet 2c	$Q = e^{(25h\ -6.5)}$	$0 < h < 0.11$	$R^2 = 0.9888$
	$Q = 0.35h\ - 0.01$	$0.12 < h < 0.34$	$R^2 = 0.9669$
Outlet 2	$Q = \frac{(h-0.01)}{0.21}$	$0 < h < 0.31$	$R^2 = 0.9525$

Table 3-3 Correlations between measured elements in suspended and dissolved forms in catchment-1; n = 26; ** significant at P <0.01; * significant at P <0.05

		Suspended					Dissolved							
		Fe	Si	Ca	Mg	K	Al	Fe	Si	Ca	Mg	K	DOC	DN
Suspended	Al	0.33	0.44*	0.49*	0.31	0.06	0.41	0.40	0.33	0.25	0.48*	0.21	0.02	-0.14
	Fe		0.57*	0.35	0.25	0.07	0.31	0.33	0.31	0.40	0.56**	0.56*	-0.16	-0.09
	Si			0.30	0.42*	-0.04	0.59**	0.50*	0.27	0.47*	0.67**	0.55**	0.07	-0.32
	Ca				0.66**	0.34	-0.02	0.59**	0.07	0.01	0.29	0.58**	-0.31	-0.08
	Mg					0.29	0.06	0.44*	-0.17	0.09	0.11	0.34	-0.26	0.11
	K						-0.28	0.13	-0.52	-0.50*	-0.10	-0.18	-0.25	-0.06
Dissolved	Al							0.14	0.32	0.82**	0.54*	0.31	0.12	-0.15
	Fe								-0.04	0.07	0.66**	0.54*	0.21	-0.03
	Si									0.48	0.42*	0.33	0.30	0.01
	Ca										0.57**	0.38	0.34	-0.02
	Mg											0.67**	0.46*	0.07
	K												0.03	-0.04
	DOC													0.23

.

Table 3-4 Correlations between measured elements in suspended and dissolved form in catchment-2; n = 26; ** significant at P <0.01; * significant at P <0.05

		Suspended					Dissolved							
		Fe	Si	Ca	Mg	K	Al	Fe	Si	Ca	Mg	K	DOC	DN
Suspended	Al	0.19	-0.26	-0.21	0.41	0.17	0.34	-0.12	0.23	0.09	0.18	-0.32	-0.26	0.31
	Fe		0.25	-0.23	0.06	-0.46*	0.61	-0.25	0.58**	0.79**	0.60**	0.32	-0.52*	-0.06
	Si			-0.29	-0.17	-0.41	0.12	0.09	0.08	0.13	0.19	0.55	-0.14	-0.28
	Ca				-0.37	0.37	-0.40*	0.34	-0.52*	-0.57**	-0.42*	-0.18	0.32	0.36
	Mg					0.44*	0.06	-0.11	0.34	0.31	-0.05	0.63	-0.67**	0.22
	K						-0.28	0.29	-0.52	-0.52	-0.60	-0.68**	-0.31	0.10
Dissolved	Al							0.01	0.84**	0.59**	0.90**	0.41*	-0.74**	0.33
	Fe								-0.15	-0.38	-0.02	0.14	0.37	0.26
	Si									0.65	0.92	0.53*	-0.76**	0.08
	Ca										0.58**	0.32	-0.50*	-0.27
	Mg											0.63**	-0.67**	0.22
	K												-0.31	0.10
	DOC													-0.04

Table 3-5 Correlation between water discharge and elements

	Suspended form		Dissolved form	
	Outlet-1	Outlet-2	Outlet-1	Outlet-2
Al	-0.28	0.05	-0.27	-0.06
Fe	0.08	-0.13	-0.41*	-0.14
Si	-0.42*	-0.16	0.13	0.01
Ca	-0.18	0.02	-0.15	0.18
Mg	-0.18	0.51	-0.24	-0.20
K	-0.29	0.36	0.01	-0.23
DOC			-0.18	-0.13
DN			0.29	-0.02

*, P <0.05; **, P <0.01

Table 3-6 Comparison of chemical properties between study sites with previous reports. †: mineral-enriched peat/topogenous peat (e.g fen, coastal), P: pore water; R: river water, ‡Exclusive ombrogenous peat (e.g. exclusive peat bog, mire, tropical peat dome)

		pH	EC	Al	Fe	Si	Ca	Mg	K	DOC	DN
		----------mg L^{-1}----------									
The current study											
Peatland-1(canal)		3.86±0.24	101±47	0.50±0.21	1.34±0.44	1.09±0.89	1.88±1.01	0.92±0.78	2.52±1.92	69.3±25.8	1.91±1.01
Peatland-2 (canal)		3.76±0.34	234±147	3.18±3.59	1.50±0.56	3.35±1.38	1.06±0.48	0.44±0.13	2.84±0.88	24.2±4.5	1.29±0.92
Mineral-enriched peatland†											
Marwanto et al. (2018)	P	4.22±0.48	133±38				7.85±4.41	0.96±0.74	3.11±1.49	55.6±19.6	3.59±3.12
Funakawa et al. (1996)	P	4.08	50.7	0.10	0.23	0.35	0.4	0.15	0.51	43.8	1.91
Ulanowski et al. (2018)	P	5.71±0.19					6.54±2.54	1.13±0.36			
Langlois et al (2018)	P	4.78±0.93									
Baum et al (2007)	R									6.9-7.4	
Moore (2003)	R									15-30	
More et al (2013)	R									20.4-21.7	
More et al (2013)	R									6	
More et al (2013)	R									13	
Takechi (2013)	R									20	
Exclusive ombrogenous peat‡											
Funakawa et al. (1996)	P	4.39	80.2	1.19	1.06	1.18	1.49	1.91	1.76	61.3	2.47
Ulanowski et al. (2018)	P	4.31±0.06					1.80±0.30	0.21±0.30			
Langlois et al (2018)	P	3.37±0.31									
Yupi (2016)	R									82–90	
(2016)	R									49–57	
Alkhatib et al (2007)	R									60.6	
Baum et al 2007	R									62.0–64.1	
More et al (2013)	R									54.7–62.4	
More et al (2013)	R									39.1–47.9	

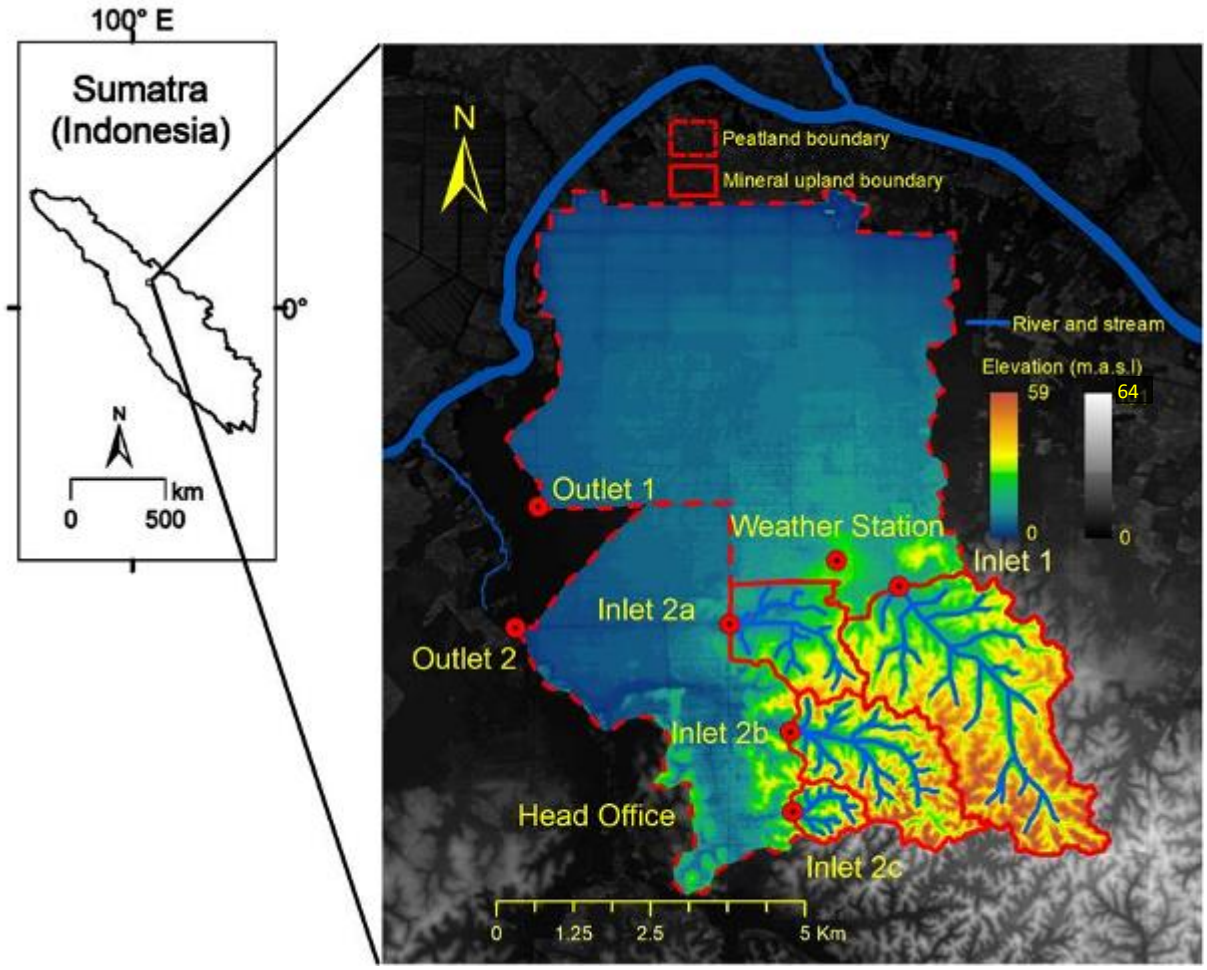

Fig. 3-1 Study site characteristics. The study site is located between mineral terrain and Siak River (thick blue line elongating from west to east). Dashed-red line indicating the hydrological border between peatland and surrounding area. Redline indicates hydrological border between mineral upland catchment and surrounding area. Peatlands are located at lower elevations indicated by green to blue color. A small stream (thin-blue line) runs from mineral upland to the peatland. Fade-thick rectangular line in the peatland indicating canal system. The background map of the study location is derived from a digital elevation model (DEMNAS, http://tides.big.go.id/DEMNAS/), resolution 8.3 m × 8.3 m and vertical accuracy of 3.7 m.

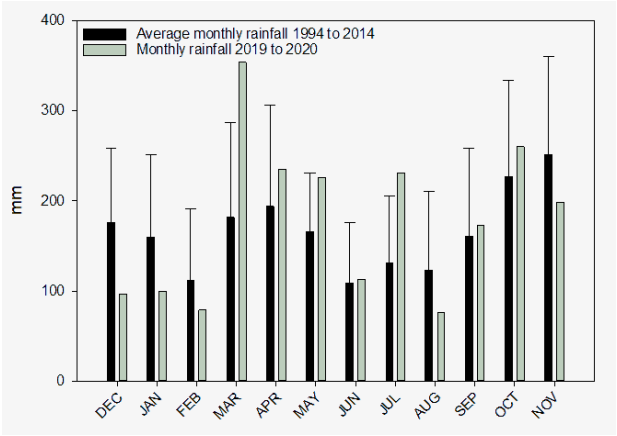

Fig. 3-2 Bar plots showing comparison between monthly average of 20-years rainfall and monthly rainfall 2019–2020 (during the study period). The lowest rainfall indicates the peak of drought (dry spell). Error bars represent standard deviation of the means.

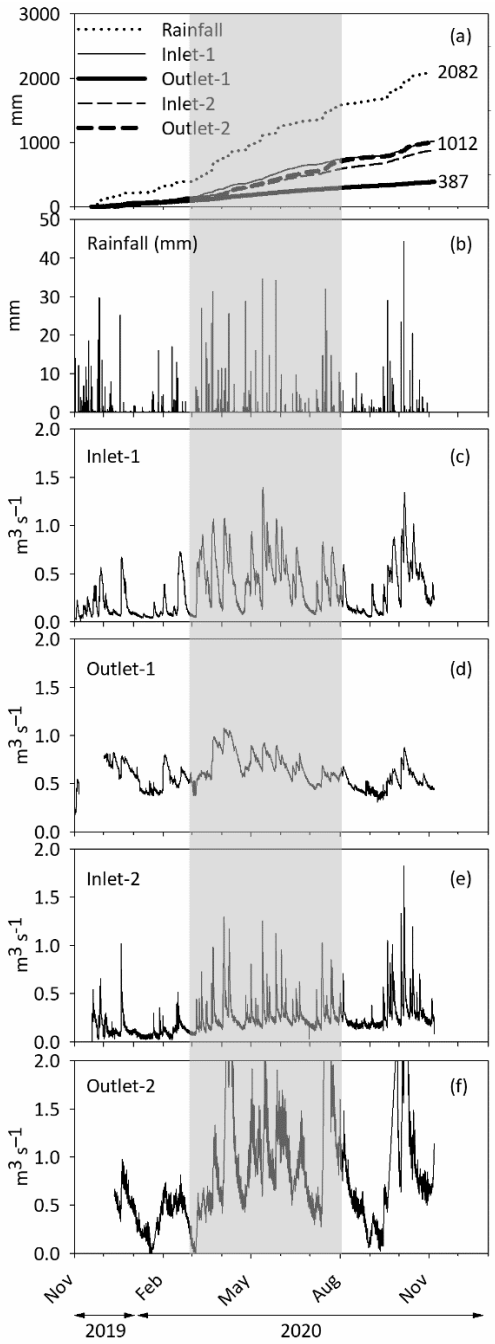

Fig. 3-3 (a) Cumulative rainfall and water discharge from the catchments: catchment-1 (inlet-1 and outlet-1) and catchment-2 (inlet-2 and outlet-2); (b) Bar plots showing 30-minutes rainfall during the study period; (c), (d), (e), and (f) Line graph showing hydrological response (water discharge) at inlet-1, outlet-1, inlet-2, and outlet-2, respectively. The grey box indicates an intense rainfall period between March and August 2020.

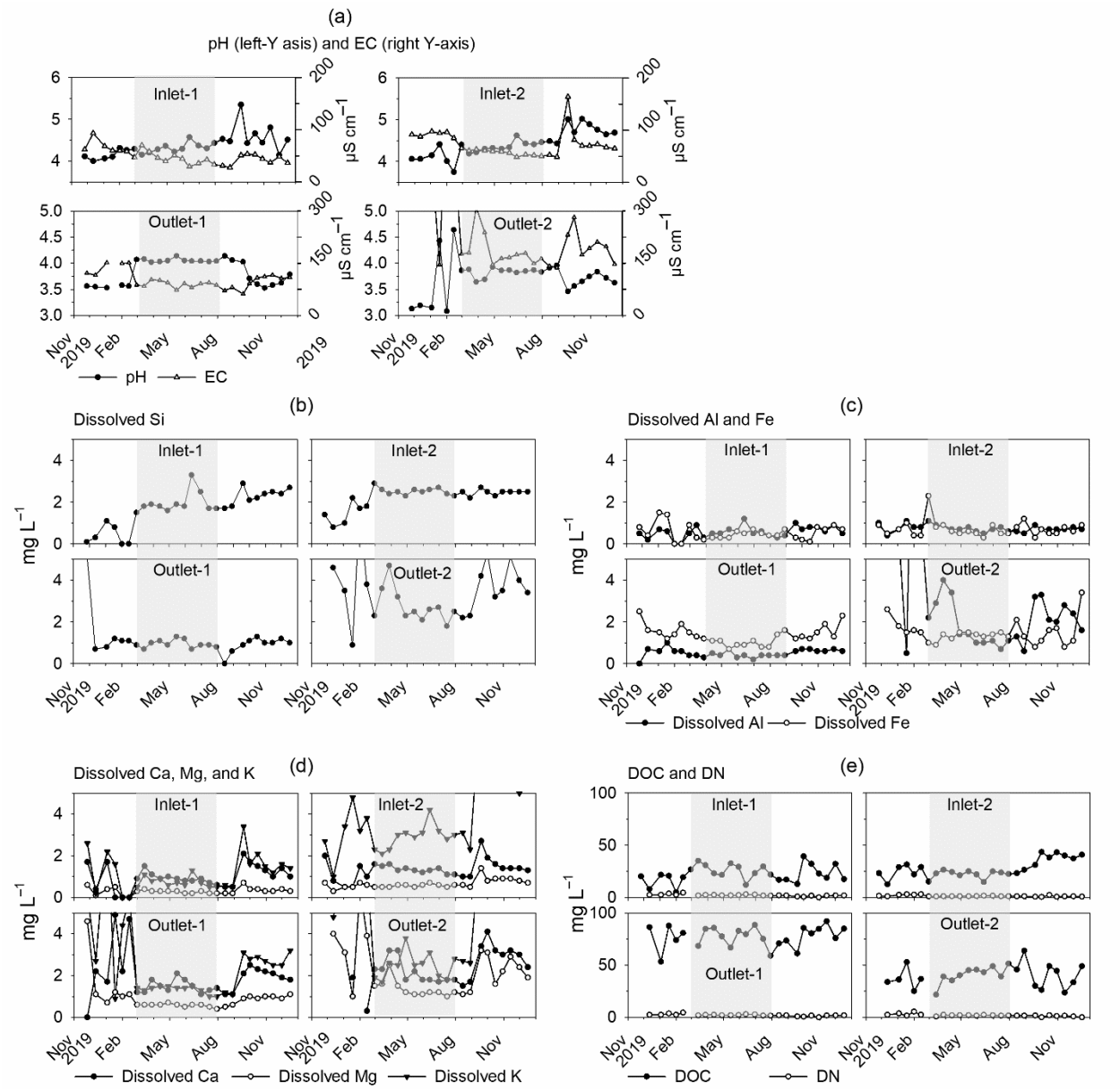

Fig. 3-4 Seasonal change in pH, EC, concentration of dissolved element and OM <0.45 μm in the study area. (a) pH and EC, (b) Si; (c) Al and Fe; (d) Ca, Mg, and K; (e) DOC and DN. Note that the axis and unit value is the same within each group.

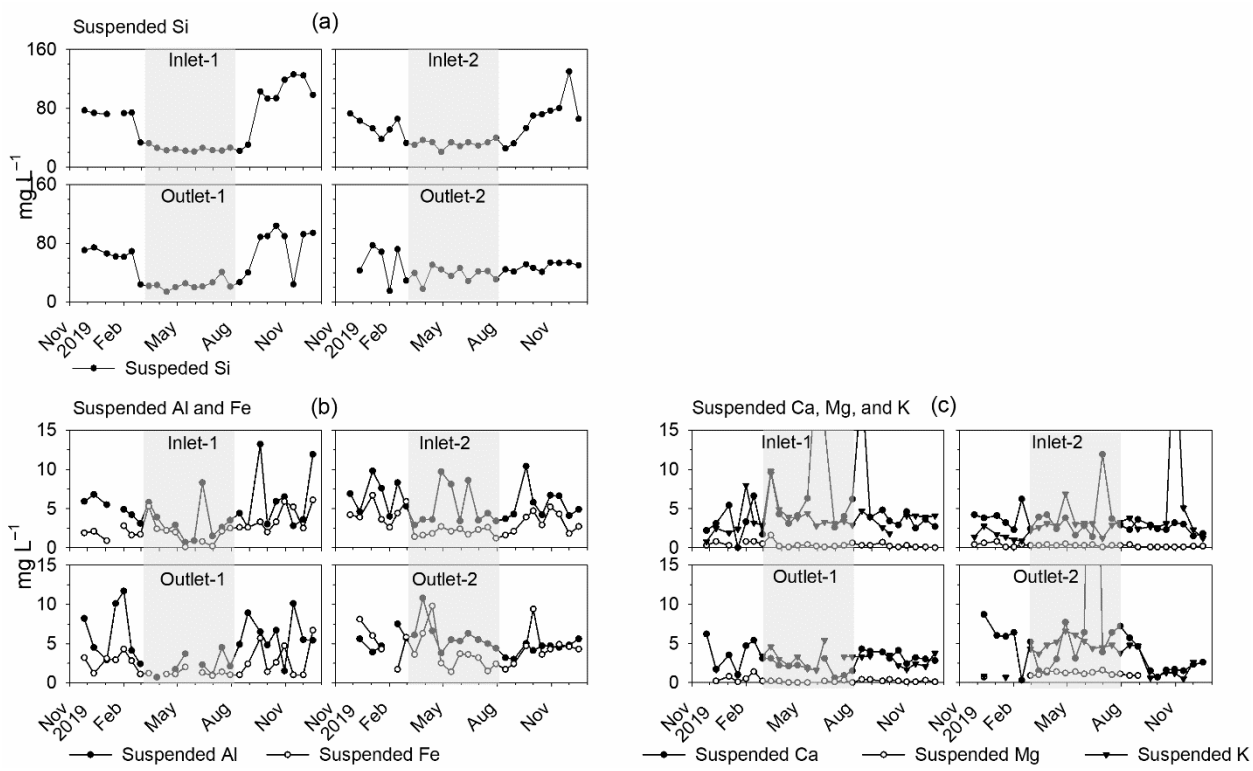

Fig. 3-5 Seasonal change in concentration of suspended form >0.45 μm. (a) Si; (b) Al and Fe; (c) Ca, Mg, and K. Note that the axis and unit value is the same within each group.

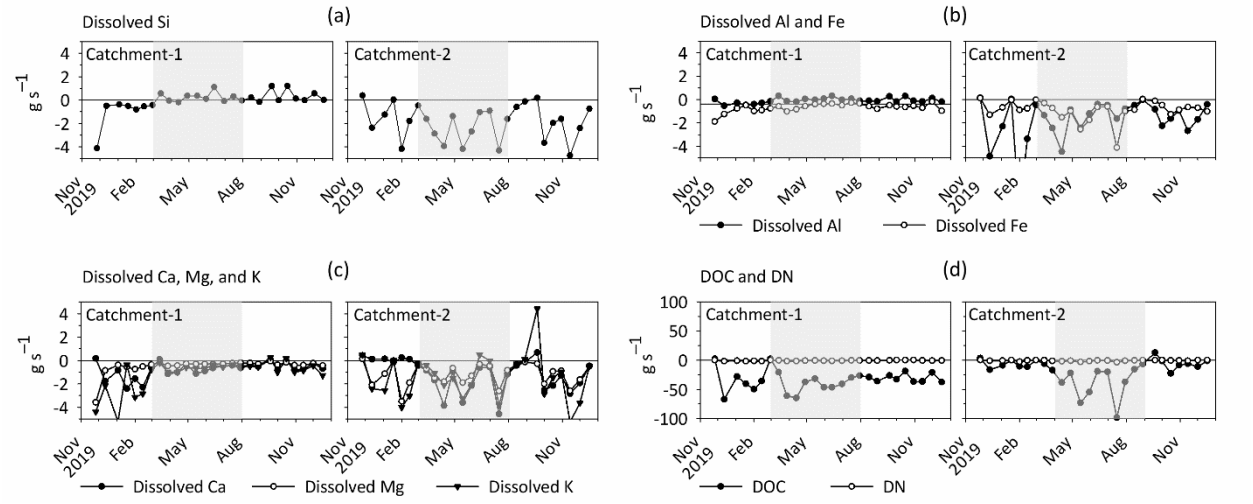

Fig. 3-6 Seasonal change in net flow of elements in dissolved form <0.45 μm: (a) Si; (b) Al and Fe; (c) Ca, Mg, and K; (d) DOC and DN. The horizontal line indicates the zero line.

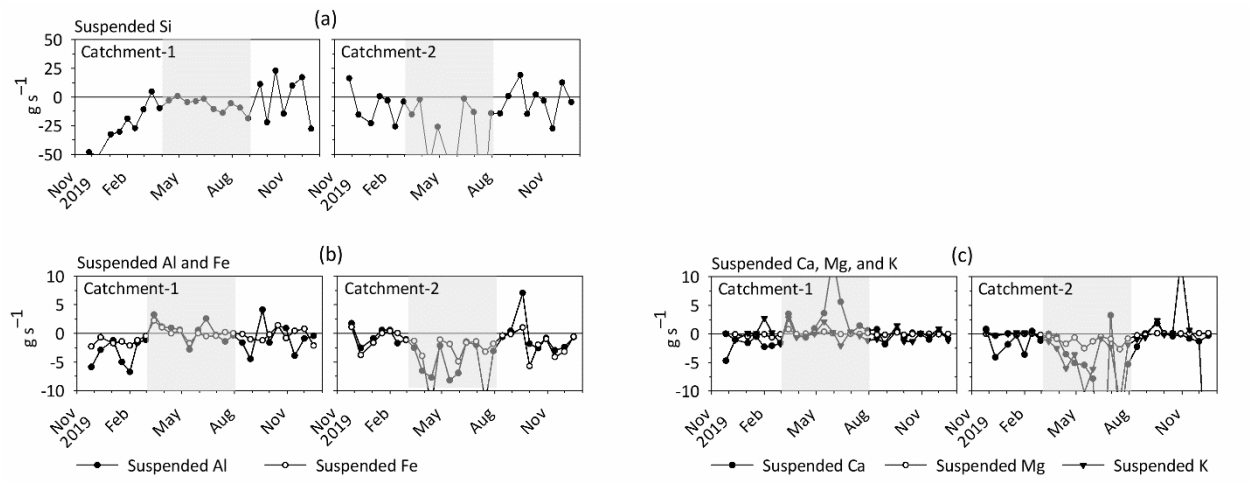

Fig. 3-7 Seasonal change in net flow of elements in suspended form >0.45 μm: (a) Si; (b) Al and Fe; (c) Ca, Mg, and K. The horizontal line indicates zero line.

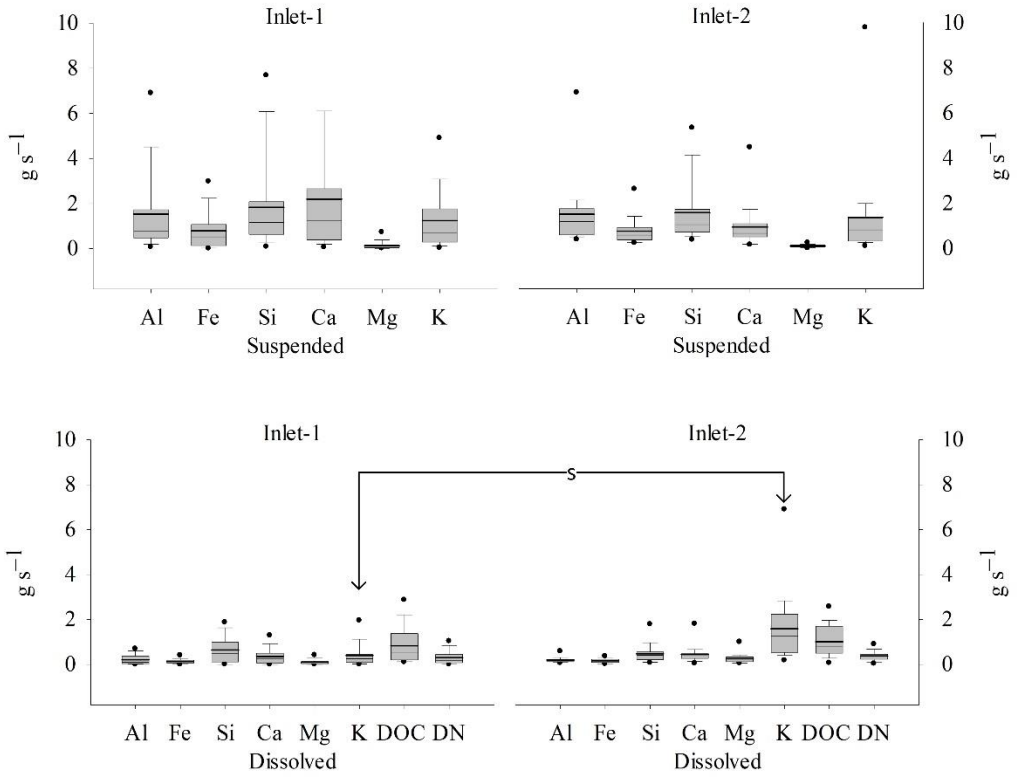

Fig. 3-8 Box-whisker plots showing the interquartile range (grey box), median (thin horizontal line), mean (thick horizontal line), maximum, and minimum observation of suspended mineral elements and DOM flow at inlet-1 and inlet-2. Only the 5th and 95th percentiles are plotted as outliers. Letter "s" indicates significant difference between inlet-1 and inlet-2 (P <0.05) by *u-test*. Note that Si and DOC are 1/10 of the real amount for clarity.

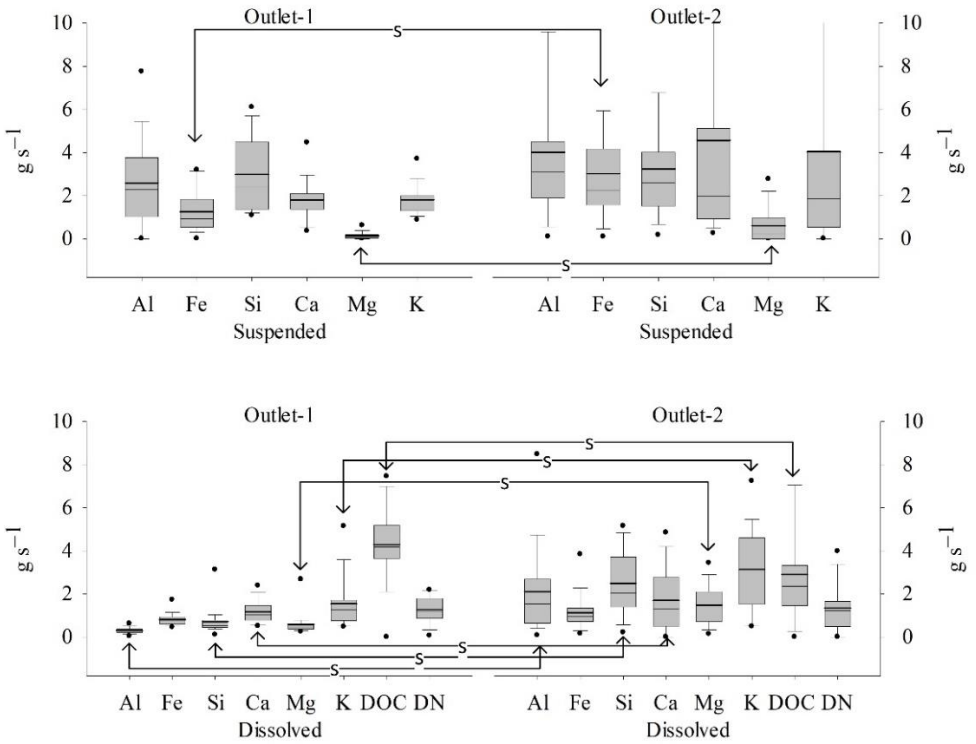

Fig. 3-9 Box-whisker plots showing the interquartile range (grey box), median (thin horizontal line), mean (thick horizontal line), maximum, and minimum observation of mineral elements and DOM flow at outlet-1 and outlet-2. Only the 5th and 95th percentiles are plotted as outliers. Letter "s" indicates significant difference between outlet-1 and outlet-2 (P <0.05) by *u-test*. Note that Si and DOC are 1/10 of the real amount for clarity.

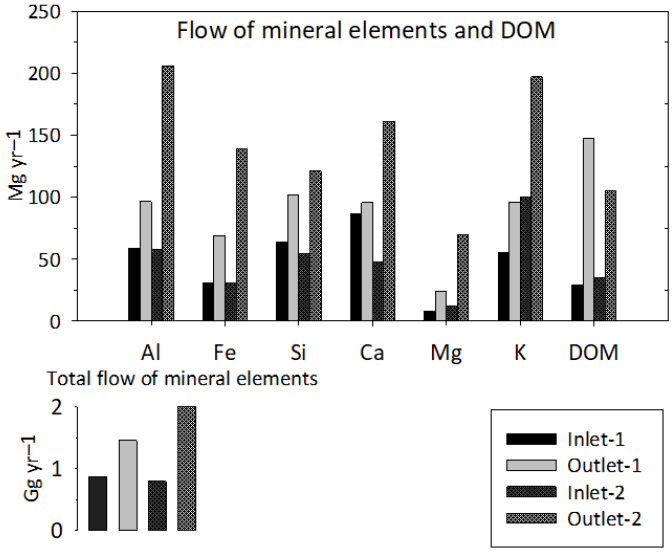

Fig. 3-10 Comparison of total mineral elements and DOM flow between catchment-1 and catchment-2. Box plot in the bottom-left shows totals mineral elements (excluding DOM) outflow from the catchments (at both outlets). Note that Si and DOM are 1/10 of the real amount for clarity.

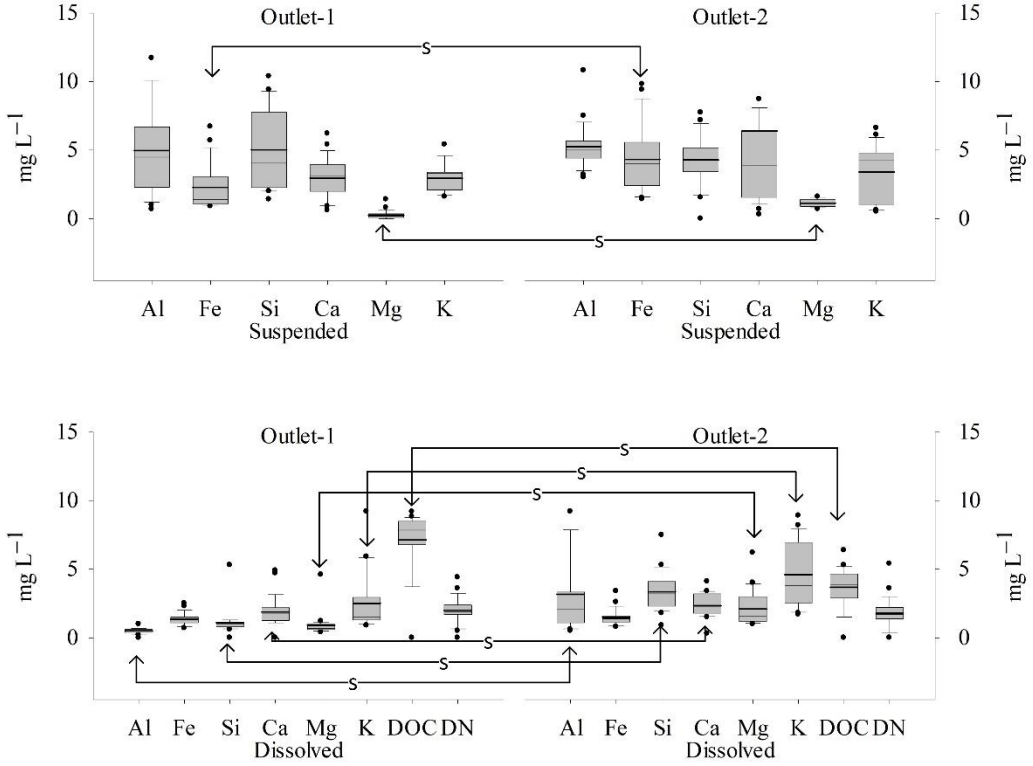

Fig. 3-11 Box-whisker plots showing the interquartile range (grey box), median (horizontal line), average (horizontal thick line) maximum and minimum observation of mineral element and DOM concentration at outlet-1 and outlet-2. Only the 5th and 95th percentiles are plotted as outliers. Letter "s" indicates significance (P <0.05) by *u-test*. Note that Si and DOM are 1/10 of the real amount for clarity.

3.6 Supplementary material of CHAPTER 3

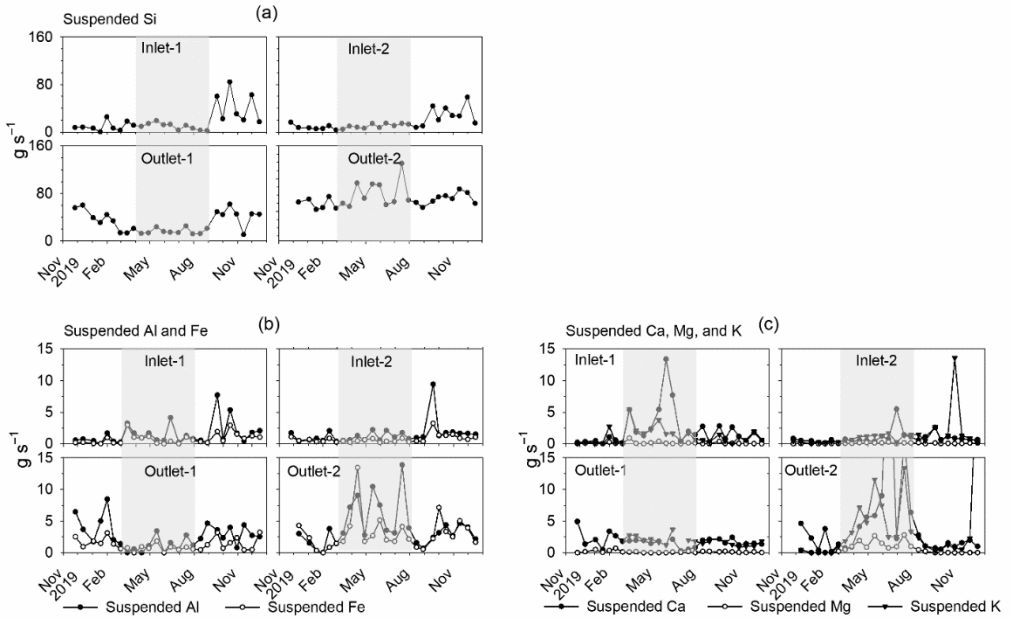

Fig. S 3-1 Seasonal change in chemical flow of suspended form <0.45 μm in the study sites. (s) Si; (b) Al and Fe; (c) Ca, Mg, and K. Note that the axis and unit value is the same within each group.

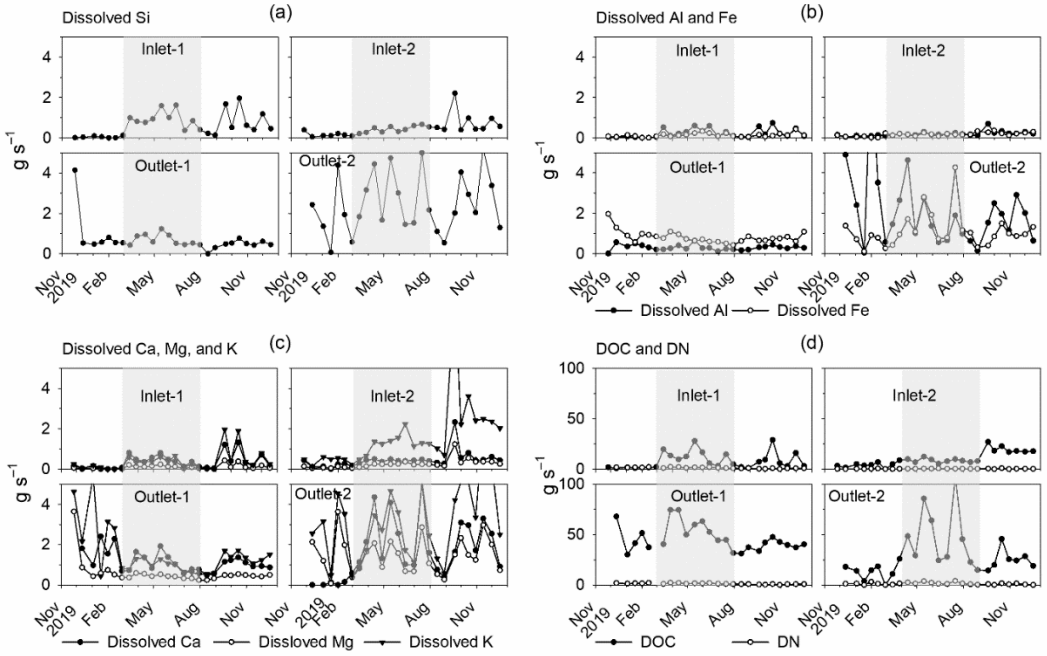

Fig. S 3-2 Seasonal change in chemical flow of dissolved form <0.45 μm in the study sites. (a) Si; (b) Al and Fe; (c) Ca, Mg, and K; (d) DOC and DN. Note that the axis and unit value is the same within each group.

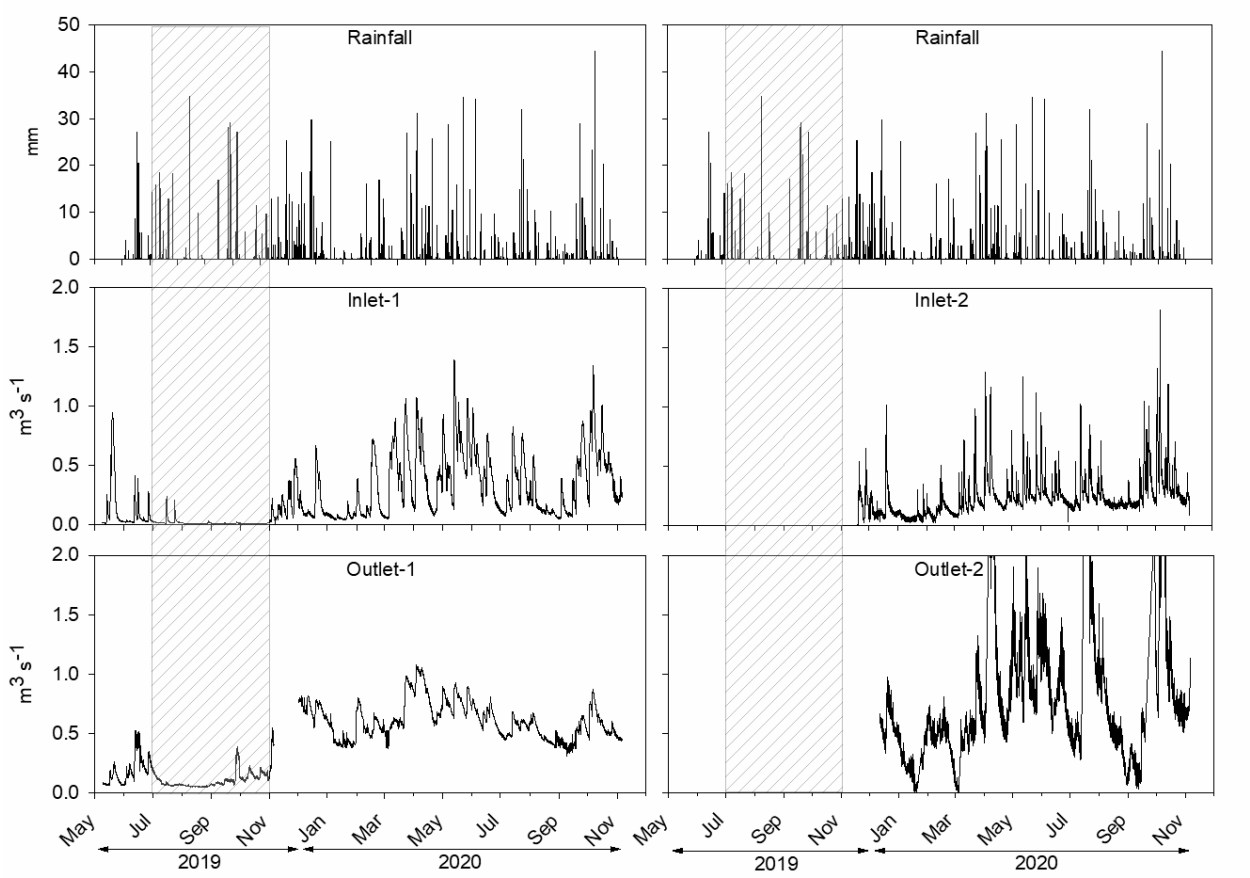

Fig. S 3-3 Rainfall data with 30-minutes interval (top) and water discharges at inlets (from mineral upland; middle) and outlets (from peatland; bottom). The box indicates long dry spell in 2019. Note that discharge data at inlet-2 and outlet-2 were not obtained until January 2020.

CHAPTER 4
MINERAL ELEMENTS LOSS IN MINERAL UPLAND UNDER OIL PALM PLANTATION

4.1 Introduction

Water erosion is one of the most powerful agents driving land to degrade, and its characteristics vary widely with soil and climate conditions throughout the globe. Reviewed from numerous erosion models, a report of longitudinal trend in erosion estimate places the tropical zones with the highest average value (29.1±51.3; $\tilde{x}$ =11.2 Mg ha^{-1} yr^{-1}) followed by sub-tropical zones (29.5±102.2; $\tilde{x}$ =9.1 Mg ha^{-1} yr^{-1}), temperate zones (16.1±33.7; $\tilde{x}$ =4.1 Mg ha^{-1} yr^{-1}), and polar and sub-polar zones (3.0±3.7; $\tilde{x}$ =1.4 Mg ha^{-1} yr^{-1}) (Borrelli et al. 2021). The high erosion in tropical regions is not surprising as human disturbance from the expansion of agricultural land is usually the cause of accelerated water erosion under high rainfall erosivity (Lal 2001; Panagos et al. 2017).

As the economy and population of tropical regions will experience rapid growth by 2050 (Harding et al. 2015), the demand for agricultural development is expected to rise. Therefore, the risk of accelerated erosion will continue. For example, in the tropical area of Indonesia, the oil palm plantation area reached 14 million hectares in 2019, accounting for about 10% of Indonesia's land (BPS 2019). Previous reports show that land conversion to a monoculture reduces permeability (Marten et al. 2016) and accelerates surface runoff (Murtilaksono et al. 2018), soil erosion (Clarke and Walsh et al. 2006; Nainar et al. 2018), and mineral nutrient loss (Maene et al. 1979; Malaysian Oil Palm Board 1994; Chew et al. 1999).

The scale of oil palm plantations ranges from hundreds of hectares to thousands of hectares, which impacts the application of erosion measurement and prediction and mineral nutrient loss. In oil palm plantations, soil erosion and nutrient loss studies generally used plot experiments (Lal 1994; Marten et al. 2016; Murtilaksono et al. 2018; Clarke et al. 2006; Nainar et al. 2018). However, these methods are difficult to apply to large areas such as catchment scales because such measurements are laborious and expensive. Considering these difficulties, soil erosion and nutrient loss can be measured at the outlet of a catchment scale.

A small upland catchment (<10 km^2) (Singh 1994; Singh 2018) is often part of bigger catchment consisting of different ecosystems. For example, in Siak Sumatra, where the current research is underway, the upland oil palm concession grows on tertiary sedimentary rocks

(Kementerian ESDM the Republic of Indonesia 2010) and Ultisols (USDA 2005) while the downstream is peatland. The upland and the peatland are connected by stream networks.

In the uplands of Sumatran Indonesia where highly weather Ultisol is present (USDA 2005), erosion can cause the loss of minerals. However, not all eroded materials can be transported to the outlet because erosion is often transport-limited (Lal 2001). Thus, it is important to quantify the ratio of the amount of eroded material that reach a certain outlet when evaluating the impact to the downstream ecosystem. Some particles are deposited locally (Foster 1982; Rose 1985), some could transport across catchments and deposit distantly toward coastal area depending upon catchment characteristics. Presumably, on-site eroded materials dominated by suspended forms (>0.45 μm) transport locally. Lighter eroded materials in solution (<0.45 μm) such as silt-sized, clay-sized, and inorganic components are believed to be transported longer distance. Lighter materials in solution is also important because it is chemically active and carry substantial elements (Owens et al. 2005). For instance, transportation of Fe and Al is reported in Fe or Al-DOC complexes (Krachler et al. 2015; Yang et al. 2017; Pott et al. 1985). However, report on the transport mechanism of suspended load and dissolved forms at catchment scale under tropical oil palm plantation is poorly understood.

The objective of this research was to clarify the amount of eroded materials containing mineral elements and its controlling factors in various small catchments (upland) with similar geological, soil, climatic conditions, and land management of oil palm plantation. Four small catchments were employed. In addition to that, seasonal change in eroded materials reaching outlet was also observed and correlated with hydrological characteristics of the catchment to determine the possible factor which might control concentration and flow of mineral elements.

4.2 Materials and methods

4.2.1 Study site location

The study sites were four small adjacent catchments, namely upland-1, upland-2a, upland-2b, and upland-2c, which had similar soil, geology, and climatic conditions. The soil type of study area was Ultisol (USDA 2005) with sandy loam texture. The geology was a tertiary sedimentary rock (Kementerian ESDM The Republic of Indonesia 2010). The uplands were situated in the Siak River Watershed in Riau, Indonesia. Each upland had a stream that drained water to peatland located downstream. The climate in this region was a typically humid ecosystem with high precipitation (2082 mm) and high daily temperatures (23–27°C)

throughout the year (Marwanto et al. 2018). The study site generally experienced a bimodal pattern of rainy seasons during October to December and March to May with dry season during July to September. The details of study site characteristics are presented in Fig. 4-1 and Table 4-1

The study site also had similar land management. The entire study sites had been cultivated by oil palm since 2002 into a farming block (300 × 1000 m). The oil palm age ranged from 18 to 20 yr old. Oil palm trunk was planted at an interval of 8 and 4 m (133 trunks ha^{-1}) (Marwanto 2018). Oil palm canopy cover almost the entire land. Soil surfaces under oil palm were also dominated by fern, shrub, and grasses. After the planting time, the soil under oil palm remained unploughed. Oil pam parts such as old fronds were regularly pruned and remained in the sites. However, each farming block was surrounded by a farming road (from 3 m to 5 m in width) constructed using local soil and gravel. There were also harvest (~2 m) and prune paths (~0.5 m) in each block which were regularly used for agronomy activities (Tarigan et al. 2018). Both farming road and path in the farming block were prone to water erosion due to intensive activities.

4.2.2 Determining catchment characteristics

Based on the DEM map (DEMNAS 2018 resolution 8.3 m x 8.3 m), delineating the study site could determine the catchment basic characteristics, such as coverage area, perimeter, and stream network. Further, based on the basic characteristics, catchment shape using criteria of Gravelius compactness coefficient (GC), stream density, and slope distribution were determined. All characteristics are determined using special tools of ArcHydro Arc GIS 10.7.1 (ESRI USA).

The GC is the most used index to define catchment shape (Sassolas-Serrayet et al. 2018). GC defines the circularity of a catchment, the relation between the perimeter of a catchment and that of a circle having a surface equal to that of a catchment.

$$\text{Gravelious}' \text{ s Coefficient (GC)} = \frac{P}{2\sqrt{\pi A}}$$

where P is the perimeter of the catchment and A is the catchment area.

Drainage density was first introduced by Horton (1945) and used extensively in many hydrological studies. Briefly, network density is a ratio between the total length of the stream and the area, defined as:

$$Drainage, density, Dd = \frac{\sum L}{A}$$

where L is the length of the main stream, and A is the area of the catchment. In this study, network density was used to suggest an accessible area in a catchment that could be the source of mineral element transportation.

Theoretically, GC and stream density estimate coverage area accessible to drive eroded materials throughout the catchment. The lower GC and the denser stream, the larger accessible eroded materials to be transported from a catchment. In addition to that, I categorized slope class following FAO (http://www.fao.org/soils-portal/data-hub/soil-maps-and-databases/harmonized-world-soil-database-v12/terrain-data/en/), that is, 0–2%, 2–5%, 5–8%, 8–16%, 16–30%, 30–45% and > 45%, then I calculated the proportional area of each class with the total area of each catchment.

4.2.3 Monitoring on hydrology and hydrochemistry

Monitoring on water discharge and water sampling was undertaken to quantify mineral element loss. Monitoring stations were set in each catchment's canal or natural stream to precisely measure discharge (water flow, m s^{-1}). A rainfall gauge (Vantage Pro 2, Davis, California, USA) was also set to record rainfall data every 30 minutes. Monitoring station at the outlet of mineral upland-1, 2a, 2b, and 2c were existing flume or weir, or simply constructed in the site where an absolute pressure type water level data logger (HOBO U21-001-04, ONSET, Massachusetts, USA) was installed (Fig. 2-1). Thus, canal or stream water level is being recorded continuously every 30 minutes. Along with flow rate measurement periodically using a current water meter (UC-300, Tamaya Inc., Tokyo, Japan), discharge rating curves were calculated to generate water flow at a 30 minutes basis (Table 4-2). Continuous water flow is a prerequisite to generate sediment yield of the catchments. A hydrograph was also performed to determine the hydrological response of each catchment.

4.2.4 Quantifying eroded materials

Multiple samples were collected in 50 ml of plastic bottles from about 20 cm below water surface two weekly for a complete dry–rainy season (November 26, 2019 to December 12, 2020). Two bottles of the 50 ml samples were preserved at 4 degrees Celsius before transporting to Japan for further laboratory analyses. One unfiltered sample was used to determine total Si, Fe, Al, Ca, Mg, and K by an inductively coupled plasma atomic emission

spectrometer (ICPE-9000, Shimadzu, Kyoto, Japan) after wet acid digestion (HF and $HClO_4$) (Hossner 1996). One filtered sample (through 0.45 μm syringe [Sartorius Inc.]) was used to determine exchangeable of Ca, Mg, K using flame emission spectroscopy (AAS AA-700, Shimadzu, Kyoto, Japan). Another one was used to determine pH and EC (Metler Toledo, Giessen, Germany) at the closest laboratory in the field. The concentration of each element was then multiplied by corresponding water discharge to determine their flow rate at each catchment. The annual flow of each element (g yr^{-1}) at the inlets and outlets of both sites was calculated by multiplying the annual flow-weighted concentration (g m^{-3}) by annual water discharge (m^3 yr^{-1}), modified from the equation by Cook et al. (2018).

4.2.5 Statistical analyses and comparison between measured erosion and estimated erosion.

Statistical analyses were done to compare the concentrations, flow rates, correlation between measure elements while comparison between measured and estimated erosion was done to clarify the ratio between potential erosion and transported eroded materials. The significant differences in chemical concentrations and flow between uplands were tested using ANOVA based on either P <0.01 and P <0.05. Spearman rank correlations were applied to investigate relationships between measured elements, DOC, pH and EC after testing for normality found that data were not normally distributed. Significance is based on P <0.01 and P <0.05. Both one-way ANOVA and Spearman test were done using Sigma Plot 11.0 software (Systat Software, California, USA). The total annual flow of each mineral was converted to oxide forms for comparison with estimated erosion using RUSLE Model. The RUSLE model was employed with assumptions that similar climatic, geology, soil, and land management input the same R, K, C, and P but LS factor. The model is explained elsewhere (Wikantika 2018; Susanti, Syafrudin, and Helmi 2019; Renard et al. 1997; Belayneh, Yirgu, and Tsegaye 2019) and the brief model running in this study is presented in the supplementary materials. The summation of mineral loss was assumed to be the total erosion reaching the outlets.

4.3 Results

4.3.1 Catchment and water discharge characteristics

Fig. 4-1 shows that bigger catchment upland-1 and upland-2b tended to be an elongated catchment. The shape of the catchment determined major stream length in which upland-1 had the most extended major stream. Upland-2c had higher drainage density and lower GC, followed by upland-2a, upland-2b, and upland-1 (Fig. 4-1 and Table 4-3). However, upland-

2b had more than 70% area with slope class > 16% (Fig slope). The second-largest area with such slope class was upland-1 (57%). Based on slope distribution, upland-2a was relatively flat as the area was dominated by slope <16%.

Fig. 4-2 shows a 30-minute rainfall event and water discharge response in the uplands. Rainfall events were distributed throughout monitoring period except for two dry spells around February 2020 and August 2020. Water discharge increased at all sites following high rainfall and decreased during the dry spells (Fig. 4-2c, 4-2d, 4-2e, and 4-2f). High water discharge was evident during the intense rainfall between March and August 2020. The upland-2c was the most responsive catchment indicated from the shortest peak time, reaching the peak after 29 hours of the rainfall event (peaking time: 3 hours), followed by upland-2b after 32 hours (peaking time: 5 hours), upland-2a after 34 hours after rainfall event (peaking time: 6 hours), and upland-1 after 39 hours after rainfall event (peaking time: 12 hours). The cumulative rainfall was 2082 mm, while cumulative water discharge of upland-1, 2a, 2b, and 2c were 1023, 1745, 387, 566 mm, respectively. Water discharges responses generally half of the total rainfall except for upland-2b, and upland-2c which had about one-fifth and one-fourth of total rainfall.

4.3.2 Seasonal variation and chemical properties

Based on the general rainfall pattern above, there were three seasonal changes in chemical properties: November 2019 to February 2020, March to August 2020, and September to November 2020. Each term describes pH, EC, mineral element, and DOC concentration and flow following the dry spells.

4.3.3 pH, EC, and mineral element and DOM concentration

Generally, pH increased while EC decreased for the period of monitoring in all uplands. The highest pH was found from September to November 2020. The pH ranged from 4.0 to 4.7, 3.5–4.5, 4.0–5.0, and 4.0–4.5, in upland-1, 2a, 2b, and 2c, respectively (Fig. 4-3a). The EC ranged from 100–20 µS cm^{-1}, 160–60 µS cm^{-1}, 80–20 µS cm^{-1}, and 100–25 µS cm^{-1}, respectively. A dramatic change in pH was found in upland-2a, 2b, and 2c between February and March 2020. At the same time, a dramatic drop of EC was evident only in upland-2a (Fig. 4-3a).

Seasonal changes in concentration of each mineral element were similar among the uplands in dissolved (Fig. 4-3) and suspended form (Fig. 4-4). The concentration of dissolved Si tended to increase throughout the study period (Fig. 4-3). Whereas the concentration of

suspended Si tended to be high from November 2019 to February 2020 and September 2020 to November 2020 but tended to be low between March 2020 and August 2020 (Fig. 4-4a). The concentration of Si in both forms was relatively higher than Al and Fe (Fig. 4-3b, 4-3c, Fig. 4-4a and 4-4b). The concentration of suspended Al, Fe, Ca, and K in both forms tended to fluctuate across the study period (Fig. 4-3c, 4-3d, Fig. 4-4b and 4-4c). The concentration of suspended and dissolved Mg was observed very low across the period of monitoring (Fig. 4-3d and Fig. 4-4c). The concentration of DOC fluctuated during the period of monitoring while the concentration of DN was low (Fig. 4-3e).

4.3.3.3 Seasonal change in flow

All upland had a similar pattern of the temporal flow of mineral element in dissolved (Fig. 4-5) and suspended form (Fig. 4-6) with a different degree. The high flow was evident for all mineral element except Mg. The high flow was particularly during intense rainfall of two terms: March to August 2020 and September to November 2020 regardless their concentrations. The high flow of both dissolved and suspended Ca and K were between March and August 2020 in upland-1 and 2a. Mg transportation was considered low (Fig. 4-5d) throughout the monitoring period. The flow of DOC was also high owing to their high rate of water discharges in upland-1 and upland-2b but not DN (Fig. 4-5d). The high flow of these mineral elements was evident in upland-1 and upland-2a but relatively low in upland-2b and upland-2c owing to their low water discharge. For instance, suspended Si, Al, and Fe were generally high after September 2020 in all uplands (Fig. 4-6a and 4-6b). The flow of suspended Si was considerably higher ten times than Al, Fe, Ca, Mg, and K (Fig. 4-6).

4.3.4 Comparison of concentrations and flows of suspended and dissolved materials in different upland areas

Fig. 4-7 and Fig. 4-8 show mean comparison of one-way ANOVA of mineral elements concentration and DOM between the uplands. pH, EC, all dissolved mineral elements, DOC, DN were significantly different between the uplands (Fig. 4-7). In comparison, the significant differences were found only for Ca and Mg in suspended forms (Fig. 4-8). Among the uplands, upland-2c had a higher concentration of Al and Fe than other uplands, particularly in dissolved forms (Fig. 4-7).

Fig. 4-9 and Fig. 4-10 show the flow of mineral elements and DOM between the uplands in both dissolved and suspended forms. Water discharge rate were significantly different between the uplands in which high water discharge were found in upland-1 (0.33±0.25

m^3 s^{-1}) and upland-2a (0.18±0.07 m^3 s^{-1}) (Fig. 4-9). Consequently, flow of all measured elements was also significantly different the uplands both suspended and dissolved forms. Higher flow of measured element was found in upland-1 and upland-2a (Fig. 4-9 and Fig. 4-10).

4.3.5 Correlation between measured elements

Fig. 4-11 and Table 4-4 show selected correlation and relationship between concentration of DOC and mineral elements. Dissolved Al were strongly correlated with DOC in all uplands. For instance, in upland-2a where DOC concentration was high (Fig. 4-7), correlation between Al and DOC was very strong (rs = –0.62; P <0.01). Except in upland-2a and upland-2b, correlation between dissolved Mg and DOC was also strong. For instance, in upland-1, correlation between mg and DOC was (rs = –0.39; P <0.05). Strong correlation between Ca and DOC was found only in upland-1 (rs = –0.39; P <0.05). Although it was not as strong as others, dissolved Fe had also correlation with DOC.

4.4 Discussion

4.4.1 Effect of landform on water discharge

Landform affected erosion and water discharge distribution in the studied uplands with similar geology, soil, climatic conditions, and land management characteristics. The fastest water discharge response to the rainfall events (Fig. 4-2) was evident upland-2c which was attributed to a steep, small and circular-shaped catchment. Also, because of the smaller size, such as upland-2c had a denser stream network (Table 4-3). Such faster discharge was less evident in upland-1 and upland-2b, probably owning to elongated shape (upland-2b) and gentle slope of upland-2a. The results reveal that slope, size, and circular shape contributed to faster water discharge by by the short distance of stream across the upland to the corresponding outlet. Water discharge response is essential to identify possible sedimentation areas downward as sediment deposition occurs when the velocity is low (Lal 2001). This finding also confirms Musy (2001) that reported that circular catchment tends to have a faster water discharge response compared to the elongated catchment.

Theoretically, the size of a catchment defines the amount of water discharge. Such finding was evident in upland-1 which had the highest water discharge. However, water discharge in upland-2b was probably underestimated while upland-2a was overestimated. Assuming that evapotranspiration under mature oil palm with ground covers is about half of the rainfall (Manoli et al. 2018), discharge in upland-2b was less than 20%, while upland-2a

was more than 80% (Table 4-3). According to discharge monitoring and visual ground check, upland-2b experienced intermittent discharge, particularly in the absence of rainfall events. In contrast, upland-2a experienced a perennial stream even though during the two dry spells. I suggested that the loss of water in upland-2a partially contributed to the excess water in upland-2a via groundwater leakage. This finding confirms Liu et al. (2020), reporting that water discharged derived by topographical delineating differed from measured water because of inter-catchment groundwater flow. Underling tertiary sedimentary rock in our study site might cause groundwater leakage as interlaying permeable-impermeable rock layer could percolate groundwater to adjacent upland (Kreitler 1989).

4.4.2 Seasonal variation of mineral element loss

The results suggested that water discharge regulated the concentration and flow of mineral elements. The high concentration of mineral elements between November 2019 to February 2020 and between September to November 2020 was attributed to the relatively low water discharge (Fig. 4-3, Fig. 4-4, and Fig 4-2). In contrast, the low concentration of those elements during March and August 2020 was attributed to the diluting process due to high water discharge (Fig. 4-3, Fig. 4-4, and Fig. 4-2). Thus, the concentration of mineral elements such as during the third term could enhance pH from September to November 2020. During that term, high pH was coincident with a high concentration of dissolved Ca and K (Fig. 4-3a and Fig. 4-4d).

In contrast, the flow of mineral elements was regulated by water discharge regardless of the concentration of the element. The high flow of mineral elements was evident during March and August 2020, even though their concentration was relatively lower than in September to November 2020 (Fig. 4-5 and Fig. 4-6). Between the uplands, catchment with high water discharge drained higher total mineral elements (Fig. 4-9 and Fig. 4-10) regardless of their concentrations. Such finding was evident in upland-1 and upland-2a. Those two uplands had a perennial stream indicated by continuous water discharge. In contrast, upland-2b and upland-2c had lower mineral element flow due to intermittent water discharge.

4.4.3 Possible mechanism of mineral transportation and mineral species

The amount of DOC could be substantial as driving force of mineral element transportations. The strong correlation between dissolved Al, Ca, and Mg with DOC indicated that transportation of such mineral element was in mineral-DOC complexes. For instance, high DOC concentration in upland-2a (35.1±10.5 mg L^{-1}) was followed with high dissolved Al

(0.8±0.2 mg L^{-1}) (Fig. 4-7). The strong correlation of Al and DOC in all upland indicated that podsolization might undergo under condition of pH 4–5 (Fig. 4-11, Fig. 4-3 and (Table 4-4) confirming the mechanism of Al-OM bindings previously reported by Pott et al. (1985). The transportation Al-DOC complex in the current study also confirms previous study in humid Ultisol by (Fujii et al. 2009). The above ground biomass was abundant as pruning returns oil palm parts to the soil. Thus, under high rainfall condition, runoff drives considerable amount of Al-DOC complex toward downstream.

Although further analysis is needed to determine the mineral species drained from each upland, based on molar ration of Si:Al, possible mineral species could be revealed. In suspended form, predominant Si was evident (Fig. 4-8). Ratio Si to Al was more than 10:1 indicating that possible primary mineral in all uplands was dominated by quartz. In comparison, the ratio of Si:Al in dissolved form was lower, about 2:1, 1:1, 6:1 and 2:1, in upland-1, upland-2a, upland-2b, upland-2c, respectively (Fig. 4-7). For example, it is suggested upland-1 and upland 2-c drained 2:1 minerals (i.e. vermiculite, montmorillonite, or mica), upland-2a drained 1:1 minerals (kaolinite), while upland-2b drained quartz or feldspar (Si:Al>2:1).

4.4.4 Comparison of erosion and mineral element loss with previous studies

Excluding upland 2b that had high mineral loss owing to excess water discharge, measured erosion (0.54–1.98 Mg ha^{-1} yr^{-1}) was lower than the estimated by RUSLE (2.33–5.04 Mg ha^{-1} yr^{-1}) (Table 4-3). The lower measured erosion implies that an amount of mineral elements deposited within upland that did not reach the outlets. This difference confirms previous reports that the displacement of eroded particles might range greatly from a few millimeters to thousands of kilometers (Lal 2001; Foster 1982; Rose 1985).

The finding contributed to the reports on mineral nutrient loss as eroded materials at catchment scale that is absent in tropical oil palm plantations. The result revealed that eroded materials ranged 0.54–4.91 Mg ha^{-1} yr^{-1} (on average of 2.3±1.8 Mg ha^{-1} yr^{-1}) (Table 4-3), lower than general erosion in tropics (29.1±51.3; $\tilde{x}$ =11.2 Mg ha^{-1} yr^{-1}) by Borrelli et al. (2021), general erosion in Indonesia (35–220 Mg ha^{-1} yr^{-1}) by Sumiahadi and Acar (2019) but still higher than cropland covered by grassland (0.7±1.6 Mg ha^{-1} yr^{-1}) reported by Labrière et al. (2015).

Considering that oil palm plantation covers vast area 14 million ha in Indonesia (BPS 2019), the result verified the importance of mineral loss under late stage of oil palm plantation

that might have implication to the downstream ecosystem. Of the total eroded materials (2.3±1.8 Mg ha^{-1} yr^{-1}) (Table 4-3), the average loss of K and Mg in upland-2c were 20.9±20.6 and 2.7±2.6 kg ha^{-1} yr^{-1}. The loss in the current study area were slightly lower compared to the loss of K (38.6 kg ha^{-1} yr^{-1}) and Mg (3.1 kg ha^{-1} yr^{-1}) reported by Vijiandran et al. (2017) under mature oil palms using an erosion plot.

4.4.5 Conclusion

Our result verified the erosion at catchment scale that is absent under oil palm plantation in Indonesia that might have implication to the downstream ecosystem. Under late stage of oil palm, the mineral upland with similar geology, climate, and soil type still experienced though it was lower compared to general erosion in tropics and Indonesia reported by models. The loss of mineral elements such as K and Mg were also lower compared to plot measurement under oil palm. The amount of measured erosion based on eroded materials reaching outlets was lower compared to the estimated erosion by RUSLE model, indicating sediment deposition might occur within uplands. The result suggest that actual measured erosion is substantial when considering mineral loss at catchment scale in regard to the implication to downstream ecosystem.

4.5 List of Tables and Figures

Table 4-1 Basic information of the study area.

(Sub) catchment name	Upland-1	Upland-2a	Upland-2b	Upland-2c
Soil classification	Ultisol†	Ultisol†	Ultisol†	Ultisol†
Geology	Tertiary sedimentary rock‡	Tertiary sedimentary rock‡	Tertiary sedimentary rock‡	Tertiary sedimentary rock‡
Land use	Oil palm (open in 2002)	Oil palm (open in 2002)	Oil palm (open in 2002)	Oil palm (open in 2002)
Catchment characteristics				
Area, *A* (ha)	1030	301	437	86
Perimeter, *P* (km)	31.0	9.1	12.8	3.9
Total length of stream, *L* (km)	18.0	8.8	11.1	3.6
Main stream length, L_m (km)	2.7	1.5	1.7	1.2
Elevation (m.asl)	10–59	5–39	4–59	8–47
Relief	Undulating	Undulating	Undulating	Undulating

Table 4-2 Rating curve equation of each monitoring point. Q: water discharge (m s^{-1}); h: water level (m).

Upland-1	$Q = e^{(5.5h - 5.9)}$	$0 < h < 0.86$	$R^2 = 0.9011$
	$Q = 0.9h - 0.41$	$0.87 < h < 1.50$	$R^2 = 0.9489$
Upland 2a	$Q = 0.882h - 0.017$	$0 < h < 0.46$	$R^2 = 0.9303$
Upland 2b	$Q = e^{(9.6h - 7.01)}$	$0 < h < 0.46$	$R^2 = 0.8474$
	$Q = 6.8h - 0.18$	$0.47 < h < 1.18$	$R^2 = 0.8890$
Upland 2c	$Q = e^{(25h - 6.5)}$	$0 < h < 0.11$	$R^2 = 0.9888$
	$Q = 0.35h - 0.01$	$0.12 < h < 0.34$	$R^2 = 0.9669$

Table 4-3 Measured catchment characteristics and comparison between measured erosion and estimated erosion by RUSLE. †: mineral element loss in oxide forms. ‡: estimated by RUSLE. Values in parentheses in mineral loss and erosion represent mean±standard deviation.

Catchment	Upland-1		Upland-2a		Upland-2b		Upland-2c	
Catchment characteristics								
Gravelius coefficients (GC)	2.7		1.5		1.7		1.2	
Stream density (km km^{-2})	1.7		2.9		2.4		4.0	
Slope distribution (FAO)	Area per catchment (%)							
I (0–2%)	7		19		3		17	
II (2–5%)	13		23		8		32	
III (5–8%)	23		34		13		21	
IV (8–16%)	40		22		35		16	
V (16–30%)	16		2		38		11	
VI (30–45%)	<1		0		3		2	
VII (>45%)	<1		0		0		0	
Rainfall and water discharge (mm)								
Annual rainfall	2082		2082		2082		2082	
Annual water discharge	1012		1745		387		566	
Mineral element loss	(kg ha^{-1} yr^{-1})	(Mg yr^{-1})	(kg ha^{-1} yr^{-1})	(Mg yr^{-1})	(kg ha^{-1} yr^{-1})	(Mg yr^{-1})	(kg ha^{-1} yr^{-1})	(kg yr^{-1})
Al (15.6±13.6 kg ha^{-1} yr^{-1})	57.1	58.8	135.5	40.8	24.4	10.7	65.1	5.6
Fe (12.8±6.9 kg ha^{-1} yr^{-1})	29.5	30.4	70.4	21.2	13.7	6	40.7	3.5
Si (159.7±144 kg ha^{-1} yr^{-1})	618.8	637.4	1243.5	374.3	287.9	126.1	539.5	46.4
Ca (18.1±20.5 kg ha^{-1} yr^{-1})	83.9	86.4	120.3	36.2	19.6	8.6	37.2	3.2
Mg (2.7±2.6 kg ha^{-1} yr^{-1})	7.7	7.9	34.2	10.3	2.7	1.2	5.8	0.5
K (20.9±20.8 kg ha^{-1} yr^{-1})	53.9	55.5	283.7	85.4	22.4	9.8	53.5	4.6
Erosion	(Mg ha^{-1} yr^{-1})	(Mg yr^{-1})	(Mg ha^{-1} yr^{-1})	(Mg yr^{-1})	(Mg ha^{-1} yr^{-1})	(Mg yr^{-1})	(Mg ha^{-1} yr^{-1})	(Mg yr^{-1})
Measured (2.3±1.8 Mg ha^{-1} yr^{-1})†	1.92	1979	4.91	1478	0.54	235	1.88	162
Estimated (3.2±.2.1 Mg ha^{-1} yr^{-1})‡	2.32	2404	0.78	235	4.68	2047	5.04	432

Table 4-4 Correlations between measured elements in dissolved forms, pH, and EC; n = 26; ** significant at P <0.01; * significant at P <0.05.

Dissolved Elements	Upland-1			Upland-2a			Upland-2b			Upland-2c		
	DOC	pH	EC	DOC	pH	EC	DOC	pH	EC	DOC	pH	EC
Al	0.39*	0.18	0.02	0.62**	-0.16	0.48*	0.42*	-0.08	0.26	0.40*	-0.46*	0.42*
Fe	-0.07	-0.20	-0.17	0.26	0.06	-0.15	0.15	0.08	-0.28	0.37	-0.37	-0.07
Ca	0.43*	0.08	0.23	0.07	0.30	0.35	0.33	-0.02	0.40	0.24	-0.07	0.29
Mg	0.39*	-0.11	0.36	-0.31	0.79**	0.03	0.23	0.13	0.47*	0.42*	-0.39	0.79**

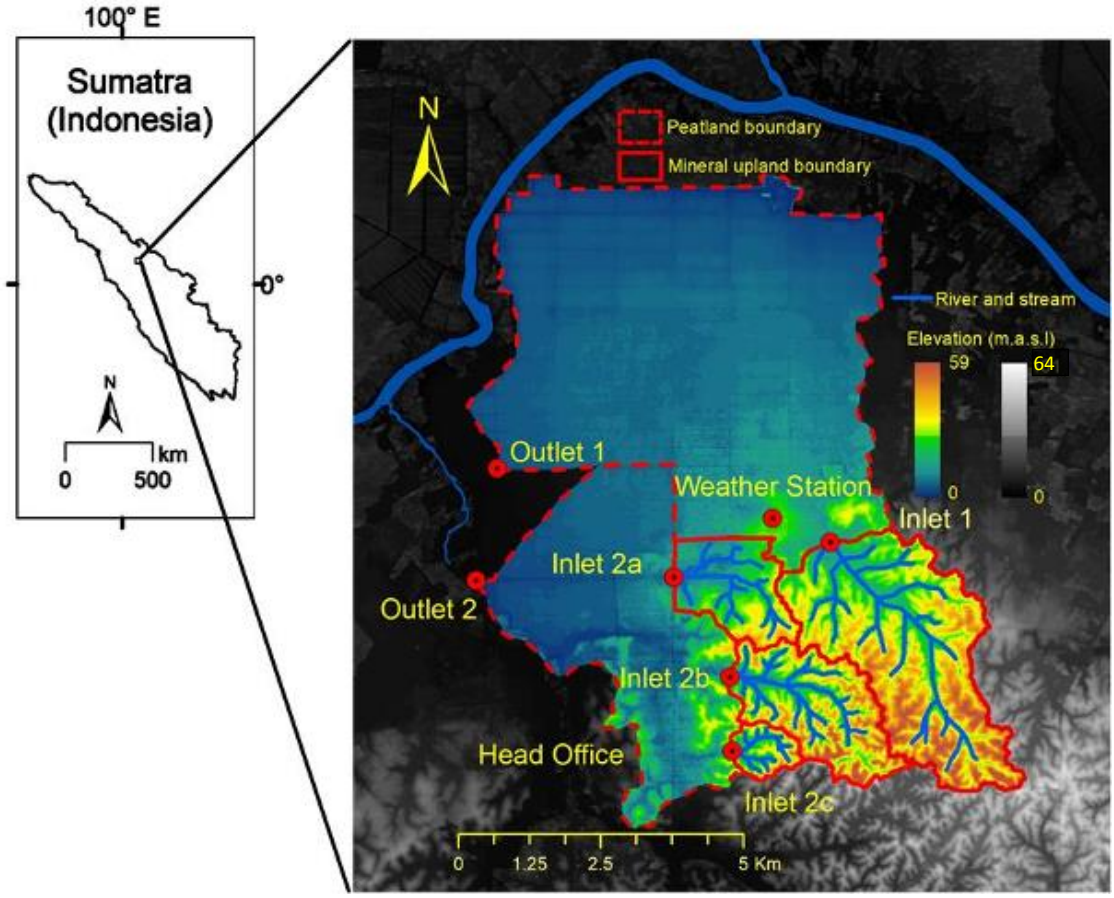

Fig. 4-1 Study site characteristics. The study site is located between mineral terrain and Siak River (thick blue line elongating from west to east). Dashed-red line indicating the hydrological border between peatland and surrounding area. Redline indicates hydrological border between mineral upland catchment and surrounding area. Peatlands are located at lower elevations indicated by green to blue color. A small stream (thin-blue line) runs from mineral upland to the peatland. Fade-thick rectangular line in the peatland indicating canal system. The background map of the study location is derived from a digital elevation model (DEMNAS, http://tides.big.go.id/DEMNAS/), resolution 8.3 m × 8.3 m and vertical accuracy of 3.7 m.

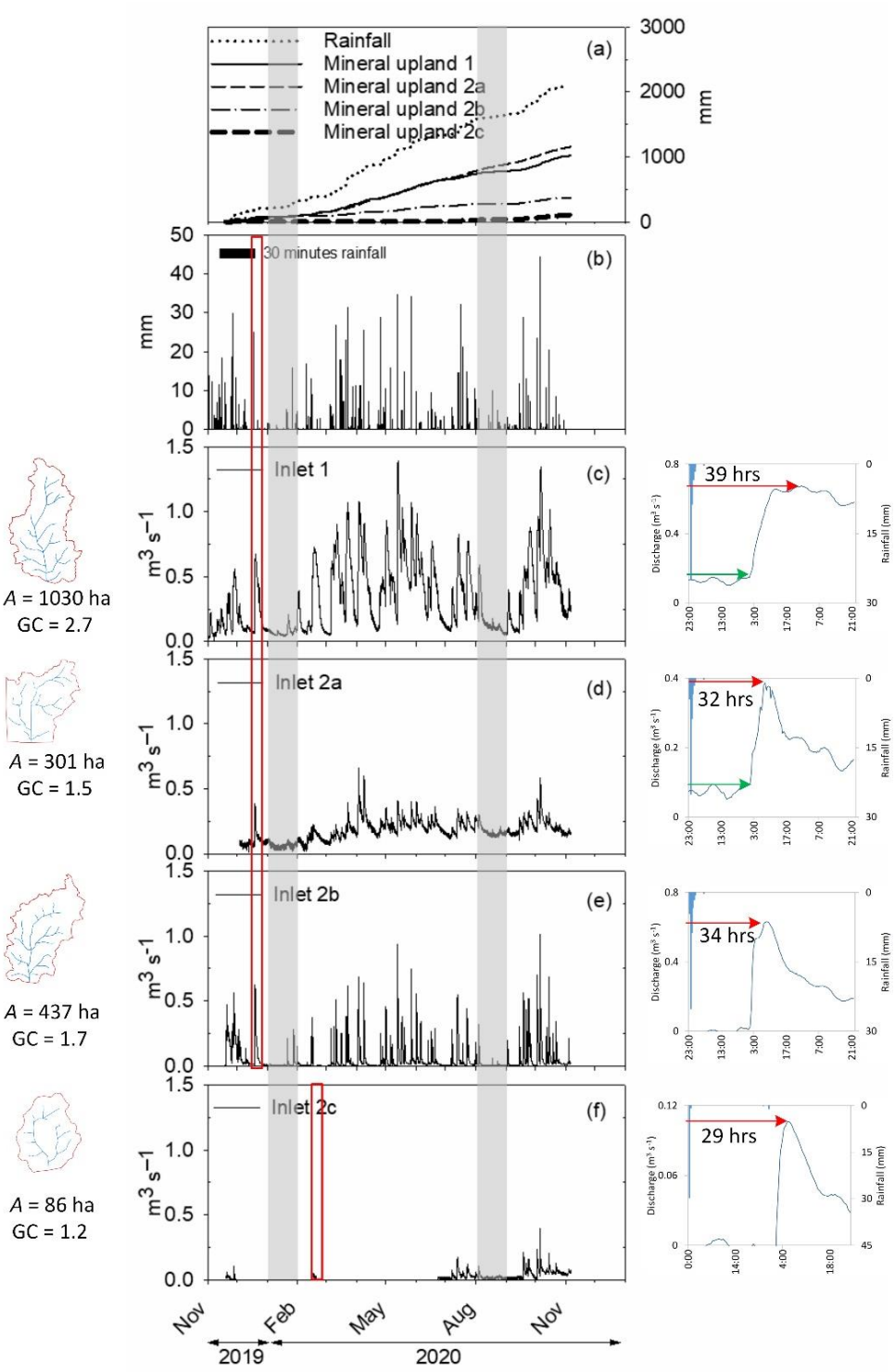

Fig. 4-2 Catchment characteristics (left), rainfall and water discharge characteristics, and particular water discharge response of the studied uplands. The red box represents selected water discharge response and corresponding rainfall events.

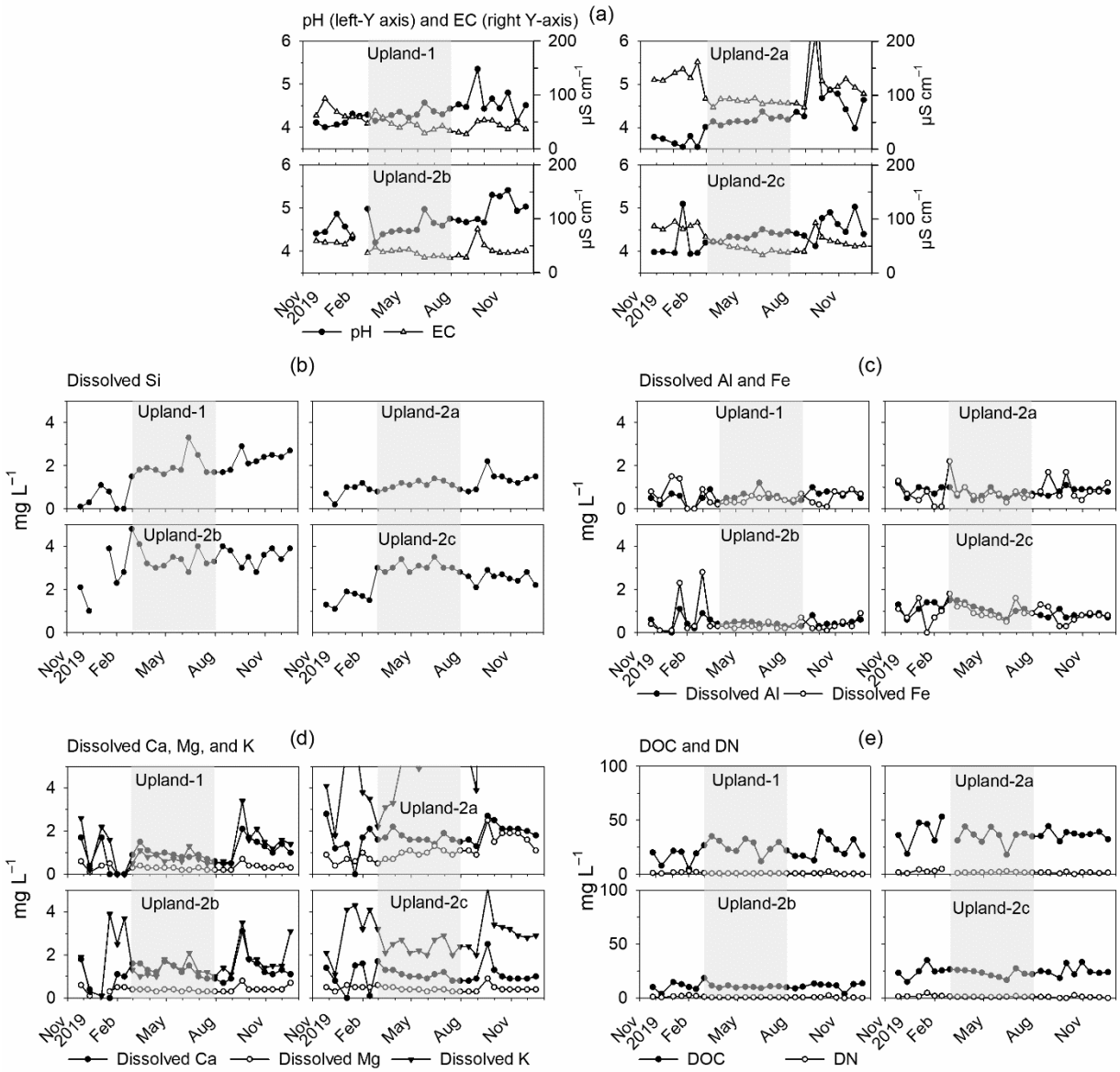

Fig. 4-3 Seasonal change in pH, EC and chemical concentration of dissolved form <0.45 µm. (a) pH and EC; (b) Si; (c) Al and Fe; (d) Ca, Mg, and K (e) DOC and DON. Note that the axis and unit value is the same within each group.

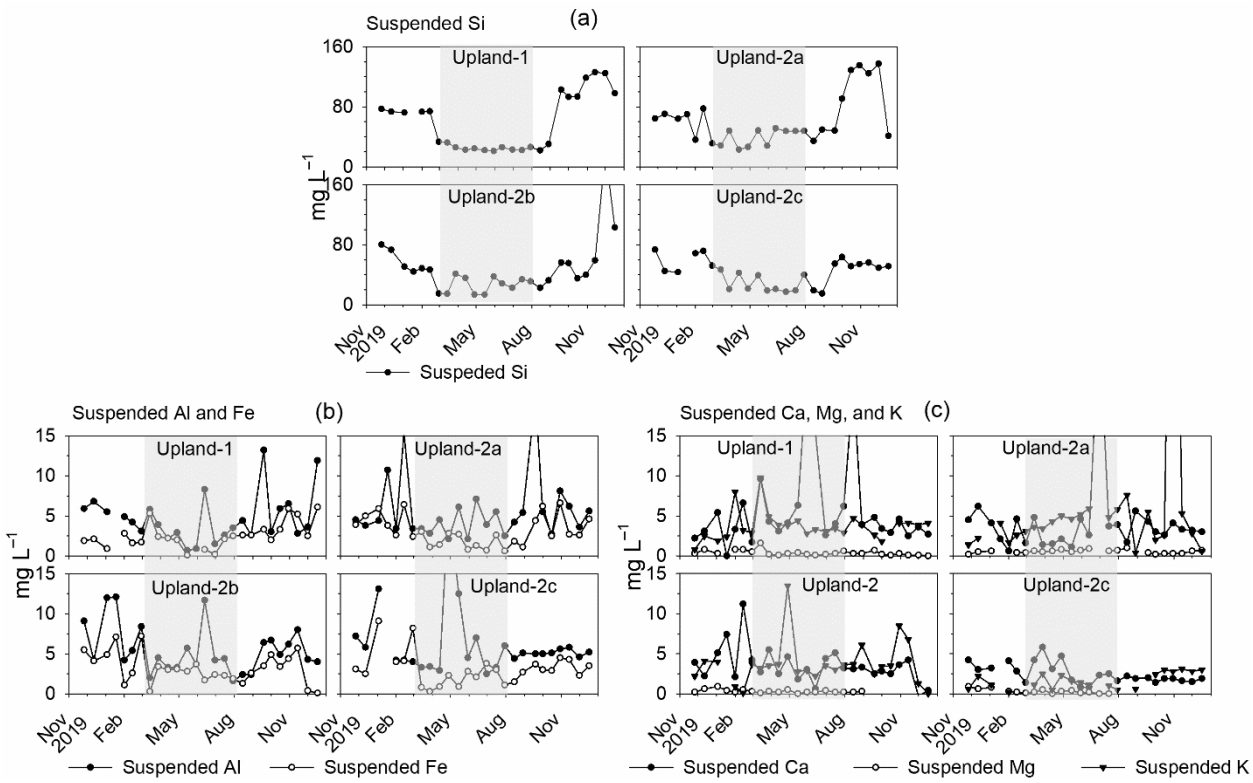

Fig. 4-4 Seasonal change in chemical concentration of suspended form >0.45 μm. (a) Si; (b) Al and Fe; (c) Ca, Mg, and K. Note that the axis and unit value is the same within each group.

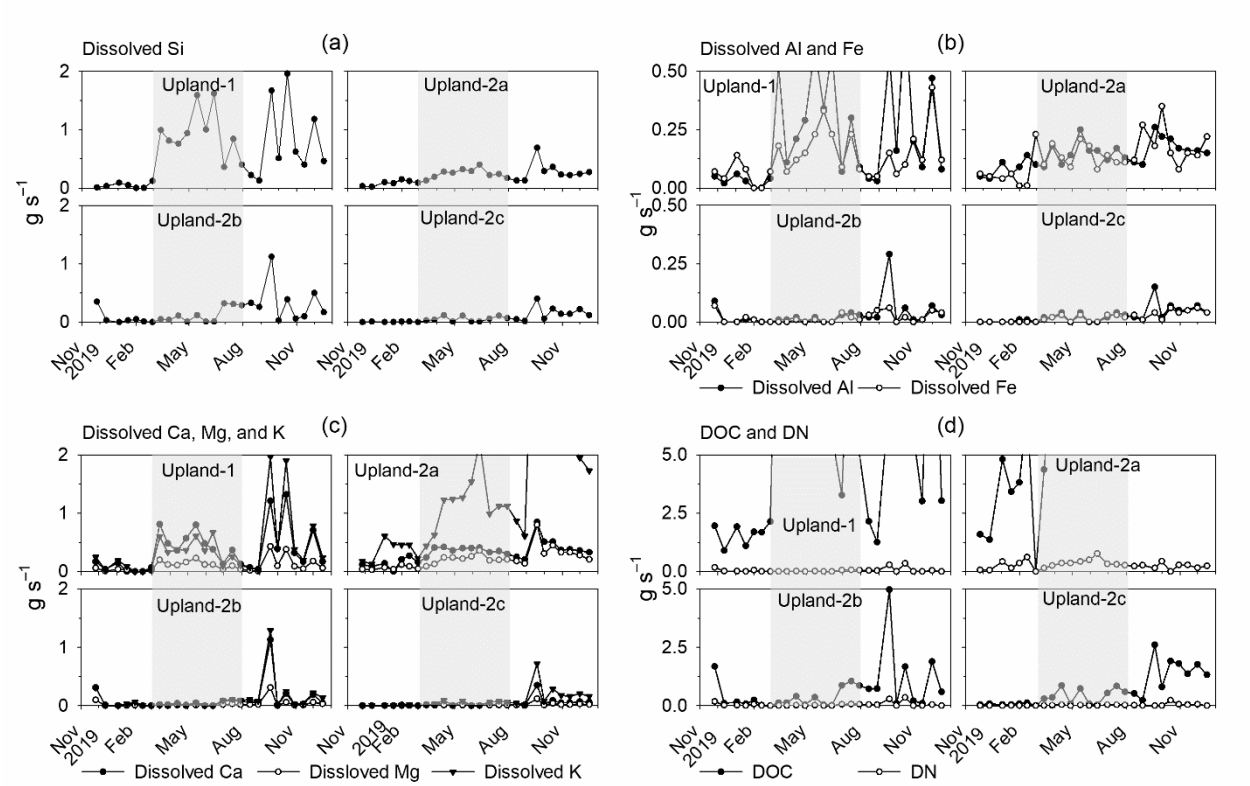

Fig. 4-5 Seasonal flow of mineral elements and DOM in dissolved form <0.45 μm: (a) Si; (b) Al and Fe; (c) Ca, Mg, and K; (d) DOC and DN. Note that the axis and unit value is the same within each group.

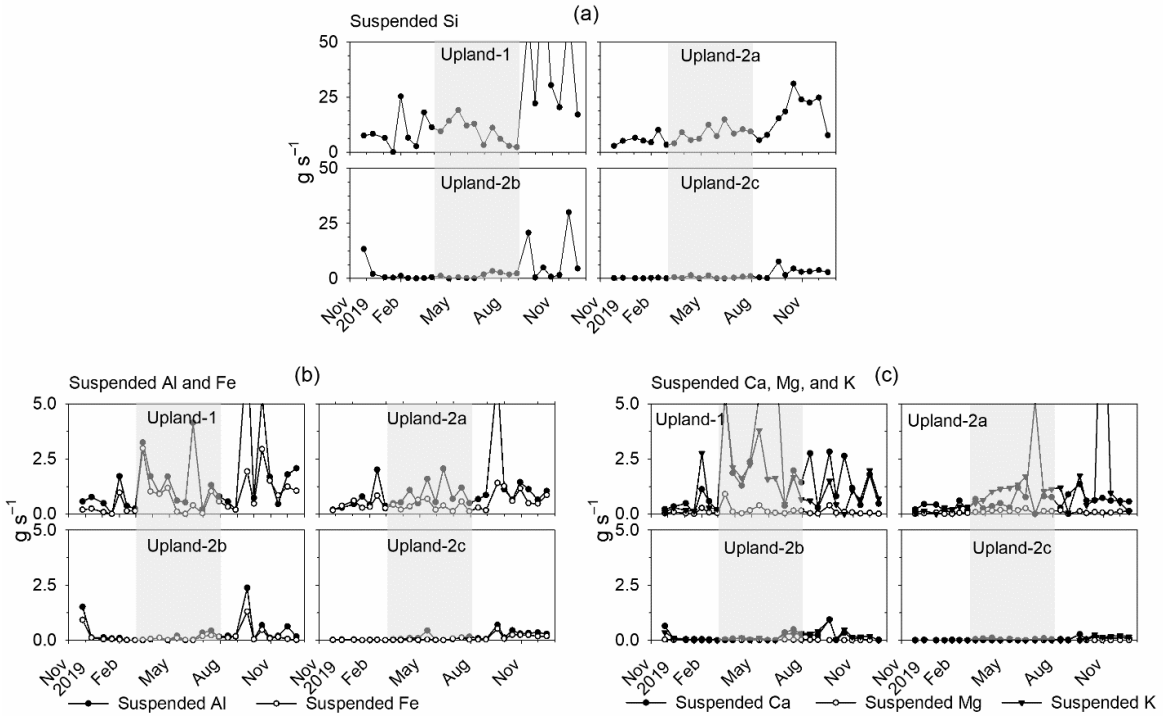

Fig. 4-6 Seasonal flow of mineral elements in suspended form >0.45 μm: (a) Si; (b) Al and Fe; (c) Ca, Mg, and K. Note that the axis and unit value is the same within each group.

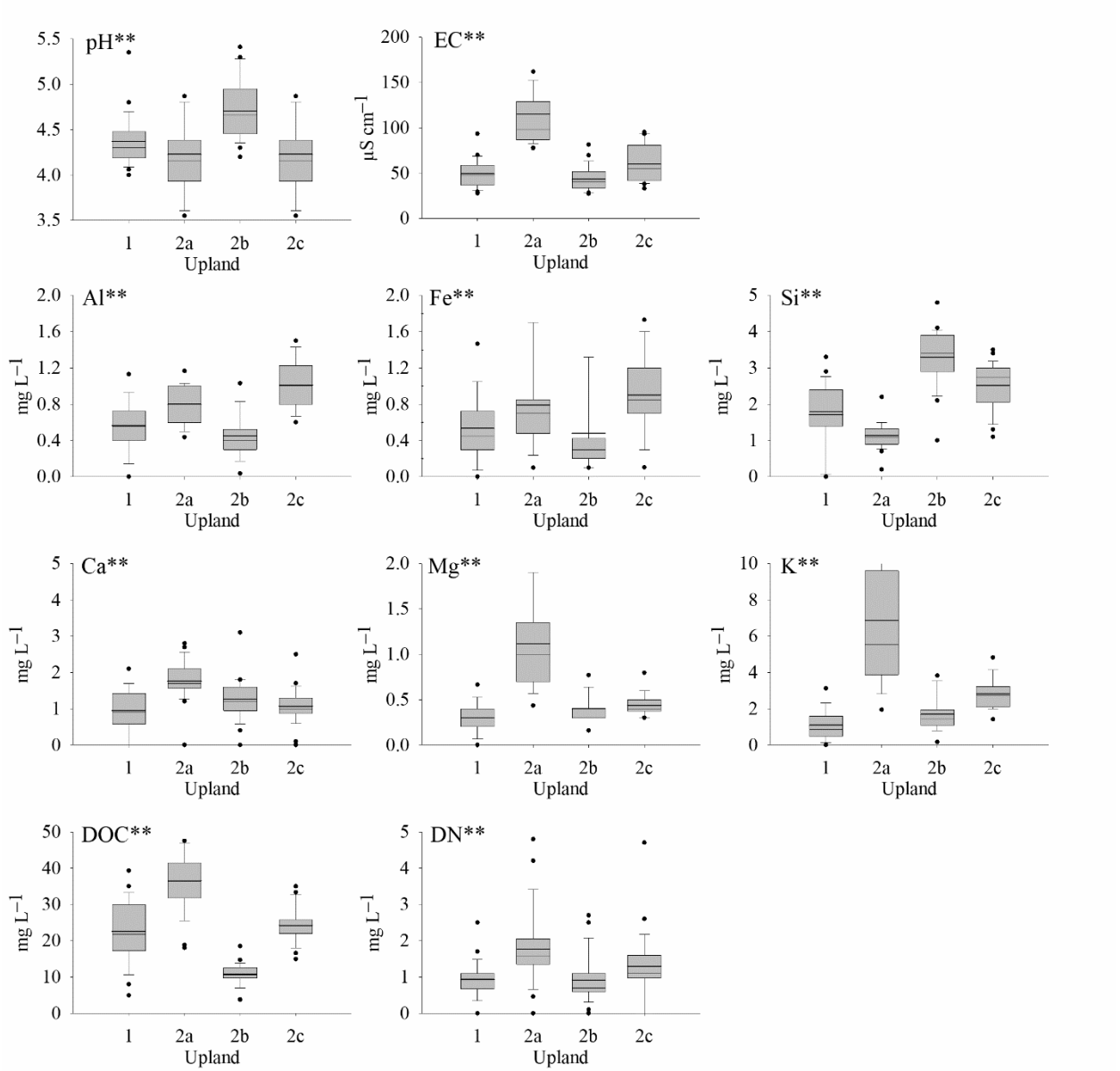

Fig. 4-7 Box-whisker plots showing the interquartile range (grey box), median (thin horizontal line), mean (thick horizontal line), maximum, and minimum observation of dissolved mineral elements and DOM concentration. Only the 5th and 95th percentiles are plotted as outliers. Mean comparison was tested by one-way ANOVA. ** is significant at P <0.01; * is significant at P <0.05

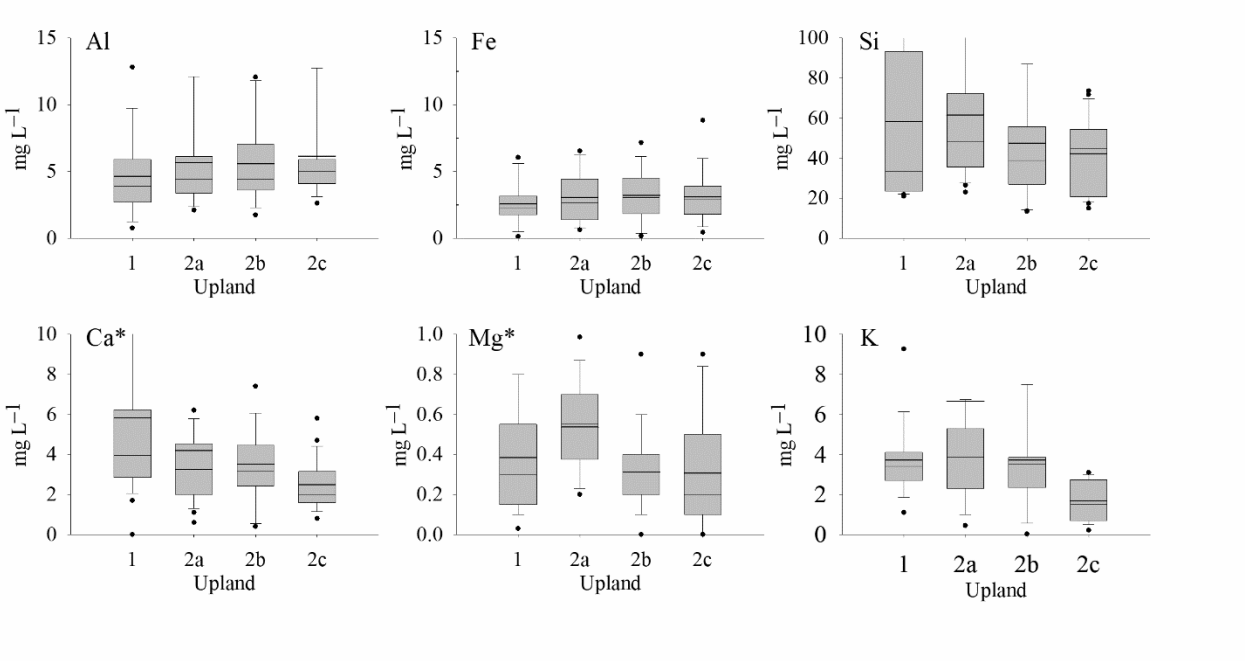

Fig. 4-8 Box-whisker plots showing the interquartile range (grey box), median (thin horizontal line), mean (thick horizontal line), maximum, and minimum observation of suspended mineral elements and DOM concentration. Only the 5th and 95th percentiles are plotted as outliers. Mean comparison was tested by one-way ANOVA. ** is significant at P <0.01; * is significant at P <0.05

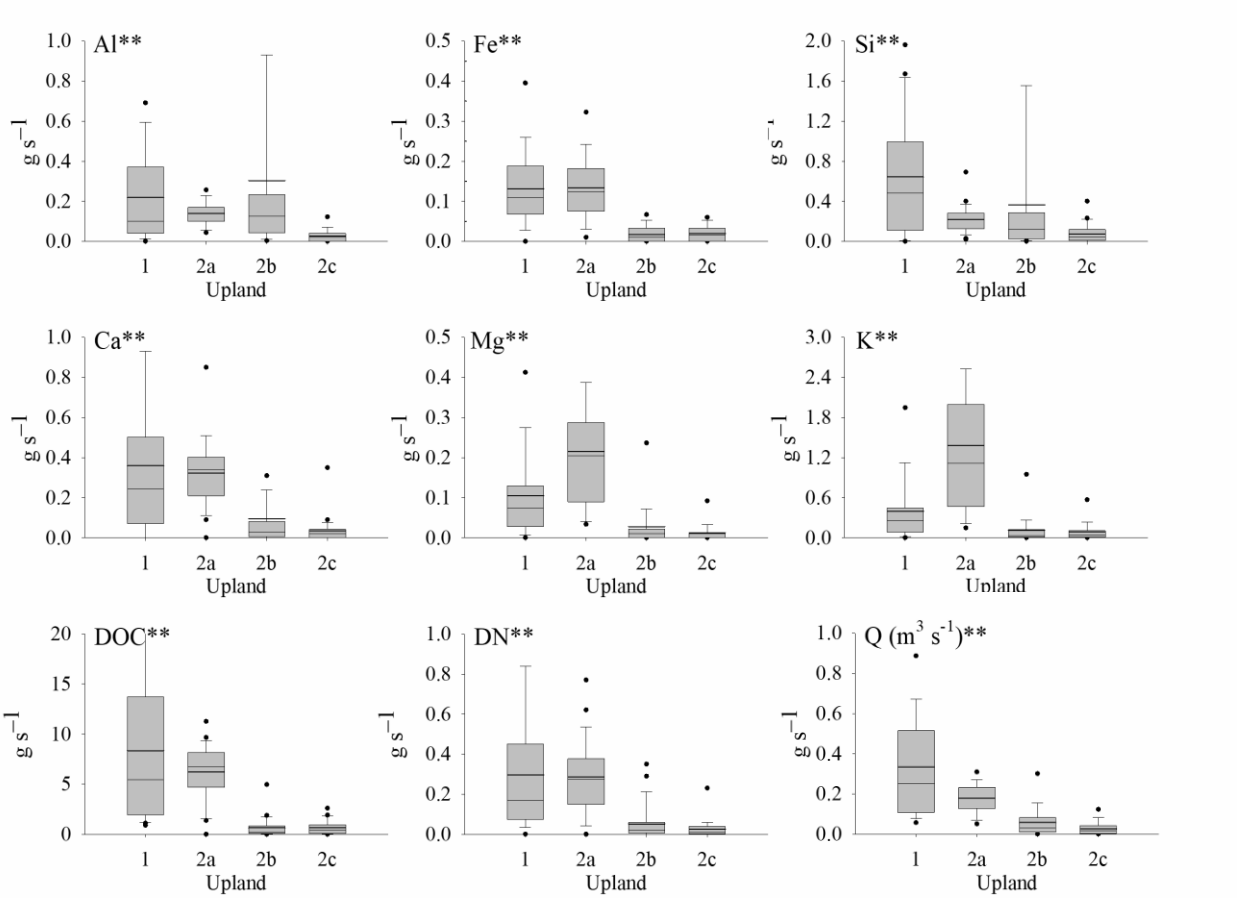

Fig. 4-9 Box-whisker plots showing the interquartile range (grey box), median (thin horizontal line), mean (thick horizontal line), maximum, and minimum observation of flow of dissolved mineral elements, DOM, and water discharge (Q). Only the 5th and 95th percentiles are plotted as outliers. Mean comparison is tested by one-way ANOVA. ** is significant at P <0.01; * is significant at P <0.05.

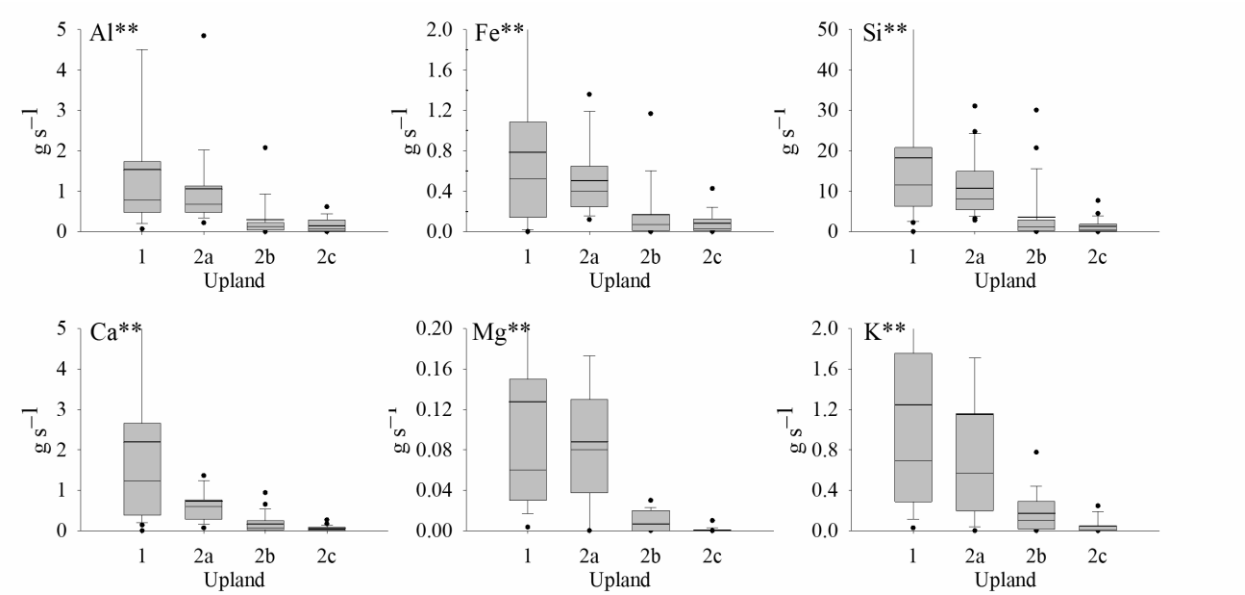

Fig. 4-10 Box-whisker plots showing the interquartile range (grey box), median (thin horizontal line), mean (thick horizontal line), maximum, and minimum observation of flow of mineral elements in suspended forms. Only the 5th and 95th percentiles are plotted as outliers. Mean comparison was tested by one-way ANOVA. ** is significant at P <0.01; * is significant at P <0.05

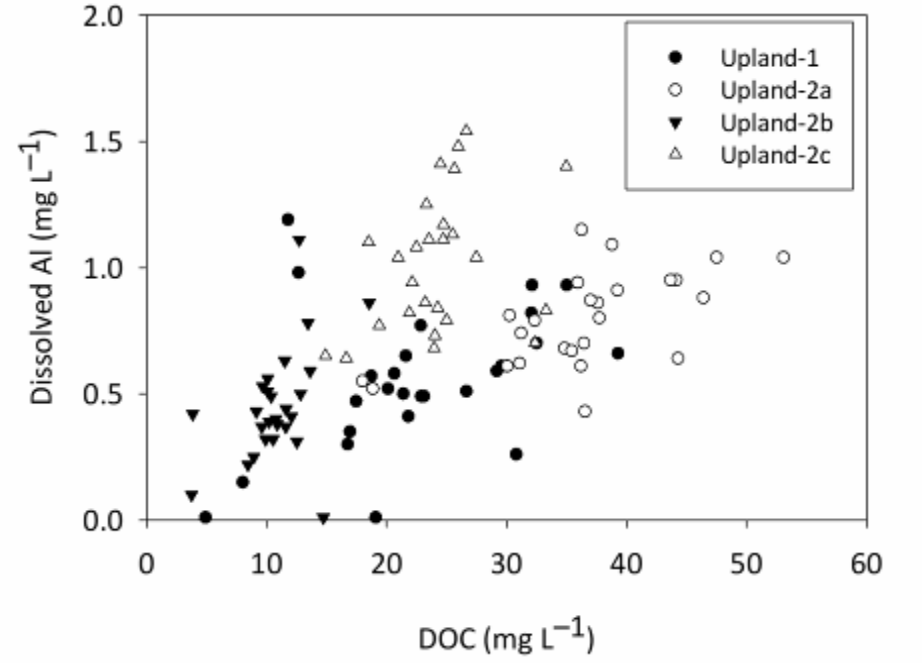

Fig. 4-11 Relationship between concentration of DOC and dissolved Al in each upland.

4.6 Supplementary material CHAPTER 4

The Revised Universal Soil Loss Erosion (RUSLE) (Mg ha^{-1} yr^{-1}) was used to estimate soil erosion in the study sites (Renard et al. 1997). The RUSLE model consists of erosivity factor (R), erodibility factor (K), length and slope factor (LS), crop factor (C), and land management practices (P). Briefly, the model is as follows

$$A = R\ K\ LS\ C\ P$$

Because the study sites had similar soil, geology, climatic conditions, and crop management, I assumed there was no significant variation among the uplands. Therefore, the R, K, C, and P were applied the same value for all uplands. The K, C and P factors for characteristics of the study area under oil palm plantation were 0.24 by, 0.5, and 0.5 (Stewart et al. 1975); (Arsyad 2010). Brief explanations of *R*, and *LS* factors are presented below.

R-factor

In this study, the relationship between the *R*-factor and the mean annual precipitation (mm) from Bols (1978) was applied.

$$R = \frac{2P^2}{100(0.073P + 0.73)}$$

Where:

R = Erosivity factor

P = Annual precipitation (mm)

LS factor

The *L*-factor is the slope length factor. It is the ratio of soil loss from the field slope to that of a standard plot length of 72.6 ft (=22.13 m) (Wischmeier and Smith 1978).

$$L = \left(\frac{\lambda}{22.13}\right)^m$$

Where λ is slope length and m is empirical coefficient (0.2 <m <0.5). In this study, I use m = 0.4 that is suggested by McCool (1989).

The S-factor is the ratio of soil loss from the field slope gradient to that from a 9% under slope otherwise identical condition (Wischmeier and Smith 1978).

$$S = 10.8 \times \sin(\theta) + 0.03, \quad \theta < 9\%; \text{ or}$$

$$S = 16.9 \times \sin(\theta) - 0.5, \quad \theta > 9\%;$$

Where θ is angle of slope (^{O}).

The slope length was defined as the distance from the point of origin of overland flow to: (a) point where the slope gradient decreases enough that deposition begins; or (b) the point where runoff enters a well-defined channel that may be part of a drainage network or a constructed channel (Wischmeier and Smith 1978).

This study used GIS-based methods to estimate slope length, represented as flow accumulation (*Flowacc*) based on the DEM. All calculation of *LS* factor and final erosion was done using a raster calculator in Map Algebra Tool Arc GIS 10.7.1. The detailed workflow of this method in GIS is presented below.

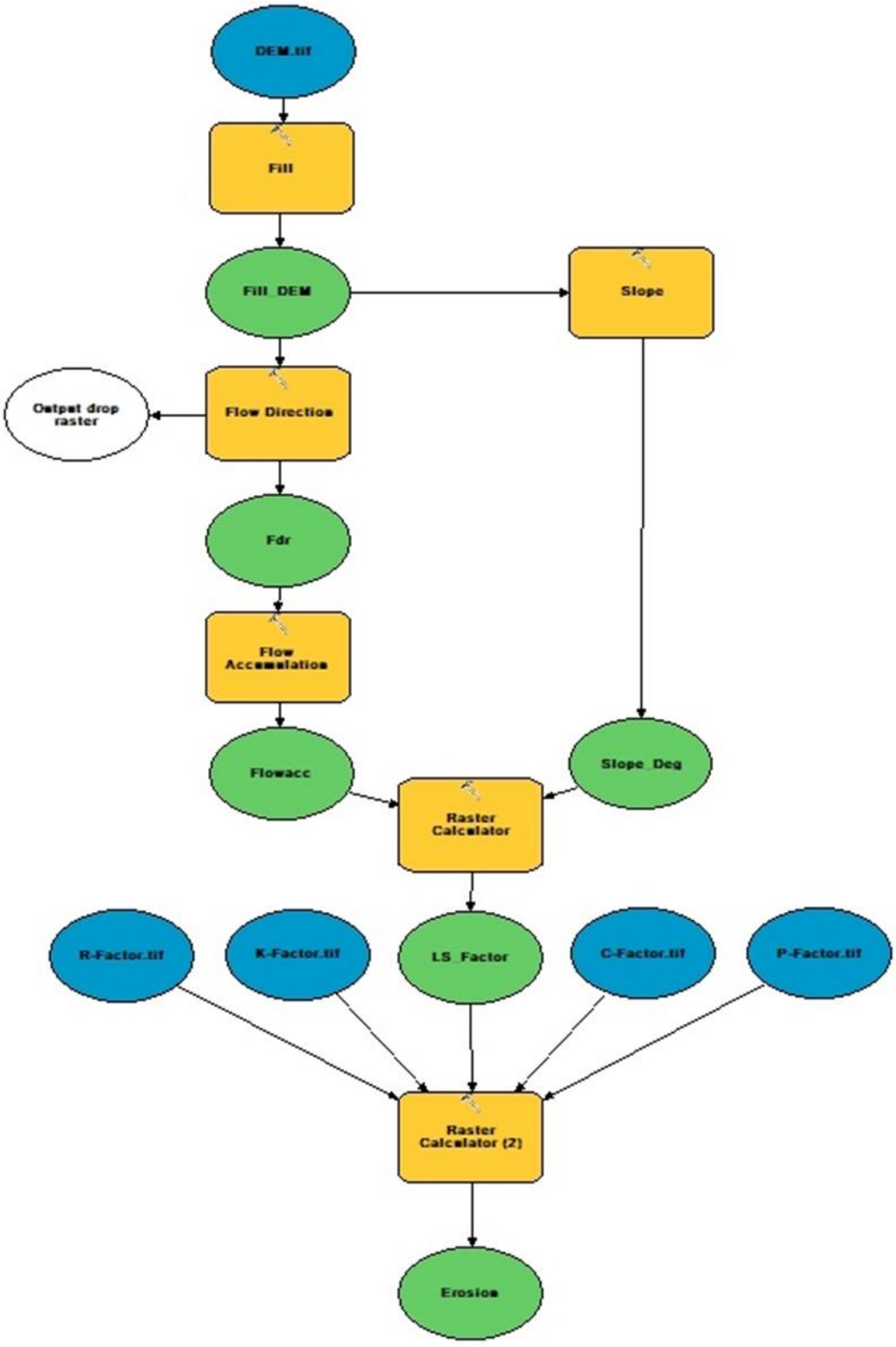

Fig. S 4-1 RUSLE model flow work using Arc GIS 10.7.1

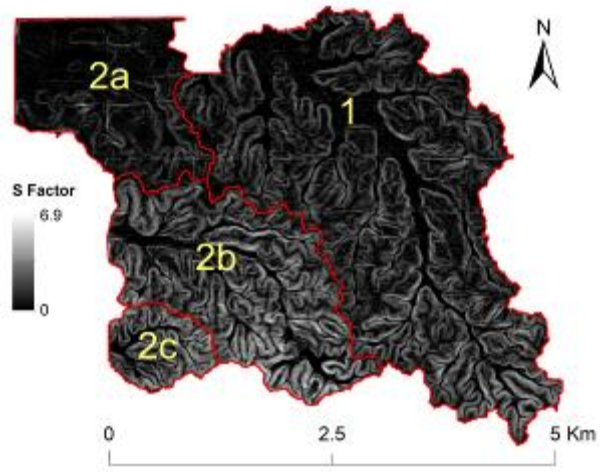

Fig. S 4-2 Slope factor (*S*) of the uplands

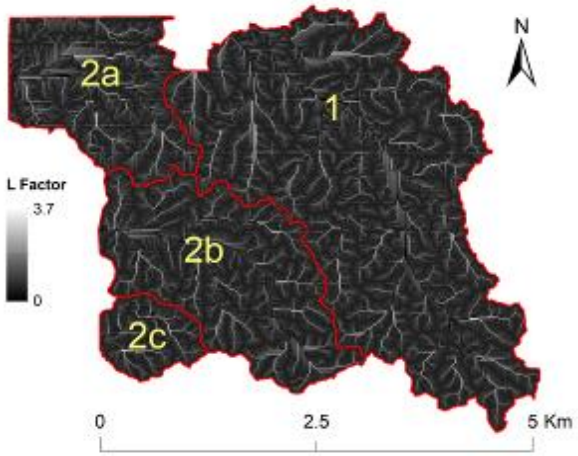

Fig. S 4-3 Length of slope factor (*L*) of the uplands

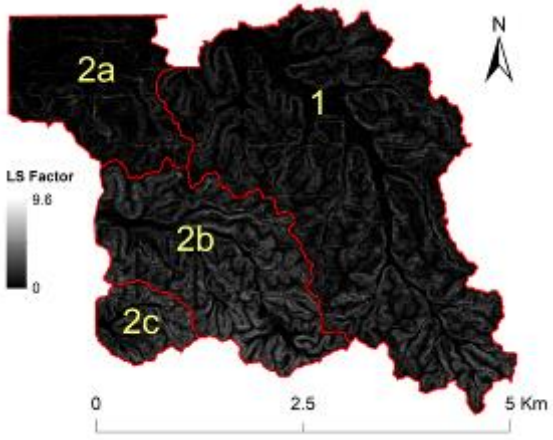

Fig. S 4-4 Combination of length and slope factor (*LS*) of the uplands

Fig. S 4-5 shows erosion distribution in the mineral upland. Upland-1 and 2b were dominated by high erosion up to 46 Mg ha^{-1} yr^{-1} at higher elevations while upland-2a was dominated by low erosion. Note that this value is based on pixel size (8.3 m). High erosion was congruent with the distribution *L* factor (Fig. S 4-3) and *S* factor (Fig. S 4-2) of each catchment. In addition, high erosion was also distributed along the farming road across the upland (Fig. S 4-5).

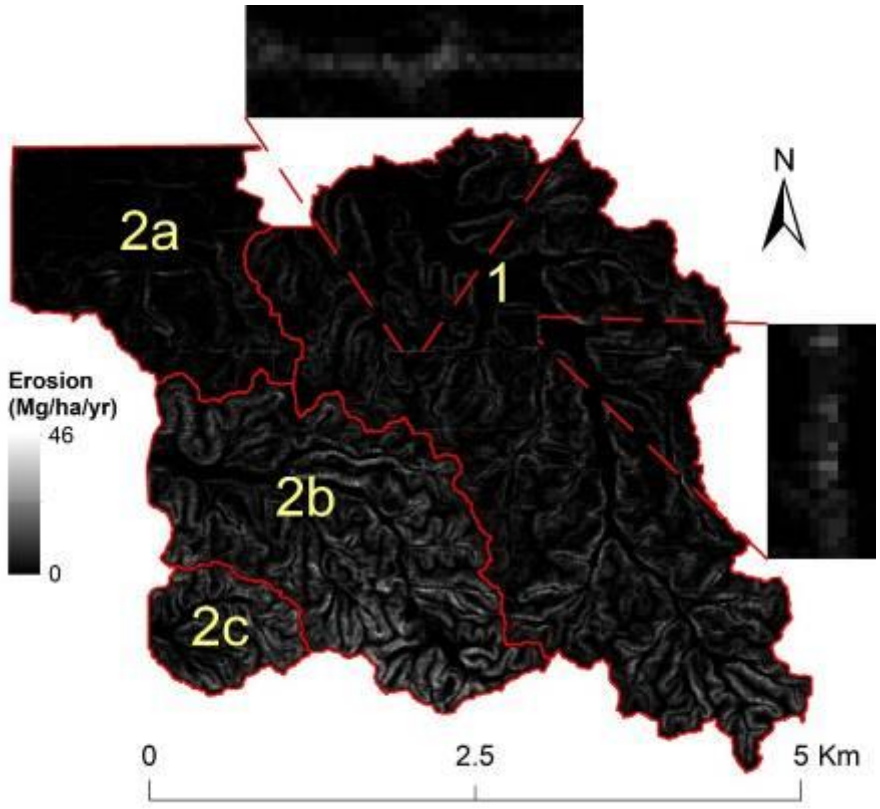

Fig. S 4-5 Erosion distribution in the study area. The red line catchment boundary. The two boxes enlarged by dashed-line show the erosion on the road.

CHAPTER 5
LANDFORM AFFECTS THE DISTRIBUTION OF MINERAL NUTRIENTS IN THE TROPICAL PEATS

5.1 Introduction

Lowland tropical peatlands in Indonesia are mainly situated along the eastern part of Sumatra (~6.4 Mha), the southern and western parts of Kalimantan (~4.8 Mha), and the southern part of Papua (~3.9 Mha) (Ritung et al. 2011) which can be up to 20 m deep (Page et al. 2006). Since several decades back, these vast and valuable ecosystems have been considered as potential agricultural lands (Driessen 1978; Andriesse 1988). However, they have attracted international recognition because of their role in regulating global environmental issues i.e. climate change (Cusell et al. 2015; Ritson et al. 2017), eutrophication, and acidification (Abrams et al. 2016; Cusell et al. 2015). A detailed evaluation of nutrient availability and distribution is required in order to promote agricultural intensification and to prevent environmental degradations.

Numerous studies have evaluated the chemical properties of tropical peat. Mineral nutrient content in tropical peat is typically very limited (Page et al. 1999; Lampela et al. 2014). In consequence, vegetation suffers from nutrient deficiency and shows stunted growth, especially in the interior of a peatland area. Using Fleischer's criteria, Driessen (1978) classified most tropical peat in Indonesia and Malaysia as oligotrophic because of its low ash and mineral nutrient content, a limiting factor that reduces its potential for agriculture (Funakawa et al. 1996).

Further studies have clarified some factors determining the distributions of mineral nutrients in tropical peatland ecosystems. A tropical peatland is typically shallow at its river-bounded fringes and thicker in the interior part (Anderson 1983), creating a dome. Anderson's model has often been used to structure nutrient distribution evaluations (Cameron et al. 1989; Page, et al. 2006). In the central part of the dome, nutrient content is generally low because the surface peat is laterally and vertically far from mineral soil sources. This is supported by research showing that the distance from the coastal levee is one of the factors that affect soil solution composition (Funakawa et al. 1996). Haraguchi et al. (2000) found that peat in the surface and the mid-depth sections of peat profiles has lower concentrations of Ca^{2+} and Mg^{2+} than the peat near the bottom because of salt retention from flows of underground water with

high elemental concentrations. A detailed study on the relationship between mineral nutrient distributions and distance to mineral bed (peat thickness) in Riau was carried out by Watanabe et al. (2013), which suggested that nutrient availability is better in the fringe bordering riverbank with the thickness less than 3 m. These reports suggest that peatland fringes bordering riverbank are richer in mineral nutrients.

A peatland fringe is a transitional zone between a peat area and the surrounding landforms. Transitional zones may function differently in terms of the mineral nutrients based on the location. In the temperate peatlands, type of mineral land and the transitional zone have been introduced as a conceptual framework describing vegetational and hydro-chemical gradients (Whitfield et al. 2009; Howie et al. 2009). Based on long-term studies, they categorize transitional zones between raised peat area and a) mineral upland, b) river levee (riverbank), c) beach, and d) flat delta (floodplain). Only type (a) receives water flow, and probably mineral nutrients, from both raised peat area and mineral upland sources. It was evident that a confined transitional zone found in a topographic depression between a raised peat area and a mineral upland of greater than 1% has a higher pH (4.8±0.9) than an unconfined transitional zone (pH 4.2±0.4) bordering a flat or receding mineral land (Langlois et al. 2015).

In contrast to the state of knowledge for temperate peatlands, the interactions between tropical peat and its surrounding landforms particularly mineral upland are rarely studied. Studies of peatland as an individual ecosystem are abundant, yet the crucial questions of how mineral nutrients are distributed, and which types of surrounding landform enrich peatland, remain. Surrounding landforms such as mineral uplands can be important mineral nutrient sources, because they are often at higher elevations than the peat, so that run-off from the mineral uplands can drive mineral nutrients downward.

The objective of this study is to clarify the effect of landform on the distribution of mineral nutrients in tropical peat that borders a mineral upland in Riau Province, Sumatra. I hypothesize that the mineral nutrient content is higher in tropical peat bordering mineral upland than in riverbank peat. It is also possible that enrichment occurs continuously across the fringe and into the interior peatland as a result of topographic gradients between mineral upland and peatland, compensating for nutrients lost due to vegetation uptake and leaching. Understanding how mineral nutrients are distributed in a tropical peatland bordering on other landforms will contribute to wise use of the peatland as well as informing strategies for restoration of integrated tropical peatland ecosystems.

5.2 Materials and Methods

5.2.1 Site Description

The study site lay 60 km from the nearest coastline, within the watershed of the Siak River, Riau Province, Indonesia, and had a mean elevation of approximately 11 m above sea level (Fig. 5-1a). Peatland has formed in a local depression, which borders mineral upland and the Siak River. The Siak River meandered around the study site and forms more than half its perimeter. The remaining part of the study site bordered the mineral upland, which was approximately 7 km from the Siak River at its closest approach. Although the peat area was close to the mineral upland, surface mineral soil was absent from the sampling points. A small stream runs out of the mineral upland to the Siak River throughout the year (Fig. 5-1a and 5-1b). This stream was thought to contribute to ongoing discharge from the mineral upland, from which the upper peatland received suspended particles. The shape and direction of the stream, however, had changed due to peat accretion and land-use changes, including the construction of a drainage system. The study site had been cultivated for oil palm since 2002, and was managed using farm road with a pair of intersecting canals (from 3 m to 5 m in width, ~2 m deep) running south-north and east-west. The canals were constructed at approximate intervals of 0.3 km (south to north) and 1 km (east to west), which made the farm blocks. The dig out materials during canal construction were put onto the road. The canal water level during the sampling period ranged from 15 cm to 120 cm below soil surface level Fig. 5-1b and 5-1c). The annual temperature ranged between 23°C and 27°C; the mean annual rainfall was about 2,080 mm yr^{-1} (Marwanto et al. 2018), with the wet season typically from December to May and the dry season June to November.

5.2.2 Sampling Design

Fertilizer were broadcasted less than one meter from the trunks of oil palms. The fertilizer application had an unclear effect on the chemical composition of the soil solution in this study site (Marwanto et al. 2018). However, to avoid any effect of fertilizer on the solid phase, sampling points were distanced about five meters from the trunks of the oil palms. Peat samples were collected at the center of the farm blocks from the surface layer at three depths (0–15 cm, 15–30 cm and 30–50 cm) on the grid at ~1 km intervals (total 32 grid points; Fig. 5-1b) using peat sampler (volume = 530 ml, length = 50 cm) (Royal Eijkelkamp, The Netherlands) for chemical analysis. Further samples were taken at 50 cm depth intervals thereafter until the mineral bed was reached. To enable investigation of the effects of the

mineral upland on the chemical properties of the surface layers, the minimum distance from the mineral upland was measured at all sampling points. Profile samplings were also obtained along transects comprised of the grid points beside the upland (T1) and the riverbank (T2) (Fig. 5-1b) for comparison of ash content; and perpendicular from the upland toward the riverbank (T3) for comparison of mineral element compositions. Core samples (diameter = 10 cm, length = 5 cm) were taken along transect T3 to measure bulk density (n = 18).

According to reports regarding the period of water level rise in the Sunda Shelf region (Wüst and Bustin 2004; Chawchai et al. 2013; Solihuddin 2014) which are coincident with the period of peat formation in Sumatra (Anderson 1983; Andriesse 1988; Cameron et al. 1989), Sumatran rivers are considered as the starting point of peat formation. I therefore considered the median water table level for the Siak River near grid square 6E (Fig. 5-1b) as the initial level of peat formation in the study site. I further assumed that mineral sediments (represented by ash content) found above this water table on both T1 and T2 were transported mainly from the mineral upland, and that those found below this water table were transported mainly from the Siak River. The nutritional condition of T1 and T2 peat samples was judged by ash content, following Driessen and Soepraptohardjo (1974) for tropical peat with absence of mineral upland.

State of peat materials (sapric, hemic, and fibric) was described according to Agus and Subiksa (2008) for fresh field samples. Briefly, sapric peat is brownish–blackish decomposed peat containing less than 15% fibrous materials. Hemic peat is brownish decomposed peat with a fibrous materials content of 15%–75%. Fibric peat is incompletely decomposed peat having more than 75% fibrous materials. I also identified and recorded charcoal, peaty clay and mineral sediment content based on visual examination of the morphology of peat constituent.

The elevation of each sampling point was measured by the static surveying technique with a handheld GNSS receiver and field controller (GRS-1 GG, TOPCON, Tokyo, Japan) with an accuracy of ±4 mm and computer software (GNSS-Pro, TOPCON, Tokyo, Japan). I set the baseline (0 m) for relative elevation at grid square 6E (Fig. 5-1b). Peat thickness from the surface to the mineral bed was measured when the soil samples were collected. The measurement of relative elevation and peat thickness made it possible to describe the shape of the peat in the study site.

5.1.1 Laboratory and Statistical Analyses

Bulk density was determined after drying at 70°C for 24 hours. Ash content was determined by weight (wt%) after burning the samples at 550°C for 8 hours in an electric muffle furnace. Electrical conductivity (EC) and pH were determined by conductivity meter and glass electrode, respectively (LAQUA F-74 BW, Horiba, Kyoto, Japan) based on an air-dried sample:water ratio of 1:10 (3 g:30 mL). Following 1 M ammonium acetate (pH 7) extraction (Soil Survey Staff 1996), exchangeable Ca^{2+} and Mg^{2+} were determined using atomic absorption spectroscopy; exchangeable K^{+} and Na^{+} were determined using flame emission spectroscopy (AAS AA-7000, Shimadzu, Kyoto, Japan). An aliquot of sample was digested with HF and $HClO_4$ (Hossner 1996), then total Ca, Mg, K, Na, Fe, and Al were determined by an inductively coupled plasma atomic emission spectrometer (ICPE-9000, Shimadzu, Kyoto, Japan).

The spatial distribution of mineral nutrients was mapped using Ordinary Kriging and stable type model in Geostatistical Analyst in Arc GIS 10.6 (ESRI, USA) from which I excluded ash content at 6E (Fig. 5-1b) as its content was considered an outlier. Correlations between the geometrical parameters (distance from the upland and peat thickness) and chemical properties of the study site were determined by Spearman rank correlation test *rs*, after testing for normality found that data were not normally distributed, using Sigma Plot 11.0 software (Systat Software, California, USA). Significance is based on *p*-values less than 0.05.

5.3 Results

5.3.1 Shapes of peat and peat bottom

The surface configuration of the study site gradually rose about 8.4 m from close to the riverbank near 6E (northwest, Fig. 5-2a) to the highest point close to the mineral upland 1A (southeast, Fig. 5-2a). Higher elevation points were concentrated in the southeast near the mineral upland, showing a gradual decline toward the Siak River. In contrast, the underlying surface (mineral bed), which was estimated from the surface configuration and peat thickness, was a rising slope with a concave configuration, with thicker peat found between the upland and the riverbank at 3B and 4B (Fig. 5-2b). The shape of the peat bottom (or mineral bed) showed a sharp slope gradient on the foothills near the mineral upland (Fig. 5-2c). About 0.5 km from the upland, the peat thickness was 5.5 m (1A), but at approximately 1 km from the riverbank (6E) it was only 0.5 m thick (Fig. 5-2c).

5.3.2 General physicochemical properties of the surface layer

Table 5-1 shows the physical and chemical properties of the peat material collected from the 32 grid points at three depths down to 50 cm. Sapric peat dominated the two layers above 30 cm deep, and fibric peat was sparse within all the three layers. At 30–50 cm deep, hemic and sapric peats were found in approximately equal quantities. Charcoal was found in the 0–15 cm and 15–30 cm layers. Mineral bed material was found at the 30–50 cm depth at the shallowest point (6E) near the riverbank. The ash content was high in the top layer, with a mean of 8.2±3.7%, showing a declining trend with depth. Bulk density in the 0–15 cm layer was approximately 1.6 times higher than in the 30–50 cm layer. The values of pH and EC were similar up to 50 cm depth (pH = 3.7±0.3; EC = 183±80 μS cm^{-1}). The levels of exchangeable Ca^{2+}, Mg^{2+}, K^{+}, and Na^{+} were 8.29 $cmol_c\ kg^{-1}$, 2.73 $cmol_c\ kg^{-1}$, 0.65 $cmol_c\ kg^{-1}$, and 0.13 $cmol_c\ kg^{-1}$, respectively, in the 0–15 cm layer and showed declining trends in the two deeper layers. At the depth of 30–50 cm, Ca^{2+} content was about one-third as much as at the 0–15 cm depth. The content of Mg^{2+} was also lower at the 30–50 cm depth, but the decrease was not as sharp as for Ca^{2+}. K^{+} and Na^{+} tended to be low throughout the three layers, compared to Ca^{2+} and Mg^{2+}.

5.3.3 Relationships among peat properties in the surface layers

Statistical analyses were used to examine relationships between the measured geometrical parameters and chemical properties (Table 5-2). Within the three surface layers, thickness, pH, and exchangeable Ca^{2+} and Na^{+} all had a negative correlation with the distance from the mineral upland, at different degrees. Thickness correlated negatively with distance from the upland (rs = –0.52; P <0.05), which suggests that the points farther from the mineral upland had thinner peat. pH had a strong and negative correlation with the distance from the mineral upland in the top (rs = –0.76; P <0.05) and middle layers (rs = –0.56; P <0.05), but the relationship tended to be weaker in the lower layer. Exchangeable Ca^{2+} had a consistently negative correlation with distance within each of the three layers, with rs values of –0.55, –0.56, and –0.45 (from shallow to deep; all had P <0.05). Exchangeable Na^{+} also had a negative correlation with distance though only in the deep layer (rs = –0.40; P <0.05). In contrast, EC correlated positively with the distance from the mineral upland, and this was apparent in the two upper layers (rs = 0.44 and rs = 0.50 in the 0–15 cm and 15–30 cm layers, respectively; both with P <0.05).

Despite having a weak correlation with distance from the mineral upland, ash content and exchangeable Mg^{2+} correlated positively with exchangeable Ca^{2+} in two of three surface layers. Ash content had a positive correlation with exchangeable Ca^{2+} in the 15–30 cm and 30–50 cm layers (rs = 0.36; P <0.05, and rs = 0.57; P <0.05, respectively). Exchangeable Mg^{2+} had a correlation with exchangeable Ca^{2+} in the 0–15 cm and 15–30 cm layers (rs = 0.39; P <0.05, and rs = 0.53; P <0.05, respectively). Exchangeable Na^{+} also had a positive correlation with Ca^{2+} in the 30–50 cm layer (rs = 0.54; P <0.05). In addition, ash content correlated positively with exchangeable Na^{+} in the 30–50 cm layer (rs = 0.46; P <0.05). Exchangeable K^{+} is correlated with Mg^{2+} in all three layers. These correlations may indicate that ash contains these cations.

Spatially, at the surface layers, higher ash content, pH, and exchangeable Ca^{2+} and Mg^{2+} are located near the mineral upland. Exchangeable Ca^{2+} was high close to the mineral upland in the 0–15 cm layer (Fig. 5-3). Although the concentration was not as high as exchangeable Ca^{2+}, higher exchangeable Mg^{2+} close to the upland was also found in the 15–30 cm (Fig. 5-3), and 30–50 cm layers (map not shown). The concentrations of exchangeable K^{+} and Na^{+} did not show any clear pattern in the 0–15 cm and 15–30 cm layers, but high levels were also found near the mineral upland in the 30–50 cm layer (maps not shown). The locations with higher content of exchangeable Ca^{2+} were consistently found near the mineral upland in all three layers (Table 5-1 and Fig. 5-3).

Given its clear relationship with distance from the mineral upland, I compared exchangeable Ca^{2+} distribution with published reports. Exchangeable Ca^{2+} in three layers was higher than the mean exchangeable Ca^{2+} found by Funakawa et al. (1996) and Watanabe et al. (2013), both of which investigated peatland without adjacent mineral upland (Fig. 5-4). In the present study, the mean of Ca^{2+} in the 0–15 cm layer was 8.29±5.08 $cmol_c\ kg^{-1}$ (Table 5-1), with higher Ca^{2+} values distributed predominantly more than 4 km away from the mineral upland (Fig. 5-4). In the 15–30 cm layer, the mean Ca^{2+} was 6.51±3.85 $cmol_c\ kg^{-1}$ (Table 5-1) with almost all points above the mean reported by Funakawa et al. (1996) (Fig. 5-4). Although the mean exchangeable Ca^{2+} in the 30–50 cm layer decreased markedly to 3.7±2.2 $cmol_c\ kg^{-1}$, it was still higher than that found by the above authors.

5.3.4 The distribution of ash content along transects T1 and T2

Except in the bottom layer (mineral bed) and the peat layers directly overlying it, T1 profiles (Fig. 5-5), located close to the mineral upland generally had higher ash content than

T2 profiles (Fig. 5-6). The mean ash content above the water table in T1 was 7.6±9.0%. Moreover, the profiles in T1 had high ash content (more than 10%) in some layers, for instance in the profile of 1A at 8.35 m (15.3%) and 5.5 m (46.1%), in the profile of 1B at 6 m (10.2%) and 5.5 m (14.7%), and in the profile of 1C at 5.5 m (13.2%) (Fig. 5-5). Sapric peat was predominantly identified in the same layers in which ash content was over 10% (Fig. 5-5). In the profile of 1F, which is close to the riverbank, ash content over 10% was not observed above water level (Fig. 5-5). In contrast, the mean ash content above the water table in T2 (Fig. 5-6) was only 3.8±2.8%, lower than the mean of T1. Only the profile of 6D at 2.15 m had an ash content over 10% (10.8%). The remaining layers, between the surface layer (0–50 cm) and the mineral bed (including high ash-layers above them), of the profiles along T2 were predominantly typical oligotrophic peats with ash content below 2% (Driessen and Soepraptohardjo 1974). However, probably due to decomposition and accumulation processes in the surface layer and seasonal flooding of the Siak River, the uppermost layers (which were also dominated by sapric peats) had high ash content (Fig. 5-6). Higher ash content was also observed in the bottom layers, in this case probably supplied by the underlying mineral bed.

5.3.5 The distribution of ash content, total element content, pH, and EC along transect T3

In the peat profiles of T3 (Fig. 5-7), ash content and total element content at the surface near the mineral upland (1C, 2C, and 3C) show higher values compared to those near the riverbank (4C, 5C, and 6C) (Fig. 5-7 and Fig. 5-8). Those higher ash contents generally exceeded 5% and 10% that fall to the criteria of mesotrophic and eutrophic peats respectively (Driessen and Soepraptohardjo 1974), and were evident at 0–30 cm in 1C and 2C. Ash content was low in the samples more than 1 m deep in general, but higher near and at the mineral bed. The total Ca content in 1C, 2C, and 3C exceeded 5 g kg–1 in the surface layers, unlike 4C, 5C, and 6C (Fig. 5-8). In the surface samples of 1C, 2C, and 3C, for instance, the levels of total Ca were 6.3 g kg–1, 7.6 g kg–1, and 6.7 g kg–1, respectively. The levels of total Ca decreased in layers more than 1 m deep through to the bottom layers. This trend corresponded to the trend of ash content from the surface to the middle of the profiles (Fig. 5-8). The distribution pattern of total Mg was similar to that of total Ca: it was not high near or at the bottom layer. Although not as high as total Ca, total Al and Fe showed similar trends to ash content, particularly in peat layers. Al and Fe are major elements of a mineral soil, and were thus abundant in the mineral soil of bottom layers, and peat layers close to them. No clear trend was observed in total K in the profiles. Higher amounts of Na were apparent in the lower layers.

As shown in the (Fig. 5-7), the mean pH was 3.6±0.3. Generally, pH was high at the surface, and slightly lower in the middle and near the bottom (mineral bed) layers. Some profiles had very low pH (<3.0) near the bottom. The EC mean value was 0.23±0.15 mS cm^{-1}; it did not show a clear pattern, unlike pH. Notwithstanding this, higher EC values, over 1 mS cm^{-1}, were found where pH was very acidic (<3.0), near and at the mineral bed below the water table of the Siak River. This was probably caused by acid sulfate generation in the underlying marine sediment.

5.4 Discussion

5.4.1 Effect of mineral upland on peat shape Sampling Design

The landform setting of the study site, a local depression between mineral upland and the bank of the Siak River, has contributed to the formation of a narrow-deep peat. The shape fits the category of basin or valley peatland which has deep peat within a short distance from the riverbank (Page et al. 2006). The part of the study site bordering the mineral upland has developed on the mineral bed above the current water table of the Siak River (Fig. 5-2). This upper peat may have formed after topogenous peat had completely filled the deposition zone between the mineral upland and the Siak River. This partially confirms the hypothesis of Driessen (2001), in which ombrogenous peat develops above topogenous peat in the later stages of peat formation, when rainfall is high and evenly distributed over the year, and the decomposition rate of plant material is low due to acidic conditions. However, I suggest that here, the upper peat has formed under waterlogged conditions caused not only by rainfall but also the discharge of the permanent stream. Due to the presence of the mineral upland, the shape of the peatland in the study site also differs from the lenticular form common in tropical peatlands. A tropical peatland generally has both the thickest peat and highest elevation at the center, known as a peat dome (Anderson 1983; Andriesse 1988; Cameron et al. 1989). In contrast, within the present study site, the highest elevation (1A) was not at the location of the thickest peat (4B). I suggest that the shape of the dome was absent or unclear in this study site due to interaction with the surrounding landforms.

5.4.2 Factors regulating nutritional status in the surface layer

Previous reports by Funakawa et al. (1996), Page et al. (1999), and Lampela et al. (2014) have suggested that mineral nutrients such as Ca and Mg are present at higher levels in surface layers, with a decrease toward deeper layers (excluding mineral-enriched layers near

the mineral bed). This is due to their stronger bonding with organic matter compared to monovalent cations. Elevated Ca in surface layers may be more pronounced in the presence of drained cultivation, such as in the current study site. After the forest was cleared, the nutrient cycle was broken and bases cations with weaker associations with organic matter, such as K and Na, then leached (Watanabe et al. 2013). This upper peat is more likely to undergo decomposition at a high rate, due to drainage (Marwanto et al. 2018). The results confirm this, as the predominant peat material in the surface layer was sapric peat, with higher mineral contents of Ca and Mg. The decomposition rate alone, however, was insufficient to explain the high concentrations of these mineral nutrients and their uneven distribution across the study site, i.e. the higher concentration near the mineral upland and lower further from it. Thus, in addition to the decomposition, I consider that the study site has been influenced by mineral soil supply from the mineral upland.

The mineral upland affected the peat's chemical properties via mineral soil transportation. Its topography is likely to generate mineral-enriched stream water as well as surface runoff, both of which drive suspended particles formed during mineral upland erosion. Eroded mineral soil, then, would associate with peat around the mineral upland, resulting in higher ash content, pH, exchangeable Ca^{2+} and Mg^{2+} (Table 5-1 and Fig. 5-3), total Ca, total Fe, and total Al at the surface layers as well as some high ash levels in the deeper layers (Fig. 5-8), while K and Na showed no clear pattern and no relationship with distance from the mineral upland. The higher ash content in some points near the upland represents mineral soil deposition, in which base cations (Fig. 5-3 and Table 5-1) and total elements (Ca, Mg, Fe and Al) (Fig. 5-8) were also high. Decrease in ash content coincided with decreases in pH, exchangeable Ca^{2+} and Mg^{2+} and total Ca and Mg, and Fe, suggesting that transported mineral soil supplied these mineral nutrients.

The current study suggests that oligotrophic environment would not be formed at the surface of tropical peatlands affected by mineral inflow from adjacent mineral uplands. Such environment differed from general characteristics of tropical peatlands without mineral inflow. The concentrations of exchangeable Ca^{2+} in surface peat, especially close to the mineral upland in the study site, were generally higher than those found in previous studies in tropical peats (Fig. 5-4). For example, at the top layer, the concentrations of exchangeable Ca^{2+} reported by Funakawa et al. (1996) and Watanabe et al. (2013) were low (7.7 $cmol_c\ kg^{-1}$ and 4.9 $cmol_c\ kg^{-1}$, respectively); both were reported from peatlands without presence of mineral upland.

5.4.3 Effect of the mineral upland on the distribution of ash content and total mineral elements in the profiles

T1 profiles had higher ash content (Fig. 5-5) than T2 profiles (Fig. 5-6). Considering the elevation gradient between the upland and the peat area, the transitional zone represented by T1 seems to be a deposition area for mineral upland runoff. Higher ash content in the T1 profiles indicates that transportation of mineral sediment from the upland occurred during the formation of peat. Surface layers characterized by ash content of greater than 10%, which are categorized as eutrophic peat (Driessen and Soepraptohardjo 1974), were more frequently found along the mineral upland (T1) than along the riverbank (T2). The lower ash levels along the riverbank indicate that upland had little influence on points farther from the mineral upland. Instead, mineral soil transportation along the riverbank (T2), represented by ash content in the lower layers near the mineral bed, probably occurred only during yearly floods of the Siak River in rainy season.

In the profiles running from the upland to the riverbank (T3), the presence of ash may again reflect the presence of mineral nutrients. The predominant total elements in the ash content along T3 were Ca, Al, and Fe. The high concentrations of total Al and Fe, which typically originate from mineral soil, were attributed to the influence of the mineral upland in the surface and underlying mineral layers. In 1C, for instance, higher ash contents in the 0–15 cm, 15–30 cm and 30–50 cm layers were coincident with high total Ca, Al, and Fe (Fig. 5-8). This trend was similar to that seen in the profiles of 2C and 3C, which became weaker in 4C. In contrast, no such trend appeared in 5C or 6C, which both had less than 10% ash content (Fig. 5-8), suggesting that the mineral upland has a lesser effect, if any, on the distribution of ash and total element content. These results indicate that the mineral upland has enriched the closer profile, as reflected in the higher pH in the same profiles and depths (Fig. 5-8). I suggest that the presence of a mineral upland, particularly in its topography and hydrology, is a key factor controlling pH and mineral nutrient distribution in tropical deep peat as well as, that is not limited to temperate peatlands such as previously reported by Paradis et al. (2015)

Considering that most tropical peats co-exist with mineral uplands in Indonesia, this implies that these peatlands will have received mineral nutrients supplied from the associated mineral uplands. For instance, Sumatra Island contains about 6.4 Mha of peatland (Ritung et al. 2011), which may receive nutrients from mineral uplands in the mountainous ridges at higher elevations. A similar process may also be present in peatlands in Kalimantan and Papua, where the peatlands are mostly located in the vast lowland plains leading downstream to the

coast. Although further evidence is needed in relation to the extent to which the uplands can affect the distribution of mineral nutrients in lowland peat, the findings provide insight into mineral nutrient distribution in tropical peatlands.

5.4.4 Conclusion

Exchangeable Ca^{2+} and Mg^{2+} levels tended to be high in surface peat and declined with depth; these cations were found close to the mineral upland. For exchangeable Ca^{2+} in particular, higher concentrations in surface peats were found more than 4 km from the mineral upland, implying that the mineral upland has enriched the study site. Exchangeable K^{+} and Na^{+} levels were less affected by this upland. Total Al and Fe levels were also high in the surface peat near the mineral upland; in comparison, they were low near the riverbank. Based on the observed distribution of ash content, exchangeable Ca^{2+} and Mg^{2+}, and total Ca, Mg, Al and Fe content, the present study suggests that the mineral upland influenced mineral nutrient distribution to the study site. The local landform should be considered when the nutritional status of tropical peatland is evaluated.

5.5 List of Tables and Figures

Table 5-1 General physical and chemical properties of surface peat. n = 32, except for bulk density (n = 18) and ash content (n = 31); †S: sapric peat; H: hemic peat; F: fibric peat; CC: charcoal; M: mineral soil; ‡ EC: electrical conductivity. S = Sapric peat; H = Hemic peat; F = Fibric peat; CC = Charcoal; M = Mineral soil; EC = Electrical conductivity; n = 32, except for bulk density (n = 18)

Layer (cm)	Peat material						Bulk density (g cm^{-3})	Ash content (%)	pH	EC ($\mu S\ cm^{-1}$)	Exchangeable cations ($cmol^{+}\ kg^{-1}$)			
	S	H	F	CC	M						Ca	Mg	K	Na
0–15	29	1	1	1	0	Average	0.26	9.0	3.7	185	8.29	2.73	0.65	0.13
						Standard deviation	0.04	6.4	0.3	57	5.08	1.10	0.34	0.07
15–30	23	7	1	1	0	Average	0.19	7.1	3.7	179	6.51	2.51	0.50	0.10
						Standard deviation	0.04	9.1	0.3	93	3.85	1.21	0.33	0.19
30–50	14	15	2	0	1	Average	0.16	4.8	3.7	184	3.71	2.12	0.42	0.10
						Standard deviation	0.02	11.9	0.2	90	2.20	0.85	0.37	0.12

Table 5-2 Correlations among measured values; n = 32 at each layer; except for ash content (n = 31); * significant at P <0.05; † peat thickness; ‡ EC: electrical conductivity; § distance from mineral terrain. n = 30 in each layer; *: significant at P value <0.05

		†Thickness	Ash content	pH	‡EC	Ca	Mg	K	Na
§Distance		0.52*	-0.25	-0.76*	0.44*	-0.55*	0.09	-0.20	0.17
†Thickness			0.02	0.40*	-0.28	0.36*	0.08	0.11	0.01
Ash content				0.10	0.22	0.49*	0.22	0.17	-0.12
pH					-0.62*	0.57*	0.25	0.18	-0.07
‡EC						-0.20	0.09	0.24	0.17
Exch. cations	Ca						0.40*	0.27	-0.18
	Mg							0.39*	-0.18
	K								-0.03

		†Thickness	Ash content	pH	‡EC	Ca	Mg	K	Na
15–30 cm									
§Distance		0.52*	-0.23	0.56	-0.50*	0.56*	-0.12	-0.22	-0.11
†Thickness			-0.13	0.25	-0.37*	0.26	0.14	0.23	0.16
Ash content				0.50*	-0.26	0.27	-0.06	0.06	0.25
pH					-0.79*	0.61*	0.21	0.09	-0.03
‡EC						-0.32	-0.11	0.01	0.09
Exch. cations	Ca						0.49*	0.22	0.05
	Mg							0.41*	-0.06
	K								-0.07
30–50 cm									
§Distance		0.52*	-0.13	-0.26	0.09*	-0.45*	0.29	-0.17	-0.40*
†Thickness			-0.24	-0.07	0.22	0.11	-0.23	0.08	0.16
Ash content				0.33	-0.25	0.43*	-0.08	-0.20	0.32
pH					-0.86*	0.26	0.04	-0.07	0.25
‡EC						0.06	0.01	0.24	-0.13
Exch. cations	Ca						0.20	0.16	0.51*
	Mg							0.44*	-0.01
	K								0.18

n = 30 in each layer; *: significant at *P* value <0.05.

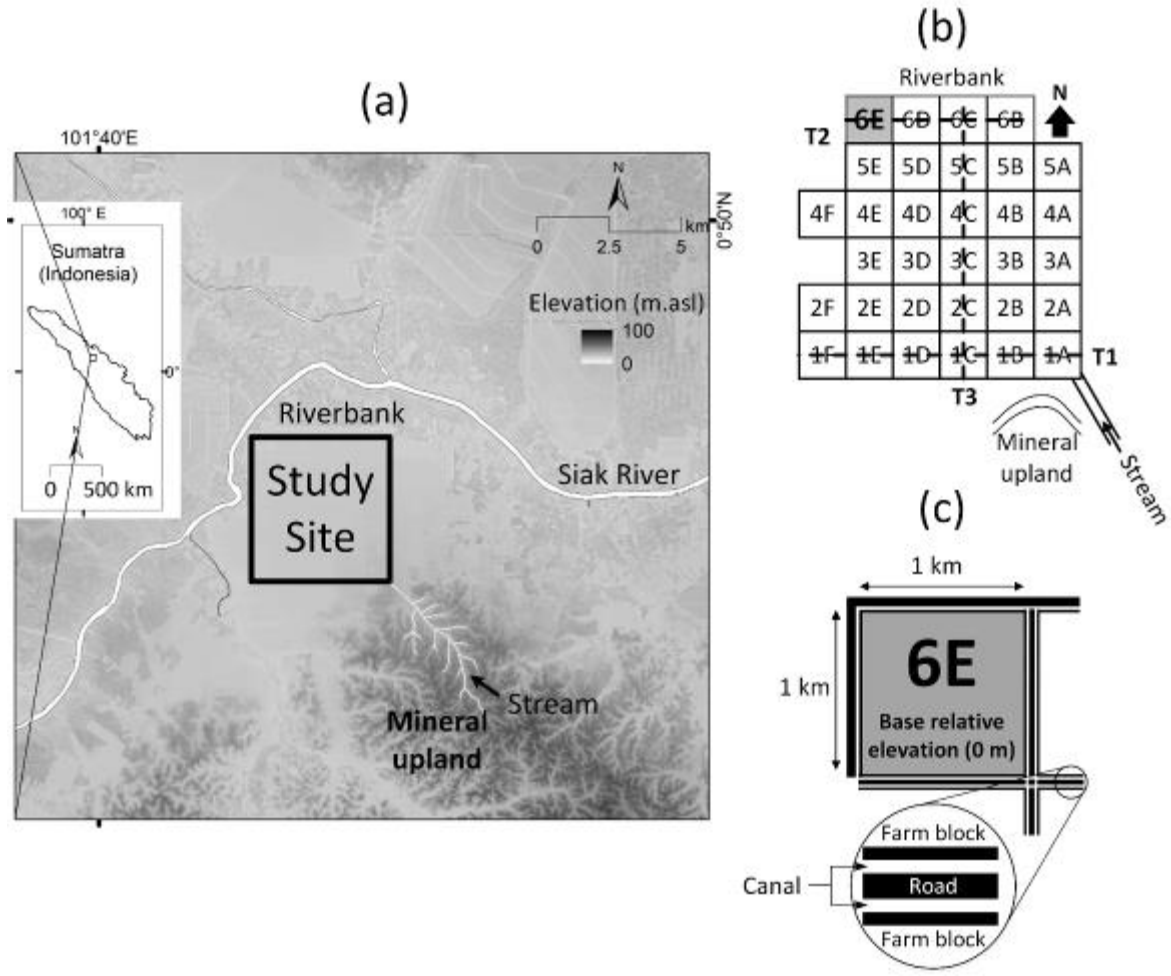

Fig. 5-1 (a) Study site location; (b) sampling design; (c) sketch of canal and farm road in the study site. The small stream (thin-white line) runs from mineral upland to the study site. The Siak River (thick-white line) flows from west to east. The dashed lines on the sampling design represent the three transect locations. The background map of the study location is derived from a digital elevation model (DEMNAS, http://tides.big.go.id/DEMNAS/), resolution 8.3 m × 8.3 m and vertical accuracy of 3.7 m.

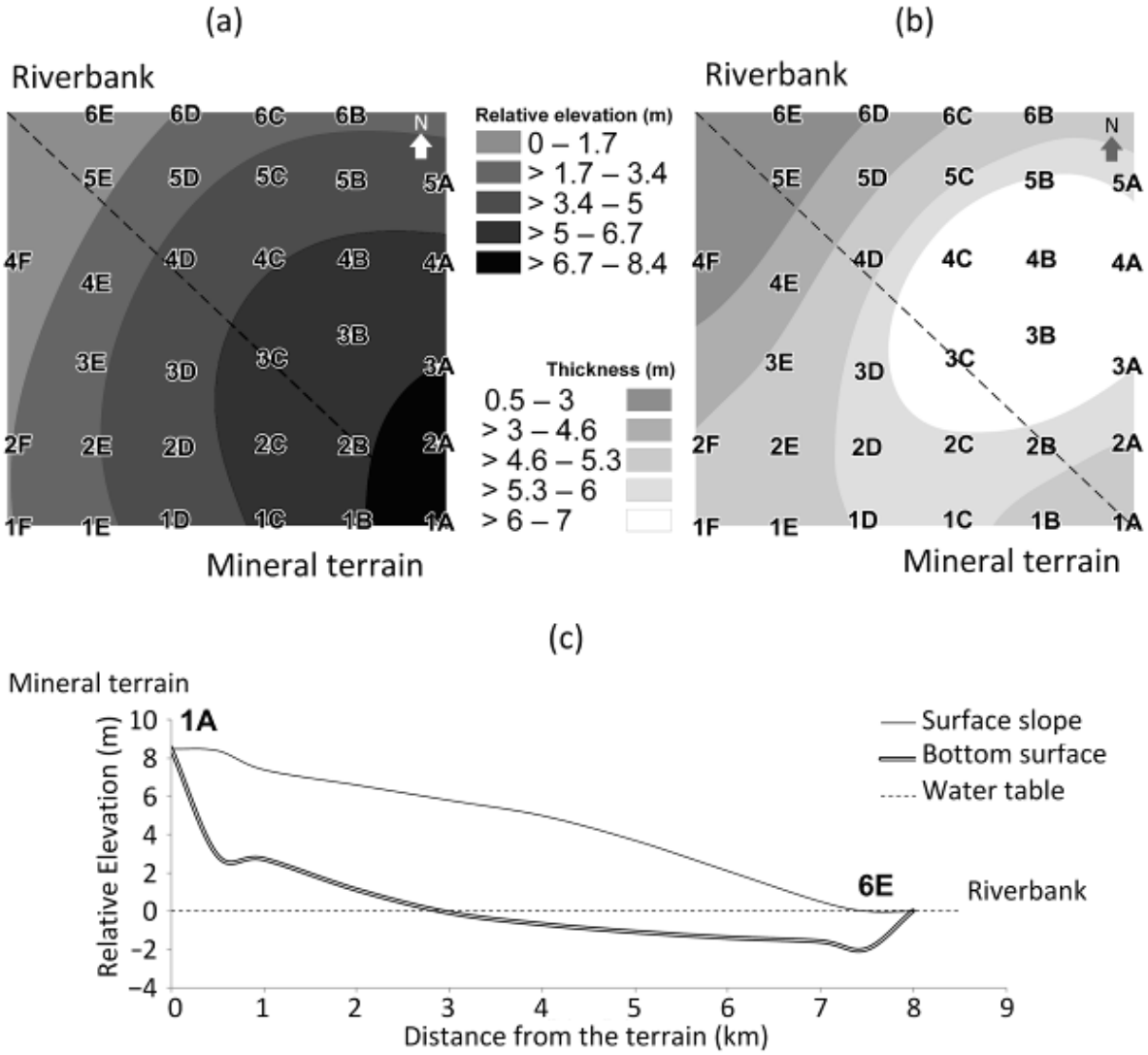

Fig. 5-2 Surface topography (a) and peat thickness (b) at the study site. The cross-section (c) represented by diagonal dashed line in (a) and (b) shows both surface topography and peat thickness from the upland to the riverbank; the Y-axis is exaggerated for clarity.

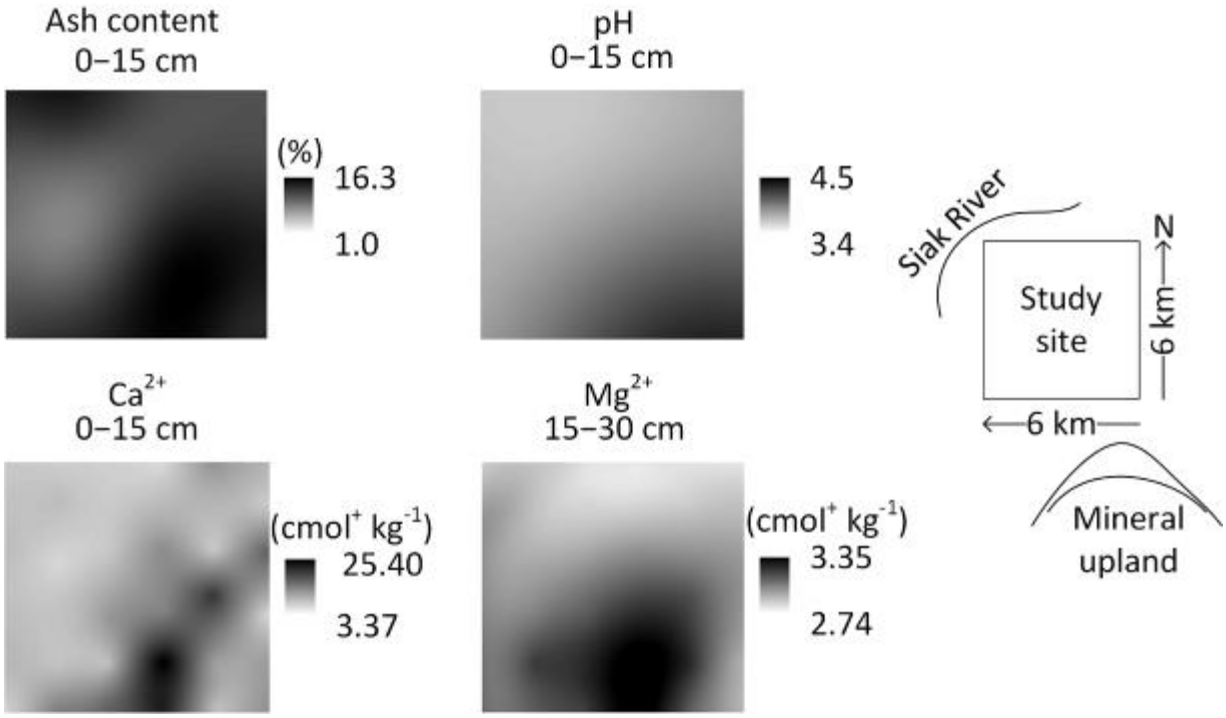

Fig. 5-3 The distributions of ash content, pH, exchangeable Ca^{2+}, and exchangeable Mg^{2+} at selected depths in the surface peat.

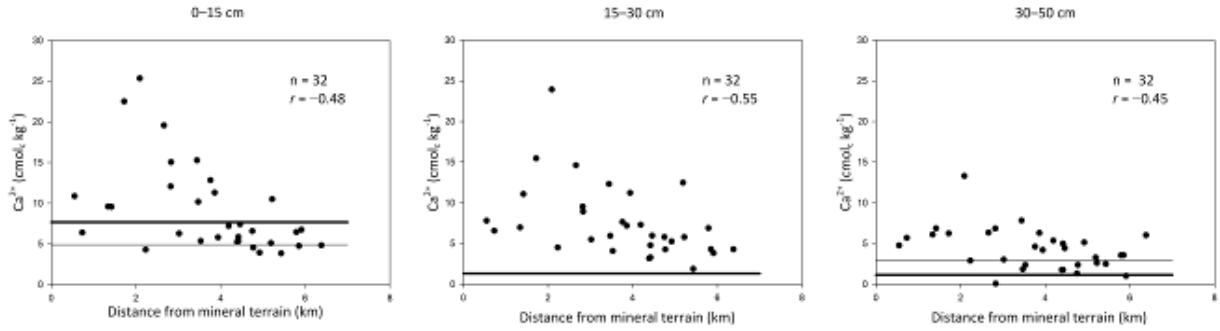

Fig. 5-4 Relationship between exchangeable Ca^{2+} and distance from the adjacent mineral upland; dots: results from the present study at the depths indicated above each plot; thick horizontal lines: mean values from Funakawa et al. (1996) at depths of 0−10 cm (above left), 10−20 cm (above middle), and 20−40 cm (above right); thin horizontal lines: mean values from Watanabe et al. (2013) at depths of 0−25 cm (above left) and 25−50 cm (above right).

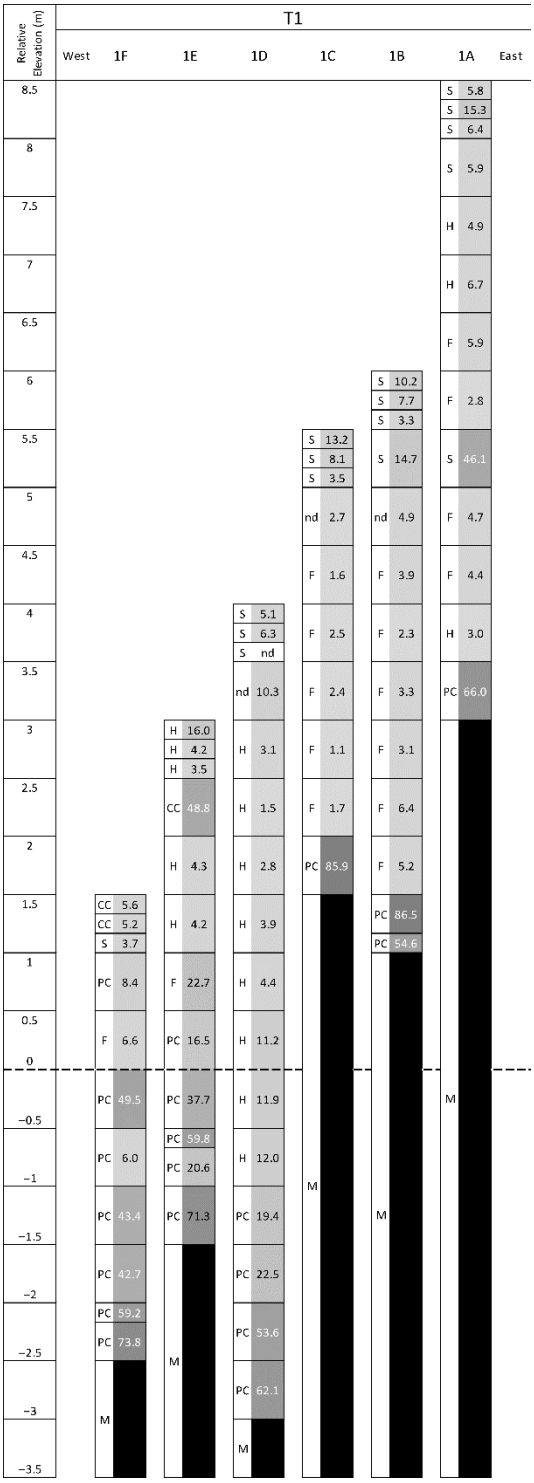

Fig. 5-5 The distribution of peat materials and ash content in the profiles of T1; shaded boxes represent ash content, with darker shading for higher values; ash content (%) shown within boxes; dashed line: median water table; Peat materials are S: sapric peat, H: hemic peat, F: fibric peat, CC: charcoal, PC: peaty clay; M: mineral bed; nd: not determined.

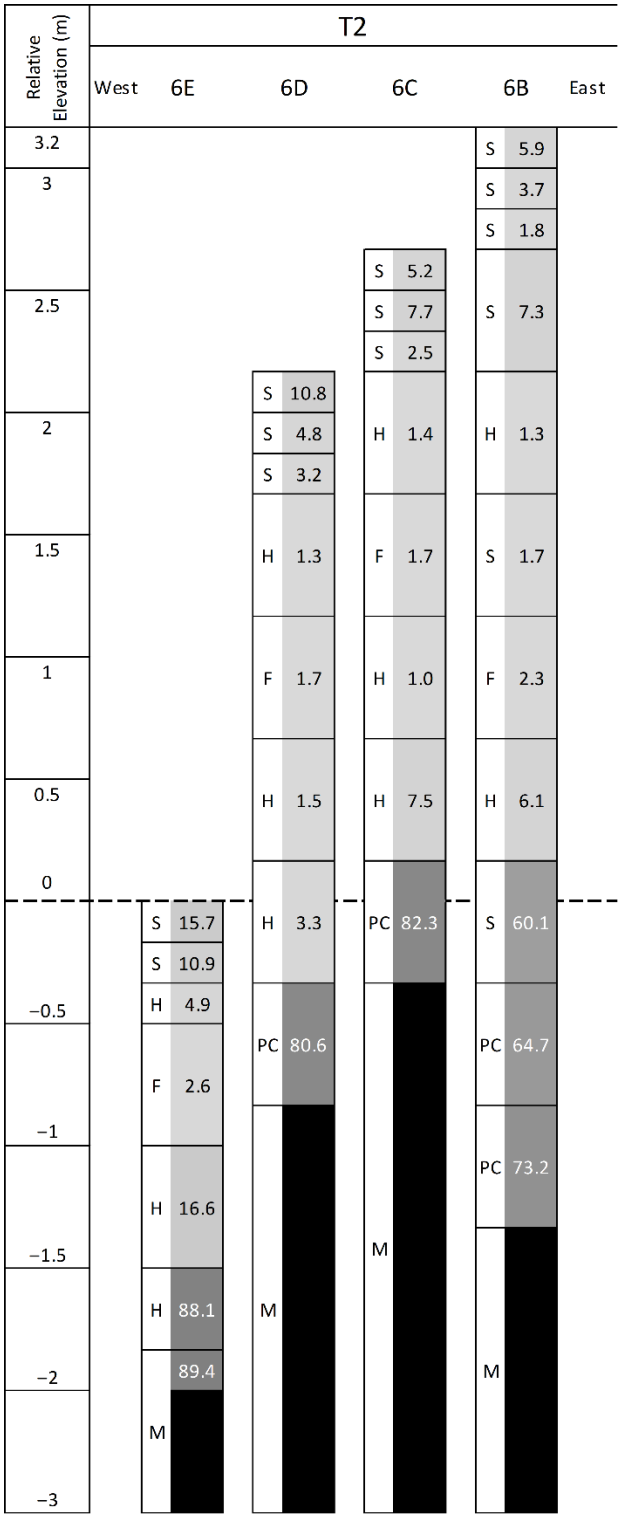

Fig. 5-6 The distribution of peat materials and ash content in the profiles of T2; shaded boxes represent ash content, with darker shading for higher values; ash content (%) shown within boxes; dashed line: median water table; Peat materials are S: sapric peat, H: hemic peat, F: fibric peat, CC: charcoal, PC: peaty clay; M: mineral bed; nd: not determined.

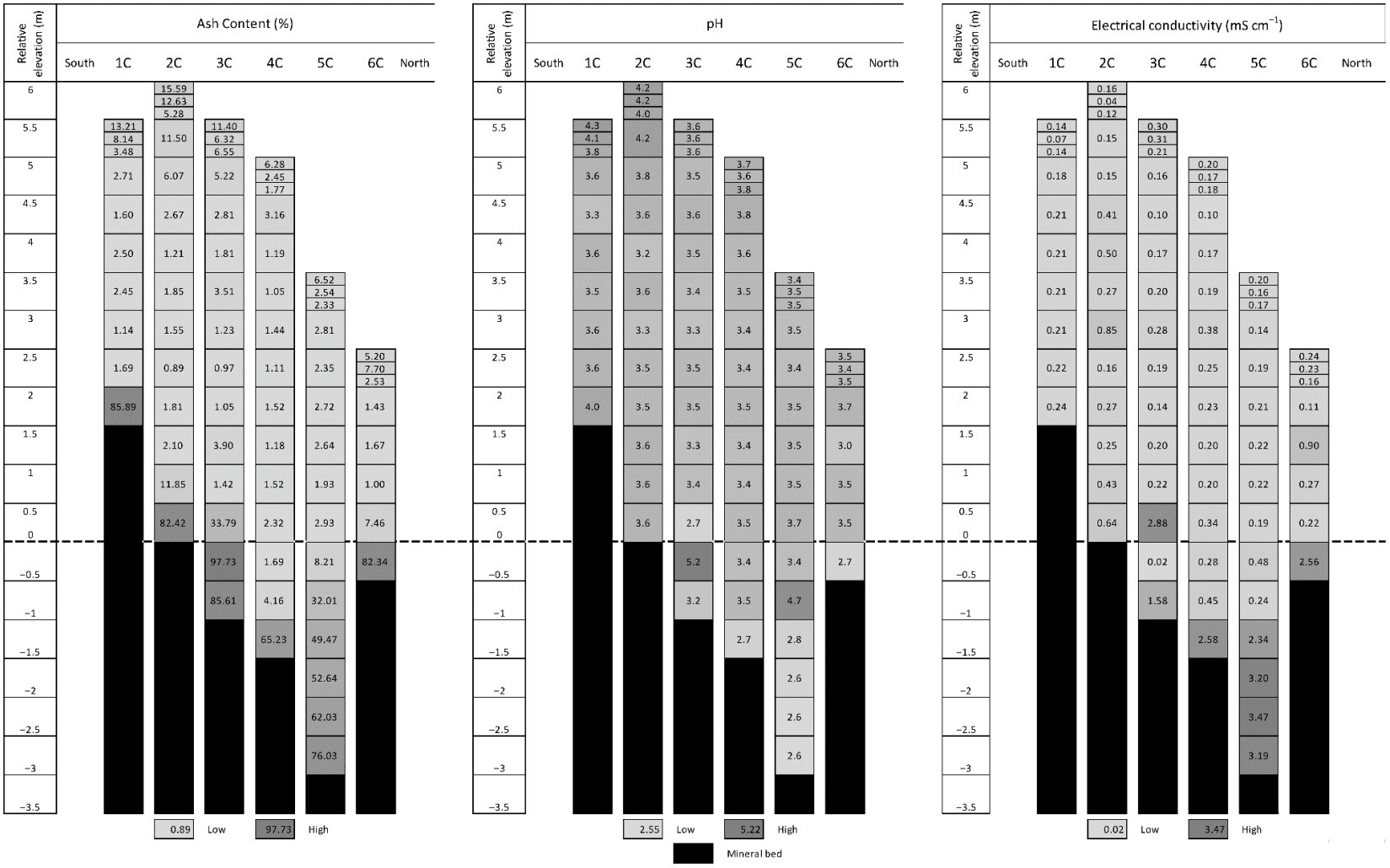

Fig. 5-7 Distribution of ash content (left), pH (middle) and electrical conductivity (right) in the profiles of T3; shaded boxes represent ash content (%), pH or EC (mS cm-1) as indicated, with darker shading for higher values; dashed line: median water table.

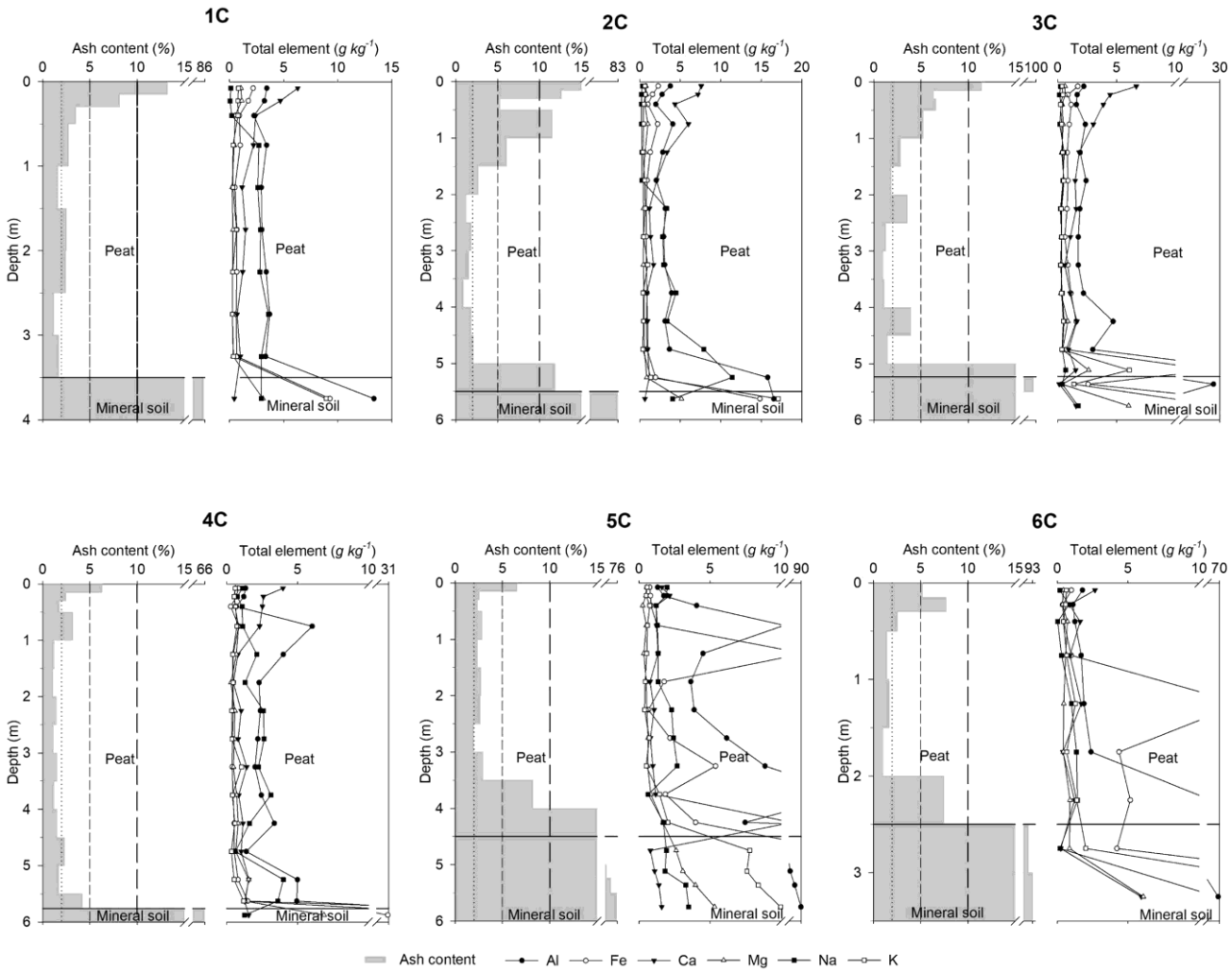

Fig. 5-8 The distribution of ash content and total elements in the profiles of T3 by grid square; peat and mineral soil layers are separated by thick horizontal lines, based on the criteria of Wüst and Bustin (2004); dotted line: oligotrophic peat; short-dashed line: mesotrophic peat; long-dashed line: eutrophic peat (based on Fleischer's criteria in Driessen and Soepraptohardjo [1974]). Note that axis break values differ between graphs.

CHAPTER 6
GENERAL DISCUSSION AND CONCLUSION

6.1 General discussion

To the best of my knowledge, no studies reported peat-mineral landform integration in a tropical mineral-peat landform regarding mineral element transportation. Understanding the integration of these two lands suggests that mineral nutrient loss from mineral land can compensate for mineral nutrients loss in peatland. We found that landform affected: 1) the erosion rate in the mineral land at catchment scale that is rarely studied so far in oil palm plantation; 2) mineral nutrient flow in the peatland; and 3) mineral nutrient distribution in peat soil. The general result of this integrated study is presented in Fig. 6-1.

The mineral element nutrient loss from the mineral land was studied to clarify its effect on the mineral element budget in the downstream peatland. The study consisted of two different peatlands (peatland-1, 3632 ha, while peatland-2 1478 ha) cultivated for oil palm, which receive streamflow from upland with similar characteristics. The mineral input could enhance chemical properties such as pH and mineral nutrients on peat water. Further investigation between peatland-1 and peatland-2 revealed that the effect of mineral element input on the seasonal change and total flow wasobvious catchment-1 than catchment-2. Catchment-1 had lower mineral element loss than catchment-2. Catchment-1 had also nearly balance seasonal budget between input and the loss. . With similar

Generally speaking, mineral input from upland enhanced the chemical properties of peat water in the canal. For instance, the averages pH at both outlets (3.86±0.24 and 3.76±0.34) were higher than that in a temperate bog (3.37±0.31) reported by Langlois et al. (2018). The mineral nutrient such as dissolved Ca in outlet-1 (1.88±1.01) and outlet-2 (1.06±0.48 mg L^{-1}) were also higher than that reported in tropical peat (1.49 mg L^{-1}) by Funakawa et al. (1996) and in temperate bog 1.80±0.30 by Langlois et al (2018). The higher Ca clarifies that continuous flow by topography (from upland) would be more critical than occasional input from the river or coast located at the lower elevation when considering mineral element input.

Peatland size would also be valuable when considering a seasonal change in mineral elements flow. For example, during high rainfall and water discharge, the loss of mineral elements from peatland-1 could be compensated by the high inflow from mineral land-1 (inlet-1), indicated by a positive net flow of Al, Fe, Ca, and K in suspended form (Fig. 3-7b, 3-7c, and 3-7d). Such compensation did not occur in peatland-2, indicated by the high loss of those

elements (Fig. 3-7b, 3-7c, and 3-7d). The high loss found in peatland-2 was caused by the higher water discharge and shorter responding time between inlet-2 and outlet-2, giving the minerals a lower chance to deposit.

The deposition of the mineral element could be by physical and chemical processes. Mineral elements in suspended forms would quickly deposit by gravitational force as water discharge got slower because of the gentle slope gradient and multiple water gates in the peatland. The nearly zero and stable net flow of Al, Fe, and Ca in dissolved forms (Fig. 3-6b and 3-6c) implies that their inflow from inlets could compensate for the loss particularly in peatland-1. Such elements in dissolved forms were distributed across the peatland via the canal network; thus, the high concentration of DOM could be the chelating agent that associates with minerals. The positive net flow of dissolved Al at peatland-1 was evident between March and November 2020 (Fig. 3-6b), which would come from the formation of Al–organic matters complexes as indicated by Funakawa et al. (1996). Association of DOM with dissolved mineral elements, such as divalent Ca and polyvalent Al, are more chemically active than monovalent cations (Owens et al. 2005), which may bind and flocculate (Römkens et al. 1996).

Landform affected erosion and water discharge distribution in the studied uplands with similar geology, soil, and climatic conditions, and land management characteristics. The fastest water discharge response to the rainfall events (Fig. 4-2) was evident upland-2c which was attributed to a steep, small and circular-shaped catchment. Also, because of the smaller size, such as upland-2c had a denser stream network (Table 4-3). Such faster discharge was less evident in upland-1 and upland-2b, probably owning to elongated shape (upland-2b) and gentle slope of upland-2a. The results reveal that slope, size, and circular shape contributed to faster water discharge by the short distance of stream across the upland to the corresponding outlet. Water discharge response is essential to identify possible sedimentation areas downward as sediment deposition occurs when the velocity is low (Lal 2001). This finding also confirms Musy (2001) that reported that circular catchment tends to have a faster water discharge response compared to the elongated catchment.

The rate and total water discharge regulated mineral element flow. During the same monitoring period in the uplands, mineral element concentration was low while the flow rate was high (Fig. 4-3, Fig. 4-4, Fig. 4-7, and Fig. 4-9). During intense rainfall and high water discharge, which might cause greater concentration, the concentration of mineral elements was actually lower than during less rainfall. The low concentration was attributed to the diluting

process owing to high water discharge. In contrast, the flow of mineral elements was regulated by water discharge regardless of the concentration of the elements. The high flow of mineral elements was evident during March and August 2020 even though their concentrations were relatively lower than those in September to November 2020.

This study verified that erosion still occurs under the late stage of oil palm plantation, and the comparison between estimated and measured amounts of erosion provides an evaluation of erosion in the tropics. Excluding upland 2b that had high mineral loss owing to excess water discharge, measured erosion (0.54–1.98 Mg ha^{-1} yr^{-1}) was lower than those estimated by RUSLE (2.33–5.04 Mg ha^{-1} yr^{-1}) (Table 4-3). The lower measured values imply that a portion of mineral elements deposited within the upland and did not reach the outlets from the upland. This difference confirms previous reports that the displacement of eroded particles might range greatly from a few millimeters to thousands of kilometers (Lal 2001; Foster 1982; Rose 1985)

The finding contributed to the reports on eroded materials at catchment scale that is absent in tropical oil palm plantations. The eroded materials ranged 0.54–4.91 Mg ha^{-1} yr^{-1} (on average of 2.3±1.8 Mg ha^{-1} yr^{-1}) (Table 4-3), lower than general erosion in tropics (29.1±51.3; $\tilde{x}$ =11.2 Mg ha^{-1} yr^{-1}) by Borrelli et al. (2021), general erosion in Indonesia (35–220 Mg ha^{-1} yr^{-1}) by Sumiahadi and Acar (2019) but still higher than cropland covered by grass vegetation (0.7±1.6 Mg ha^{-1} yr^{-1}) reported by Labrière et al. (2015).

Considering that oil palm plantation covers a vast area of 14 million ha in Indonesia (BPS 2019), the result verified the importance of mineral loss under the late stage of oil palm plantation that might have implication to the downstream ecosystem. Of the total eroded materials (2.3±1.8 Mg ha^{-1} yr^{-1}) (Table 4-3), the average loss of K and Mg in upland-2c were 20.9±20.6 and 2.7±2.6 kg ha^{-1} yr^{-1}. The loss in the current study area was slightly lower compared to the loss of K (38.6 kg ha^{-1} yr^{-1}) and Mg (3.1 kg ha^{-1} yr^{-1}) reported by Vijiandran et al. (2017) using an erosion plot with mature oil palms.

The clear evidence of mineral inputs was the enrichment of mineral elements in the peatland. The peat from the surface and profile transect was systematically collected to investigate the spatial distribution of mineral nutrients. The result compared the mineral nutrient level between surface soil layers and between the edge of the peatland (riverbank and mineral land).

The landform setting of the study site has contributed to the formation of narrow-deep peat. The peatland had deep peat within a short distance from the riverbank, which fits the category of basin or valley peatland (Page et al. 2006). In addition to that, the shape of the peatland in the study site also differs from the common lenticular form in tropical peatlands. The results suggest that the shape of the dome was absent or unclear in the study site due to interaction with the surrounding landforms. A tropical peatland generally has the thickest peat and highest elevation at the center, known as a peat dome (Anderson 1983; Andriesse 1988; Cameron et al. 1989). In contrast, within the present study site, the highest elevation (1A) was not at the location of the thickest peat (4B).

The higher mineral nutrient tended to be distributed in the surface layers. In addition to the high decomposition rate in the surface, the results suggested mineral soil supply from the mineral upland. The mineral upland affected the peat's chemical properties via mineral soil transportation. The topography of the complex landform is likely to generate mineral-enriched stream water and surface runoff, both of which drive suspended particles formed during mineral upland erosion. Eroded mineral soil, then, would associate with peat around the mineral upland, resulting in higher ash content, pH, exchangeable Ca^{2+} and Mg^{2+} (Table 5-1 and Fig. 5-3), total Ca, total Fe, and total Al at the surface layers (Fig. 5-8). At the same time, K and Na showed no clear pattern and no relationship with distance from the mineral upland owing to their lower bonding strength to organic matter. The higher ash content in some points near the upland represents mineral soil deposition, in which base cations (Fig. 5-3 and Table 5-1) and total elements (Ca, Mg, Fe, and Al) (Fig. 5-8) were also high.

The results of the profile transect indicated that the mineral upland had enriched at the closer profiles, as reflected in the higher pH in the same profiles and depths (Fig. 5-8). The total predominant elements in the ash content along T3 were Ca, Al, and Fe. The high concentrations of total Al and Fe, which typically originate from mineral soil, were attributed to the influence of the mineral upland in the surface and underlying mineral layers. In 1C, for instance, higher ash contents in the 0–15 cm, 15–30 cm, and 30–50 cm layers coincided with high total Ca, Al, and Fe (Fig. 5-8). In contrast, no such trend appeared in 5C or 6C, which both had less than 10% ash content (Fig. 5-8), suggesting that the mineral upland has a lesser effect, if any, on the distribution of ash and total element content in the farther distance. I suggest that the presence of a mineral upland, particularly its topography and hydrology, is a crucial factor controlling pH and mineral nutrient distribution in deep tropical peat. It is not limited to temperate peatlands, such as previously reported by Paradis et al. (2015).

6.2 Concluding remarks

6.2.1 General conclusion

Landform affects the mineral loss, budget, and distribution in a complex peat-mineral land under tropical oil palm plantation. The-nearly zero and stable net flow of mineral elements in suspended and dissolved forms in catchment-1 implies that the inflow of those elements from inlets could prevent further loss due to intensive rainfall. The retention of the mineral element is indicated by positive net flow such as Si, Al, Fe, and Ca from September to November 2020. On the contrary, peatland-2 showed the loss indicated by negative net flow, particularly from March and August 2020. Therefore, the total flow of elements in catchment-1 (outlet-1) was significantly lower than in catchment-2 (outlet-2). The size of peatland-1 in catchment-1, which is ca. two times bigger than peatland-2 (catchment-2) and has a longer canal, would result in lower mineral elements (Al, Fe, Si, Ca, K and Mg) flow. Also, a comparison with previous studies without mineral upland association suggests that the study sites had higher mineral elements and lower DOC. This study suggests that transfer of mineral elements across integrated peat−mineral catchment is beneficial for compensating mineral elements into nutrient-poor peatland and preventing potential DOC release downstream.

Our result also verified the erosion at the catchment scale that is absent under oil palm plantations in Indonesia, which might have implications for the downstream ecosystem. Under the late stage of oil palm, the mineral upland with similar geology, climate, and soil type still experienced erosion though it was lower than that in tropics and Indonesia estimated by models (Labrière et al. 2015). The loss of mineral elements such as K and Mg was also lower compared to that measured at plot scale under oil palm. The amount of measured erosion based on eroded materials reaching outlets was lower compared to that estimated by the RUSLE model, indicating sediment deposition might occur within the uplands. The results suggest that actually measured erosion is substantial when considering mineral loss at the catchment scale, having the implication to the downstream ecosystem.

In the soil of the peatland-1, exchangeable Ca^{2+} and Mg^{2+} levels tended to be high in surface peat and declined with depth; higher contents of these cations were found in area close to the mineral upland. For exchangeable Ca^{2+} in particular, higher concentrations in surface peats were found more than 4 km from the mineral upland, implying that the mineral upland has enriched the study site. Exchangeable K^{+} and Na^{+} levels were less affected by this upland, probably because of their lower affinity to organic matter. Total Al and Fe levels were also

high in the surface peat near the mineral upland; in comparison, they were low near the riverbank. Based on the observed distribution of ash content, exchangeable Ca^{2+} and Mg^{2+}, and total Ca, Mg, Al, and Fe contents, the present study suggests that the mineral upland influenced mineral nutrient distribution to the study site. The local landform should be considered when the nutritional status of tropical peatland is evaluated.

6.2.2 Unanswered questions, recommendations, and future research direction

Although the current study has employed two different peatland sizes (3000 ha and 1400 ha), peatland temporarily drained the mineral elements, particularly smaller peatland-2 significantly released mineral elements to the river, especially during the rainy season with intense rainfall. Given the idea that most peatlands in Indonesia lay at lower elevations, peat-mineral landform as an integral ecosystem must be distributed across the region. Peatland's threshold size, which can effectively retain mineral elements from associated mineral land without flushing out the elements like in peatland-2, remains an open question. More studies are needed, especially for more extensive landforms and different land use, to develop the conceptual framework of peat-mineral landform integration in terms of various sizes and landform characteristics.

Considering peatland-1 (catchment-1) and peatland-2 (catchment-2) still temporarily drained mineral elements, I recommend that making a longer watercourse would optimize sediment deposition and nutrient retention during the rainy season. Equipped by multiple water gates at every intersection, the watercourse could be distributed across the peatland; hence mineral nutrients in water would intrude into farm block via smaller canal and be retained. Mineral elements enrichment can enhance peat soil's fertility (Wang et al. 2016), thus potentially support crop productivity. Additionally, association of mineral elements with DOC might reduce organic carbon flow to under stream, preventing potential anoxia in the Siak River (Rixen et al. 2008).

Also, in the peat soil, considering that most tropical peats co-exist with mineral uplands in Indonesia, most peatlands will have received mineral nutrients supplied from the associated mineral uplands. Our findings provide insight into mineral nutrient distribution in tropical peatlands. However, further evidence is needed in relation to the extent to which the uplands can affect the distribution of mineral nutrients in lowland peat. For instance, Sumatra Island contains about 6.4 Mha of peatland (Ritung et al. 2011), which may receive nutrients from mineral uplands in the mountainous ridges at higher elevations. A similar process may also be

present in peatlands in Kalimantan and Papua, where the peatlands are mostly located in the vast lowland plains leading downstream to the coast.

6.3 List of Figure (s)

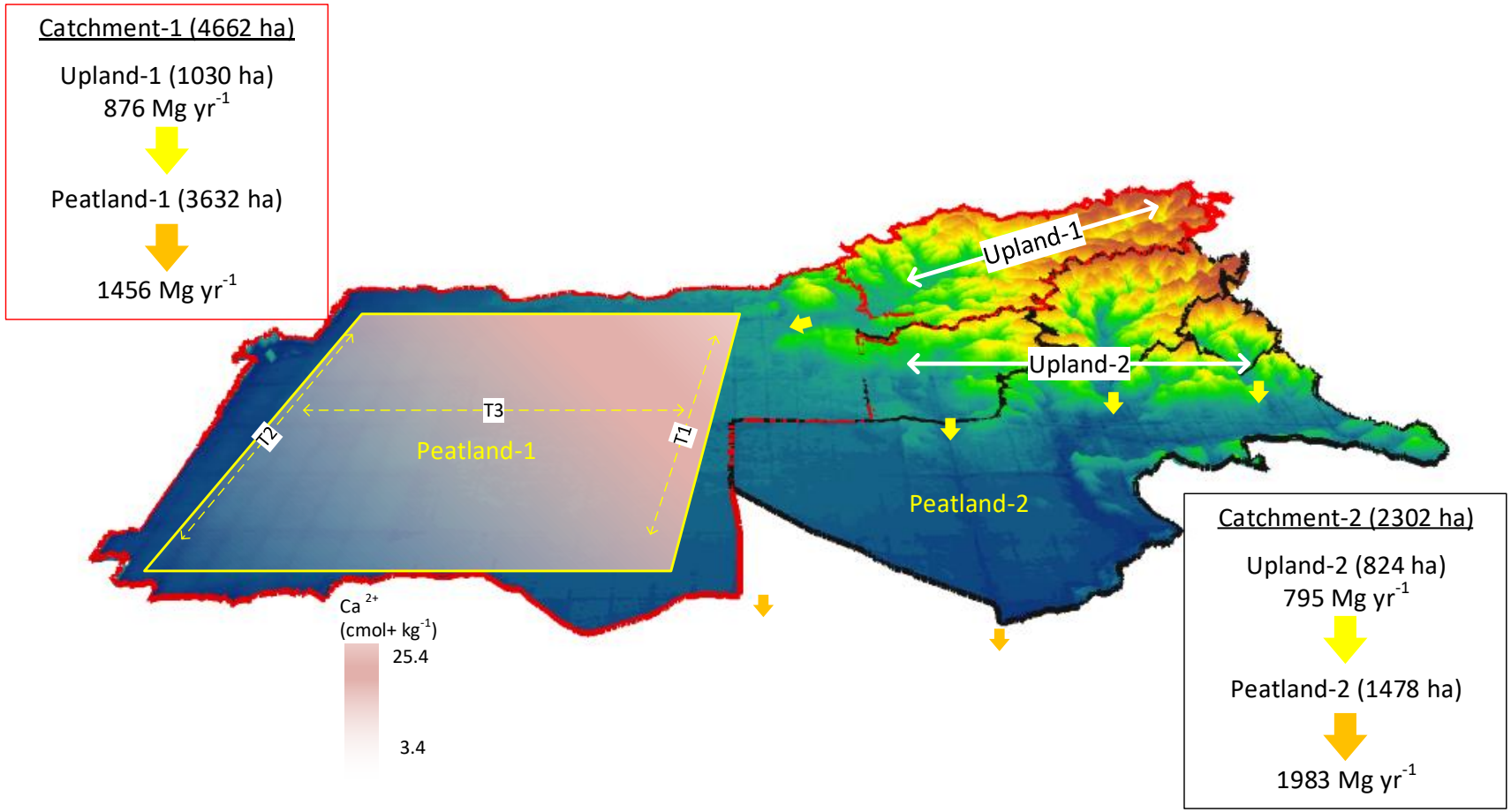

Fig. 6-1 Schematic diagram of integrated mineral element transport across mineral–peat landform under oil palm plantation in Riau-Indonesia

References

Abrams, Jesse F., Sönke Hohn, Tim Rixen, Antje Baum, and Agostino Merico. 2016. "The Impact of Indonesian Peatland Degradation on Downstream Marine Ecosystems and the Global Carbon Cycle." *Global Change Biology* 22 (1): 325–37. https://doi.org/10.1111/gcb.13108.

Agus, F., and I.G. Made Subiksa. 2008. *Lahan Gambut : Potensi Untuk Pertanian Dan Aspek Lingkungan*. *Balai Penelitian Tanah Dan World Agroforestry Centre (ICRAF)*. https://doi.org/10.1016/j.foreco.2014.08.031.

Andriesse J. P. 1988. *Nature and Management of Tropical Peat Soils*. *FAO Soils Bulletin*. Vol. 59. Rome: FAO.

Arsyad S 2010 Konservasi Tanah dan Air (Bogor: IPB Press)

Ballinger, Andrea, and P. S. Lake. 2006. "Energy and Nutrient Fluxes from Rivers and Streams into Terrestrial Food Webs." *Marine and Freshwater Research* 57 (1): 15–28. https://doi.org/10.1071/MF05154.

Belayneh, Mengie, Teshome Yirgu, and Dereje Tsegaye. 2019. "Potential Soil Erosion Estimation and Area Prioritization for Better Conservation Planning in Gumara Watershed Using RUSLE and GIS Techniques'." *Environmental Systems Research* 8 (1). https://doi.org/10.1186/s40068-019-0149-x.

Bols, P. L. (1978). The iso-erodent map of Java and Madura. Belgian Technical Assistance Project ATA 105, Soil Research Institute, Bogor.

Borrelli, Pasquale, Christine Alewell, Pablo Alvarez, Jamil Alexandre Ayach Anache, Jantiene Baartman, Cristiano Ballabio, Nejc Bezak, et al. 2021. "Soil Erosion Modelling: A Global Review and Statistical Analysis." *Science of the Total Environment* 780. https://doi.org/10.1016/j.scitotenv.2021.146494.

Cameron, Cornelia C., Joan S. Esterle, and Curtis A. Palmer. 1989. "The Geology, Botany and Chemistry of Selected Peat-Forming Environments from Temperate and Tropical Latitudes." *International Journal of Coal Geology* 12 (1–4): 105–56. https://doi.org/10.1016/0166-5162(89)90049-9.

Chawchai, S., A. Chabangborn, M. Kylander, L. Löwemark, C. M. Mörth, M. Blaauw, W. Klubseang, P. J. Reimer, S. C. Fritz, and B. Wohlfarth. 2013. "Lake Kumphawapi - an Archive of Holocene Palaeoenvirontal and Palaeoclimatic Changes in Northeast Thailand." *Quaternary Science Reviews* 68: 59–75. https://doi.org/10.1016/j.quascirev.2013.01.030.

Chew P.S., K.K. Kee and K.J. Goh.1999. Cultural practices and their impacts. In: Oil Palm and the Environment – A Malaysian Perspective, ed. G.Singh, C.K. Huan, T.Leng and D.L. Kow. Malaysian Oil Palm Growers' Council, Kuala Lumpur

Clarke, M. A., and R. P.D. Walsh. 2006. "Long-Term Erosion and Surface Roughness Change of Rain-Forest Terrain Following Selective Logging, Danum Valley, Sabah, Malaysia." *Catena* 68 (2–3): 109–23. https://doi.org/10.1016/j.catena.2006.04.002.

Colchester, Marcus, Norman Jiwan, Martua Sirait, Asep Yunan Firdaus, A Surambo, and Herbert Pane. 2006. *Promised Land : Palm Oil and Land Acquisition in Indonesia - Implications for Local Communities and Indigenous Peoples HuMA and the World Agroforestry Centre . Promised Land : Palm Oil and Land Acquisition in Indonesia - Implications for Local Communities*.

Cook, S., Whelan, M. J., Evans, C. D., Gauci, V., Peacock, M., Garnett, M. H., … Page, S. E. (2018). Fluvial organic carbon fluxes from oil palm plantations on tropical peatland. *Biogeosciences Discussions*, 1–33. https://doi.org/10.5194/bg-2018-417

Cusell, Casper, Ivan S. Mettrop, E. Emiel Van Loon, Leon P.M. Lamers, Michel Vorenhout, and Annemieke M. Kooijman. 2015. “Impacts of Short-Term Droughts and Inundations in Species-Rich Fens during Summer and Winter: Large-Scale Field Manipulation Experiments.” *Ecological Engineering* 77: 127–38. https://doi.org/10.1016/j.ecoleng.2015.01.025.

Davies, Patrick. 1995. “Greasy Palms.” *Nursing Standard* 9 (17): 56–56. https://doi.org/10.7748/ns.9.17.56.s67.

Driessen, P. M. 2001. “Lecture Notes on the Major Soils of the World”. Cleveland Clinic Journal of Medicine. Vol. 54. doi:10.3949/ccjm.54.4.354.

Driessen, P. M. 1978. Peat soils. In IRRI Ed., “Soils and Rice”, pp. 763-769. IRRI, Los Baños, Philippines.

Driessen, P. M, and M Soepraptohardjo. 1974. “Soils for Agricultural Expansion in Indonesia. ” Soil Research Institute. Bogor, Indonesia.Fujii, Kazumichi, Mari Uemura, Chie Hayakawa, Shinya Funakawa, Sukartiningsih, Takashi Kosaki, and Seiichi Ohta. 2009. “Fluxes of Dissolved Organic Carbon in Two Tropical Forest Ecosystems of East Kalimantan, Indonesia.” *Geoderma* 152 (1–2): 127–36. https://doi.org/10.1016/j.geoderma.2009.05.028.

Funakawa, Shinya, Koyo Yonebayashi, Foh Shoon Jong, and Chai Oi Khun Ernest. 1996. “Nutritional Environment of Tropical Peat Soils in Sarawak, Malaysia Based on Soil Solution Composition.” *Soil Science and Plant Nutrition* 42 (4): 833–43. https://doi.org/10.1080/00380768.1996.10416630.

Gibbs, Holly K., Matt Johnston, Jonathan A. Foley, Tracey Holloway, Chad Monfreda, Navin Ramankutty, and David Zaks. 2008. “Carbon Payback Times for Crop-Based Biofuel Expansion in the Tropics: The Effects of Changing Yield and Technology.” *Environmental Research Letters* 3 (3). https://doi.org/10.1088/1748-9326/3/3/034001.

Haraguchi, Akira, Sawahiko Shimada, and Hideki Takahashi. 2000. “Distribution of Peat and Its Chemical Properties around Lahei in the Catchment of the Mangkutup River, Central Kalimantan.” *Tropics* 10 (2): 265–72. https://doi.org/10.3759/tropics.10.265.

Harding, Sandra, Rodney McComiskie, Mark Wolff, Dennis Trewin, and Stephanie Hunter. 2015. “State of The Tropics 2014 Report.” *James Cook University* 43 (1): 146–49. https://doi.org/10.1177/0011000014564251.

Horton, B Y Robert E. 1945. “EROSIONAL DEVELOPMENT OF STREAMS AND THEIR DRAINAGE BASINS; HYDROPHYSICAL APPROACH TO QUANTITATIVE MORPHOLOGY” 56 (March): 275–370.

Hossner, L. R. 1996. Dissolution for total elemental analysis. In D. L. Sparks Ed., “Methods of Soil Analysis. Part 3. Chemical Methods”, pp. 49-64. SSSA, Madison, WI

Howie, S. A., P. H. Whitfield, R. J. Hebda, T. G. Munson, R. A. Dakin, and J. K. Jeglum. 2009. “Water Table and Vegetation Response to Ditch Blocking: Restoration of a Raised Bog in Southwestern British Columbia.” *Canadian Water Resources Journal* 34 (4): 381–92. https://doi.org/10.4296/cwrj3404381.

Iskandar, Wahyu, Tetsuhiro Watanabe, Setiari Marwanto, Supiandi Sabiham, and Shinya Funakawa. 2020. “Landform Affects the Distribution of Mineral Nutrients in the Tropical Peats: A Case Study in a Peatland of Siak, Indonesia.” *Soil Science and Plant Nutrition* 00 (00): 1–13. https://doi.org/10.1080/00380768.2020.1783965.

Koh, Lian Pin, and David S. Wilcove. 2008. “Is Oil Palm Agriculture Really Destroying Tropical Biodiversity?” *Conservation Letters* 1 (2): 60–64. https://doi.org/10.1111/j.1755-263x.2008.00011.x.

Krachler, Regina, Rudolf F. Krachler, Gabriele Wallner, Stephan Hann, Monika Laux, Maria F.

Cervantes Recalde, Franz Jirsa, et al. 2015. “River-Derived Humic Substances as Iron Chelators in Seawater.” *Marine Chemistry* 174: 85–93. https://doi.org/10.1016/j.marchem.2015.05.009.

Kreitler, Charles W. 1989. “Hydrogeology of Sedimentary Basins.” *Journal of Hydrology* 106 (1–2): 29–53. https://doi.org/10.1016/0022-1694(89)90165-0.

Labrière, Nicolas, Bruno Locatelli, Yves Laumonier, Vincent Freycon, and Martial Bernoux. 2015. “Soil Erosion in the Humid Tropics: A Systematic Quantitative Review.” *Agriculture, Ecosystems and Environment* 203: 127–39. https://doi.org/10.1016/j.agee.2015.01.027.

Lal, R. 2001. “Soil Degradation by Erosion.” *Land Degradation and Development* 12 (6): 519–39. https://doi.org/10.1002/ldr.472.

Lal, Rattan. 1995. “Erosion-Crop Productivity Relationships for Soils of Africa.” *Soil Science Society of America Journal* 59 (3): 661–67. https://doi.org/10.2136/sssaj1995.03615995005900030004x.

Lampela, Maija, Jyrki Jauhiainen, and Harri Vasander. 2014. “Surface Peat Structure and Chemistry in a Tropical Peat Swamp Forest.” *Plant and Soil* 382 (1–2): 329–47. https://doi.org/10.1007/s11104-014-2187-5.

Langlois, Mélanie N, Jonathan S Price, and Line Rochefort. 2015. “Science of the Total Environment Landscape Analysis of Nutrient-Enriched Margins (Lagg) in Ombrotrophic Peatlands.” *Science of the Total Environment* 505: 573–86. https://doi.org/10.1016/j.scitotenv.2014.10.007.

Liu, Yan, Thorsten Wagener, Hylke E. Beck, and Andreas Hartmann. 2020. “What Is the Hydrologically Effective Area of a Catchment?” *Environmental Research Letters* 15 (10). https://doi.org/10.1088/1748-9326/aba7e5.

Manoli, Gabriele, Ana Meijide, Neil Huth, Alexander Knohl, Yoshiko Kosugi, Paolo Burlando, Jaboury Ghazoul, and Simone Fatichi. 2018. “Ecohydrological Changes after Tropical Forest Conversion to Oil Palm.” *Environmental Research Letters* 13 (6). https://doi.org/10.1088/1748-9326/aac54e.

Mohamad, N. A., A. Nainar, K. V. Annammala, D. Sugumaran, M. H. Jamal, and Z. Yusop. 2020. “Soil Erosion in Disturbed Forests and Agricultural Plantations in Tropical Undulating Terrain: In Situ Measurement Using a Laser Erosion Bridge Method.” *Journal of Water and Climate Change* 11 (4): 1032–41. https://doi.org/10.2166/wcc.2019.063.

Moore, Sam, Chris D. Evans, Susan E. Page, Mark H. Garnett, Tim G. Jones, Chris Freeman, Aljosja Hooijer, Andrew J. Wiltshire, Suwido H. Limin, and Vincent Gauci. 2013. “Deep Instability of Deforested Tropical Peatlands Revealed by Fluvial Organic Carbon Fluxes.” *Nature* 493 (7434): 660–63. https://doi.org/10.1038/nature11818.

Moore, T.R. (1989) Dynamics of dissolved organic carbon in forested and disturbed catchments, Westland, New Zealand.b1. Maimai. WaterResources Research, 25(6), 1321–1330. Moore, T.R. (2003) Dissolved organic carbon in a Northern Boreal landscape. Global Biogeochemical Cycles, 17(4), 20-1–20-8.

Moore, S., Gauci, V., Evans, C.D. & Page, S.E. (2011) Fluvial organic carbon losses from a Bornean blackwater river. Biogeosciences, 8, 901–909.

Moore, T.R. & Jackson, R.J. (1989) Dynamics of dissolved organic carbon in forested and disturbed catchments, Westland, New Zealand. 2. Larry River. Water Resources Research, 25(6), 1331–1339.

Murtilaksono, K., M. Ariyanti, Y. Asbur, H. H. Siregar, E. S. Sutarta, S. Yahya, S. Sudrajat, S. Suwarto, S. Suroso, and M. A. Yusuf. 2018. “Surface Runoff and Soil Erosion in Oil Palm Plantation of Management Unit of Rejosari, PT Perkebunan Nusantara VII, Lampung.” *IOP Conference Series: Earth and Environmental Science* 196 (1): 1–6. https://doi.org/10.1088/1755-1315/196/1/012002.

Musy, A. 2001. e-drologie. Ecole Polytechnique Fédérale, Lausanne, Suisse

Nainar, A., N. Tanaka, K. Bidin, K. V. Annammala, R. M. Ewers, G. Reynolds, and R. P.D. Walsh. 2018. "Hydrological Dynamics of Tropical Streams on a Gradient of Land-Use Disturbance and Recovery: A Multi-Catchment Experiment." *Journal of Hydrology* 566 (April): 581–94. https://doi.org/10.1016/j.jhydrol.2018.09.022.

Owens, Philip N., R. J. Batalla, A. J. Collins, B. Gomez, D. M. Hicks, A. J. Horowitz, G. M. Kondolf, et al. 2005. "Fine-Grained Sediment in River Systems: Environmental Significance and Management Issues." *River Research and Applications* 21 (7): 693–717. https://doi.org/10.1002/rra.878.

Page, S. E., J. O. Rieley, and R. Wüst. 2006. "Chapter 7 Lowland Tropical Peatlands of Southeast Asia." In *Developments in Earth Surface Processes*, 9:145–72. https://doi.org/10.1016/S0928-2025(06)09007-9.

Page, S E, J O Rieley, W Shotyk, and D Weiss. 1999. "Interdependence of Peat and Vegetation in a Tropical Peat Swamp Forest." *Philosophical Transactions of the Royal Society of London. Series B, Biological Sciences* 354 (1391): 1885–97. https://doi.org/10.1098/rstb.1999.0529.

Panagos, Panos, Pasquale Borrelli, Katrin Meusburger, Bofu Yu, Andreas Klik, Kyoung Jae Lim, Jae E. Yang, et al. 2017. "Global Rainfall Erosivity Assessment Based on High-Temporal Resolution Rainfall Records." *Scientific Reports* 7 (1): 1–12. https://doi.org/10.1038/s41598-017-04282-8.

Paradis, Étienne, Line Rochefort, and Mélanie Langlois. 2015. "The Lagg Ecotone: An Integrative Part of Bog Ecosystems in North America." *Plant Ecology* 216 (7): 999–1018. https://doi.org/10.1007/s11258-015-0485-5.

Polis, Gary A., Wendy B. Anderson, and Robert D. Holt. 1997. "Toward an Integration of Landscape and Food Web Ecology: The Dynamics of Spatially Subsidized Food Webs." *Annual Review of Ecology and Systematics* 28: 289–316. https://doi.org/10.1146/annurev.ecolsys.28.1.289.

Pott, David B., James J. Alberts, and Alan W. Elzerman. 1985. "The Influence of PH on the Binding Capacity and Conditional Stability Constants of Aluminum and Naturally-Occurring Organic Matter." *Chemical Geology* 48 (1–4): 293–304. https://doi.org/10.1016/0009-2541(85)90054-3.

Renard et al., 1997. 1997. "Predicting Soil Erosion by Water: A Guide to Conservation Planning With the Revised Universal Soil Loss Equation (RUSLE)."

Ritson, Jonathan P., Richard E. Brazier, Nigel J.D. Graham, Chris Freeman, Michael R. Templeton, and Joanna M. Clark. 2017. "The Effect of Drought on Dissolved Organic Carbon (DOC) Release from Peatland Soil and Vegetation Sources." *Biogeosciences* 14 (11): 2891–2902. https://doi.org/10.5194/bg-14-2891-2017.

Ritung, Sofyan, Wahyunto, Kusumo Nugroho, Sukarman, Hikmatullah, Suparto, and Chendy Tafakresnanto. 2011. "Peta Lahan Gambut Indonesia Skala 1:250.000." December 2. Bogor: BBLSDP-Balitbang Kementerian Pertanian.

Römkens, Paul F., J. Brill, and Will. Salomons. 1996. "Interaction between Calcium and Dissolved Organic Carbon: Implications for Metal Mobilization." *Applied Geochemistry* 11.

Saka, S., M. V. Munusamy, M. Shibata, Y. Tono, and H. Miyafuji. 2008. "Chemical Constituents of Different Part of Oil Palm.Pdf."

Sassolas-Serrayet, Timothée, Rodolphe Cattin, and Matthieu Ferry. 2018. "The Shape of Watersheds." *Nature Communications* 9 (1): 1–8. https://doi.org/10.1038/s41467-018-06210-4.

Shibata, Makoto, Soh Sugihara, Antoine David Mvondo-Ze, Shigeru Araki, and Shinya Funakawa. 2017. "Nitrogen Flux Patterns through Oxisols and Ultisols in Tropical Forests of Cameroon,

Central Africa." *Soil Science and Plant Nutrition* 63 (3): 306–17. https://doi.org/10.1080/00380768.2017.1341285.

Singh, Vijay P. 2018. "Hydrologic Modeling: Progress and Future Directions." *Geoscience Letters* 5 (1). https://doi.org/10.1186/s40562-018-0113-z.

Soil Survey Staff. 1996. "Soil survey laboratory methods manual", USDA-NRCS, Washington, DC

Solihuddin, Tubagus. 2014. "A Drowning Sunda Shelf Model during Last Glacial Maximum (LGM) and Holocene: A Review." *Indonesian Journal on Geoscience* 1 (2): 99–107. https://doi.org/10.17014/ijog.v1i2.182.

Sumiahadi, Ade, and Ramazan Acar. 2019. "Soil Erosion in Indonesia and Its Control." *Proceedings of International Symposium for Environmental Science and Engineering Research (ISESER2019)*, no. November: 545–54.

Susanti, Yuari, S. Syafrudin, and Muhammad Helmi. 2019. "Soil Erosion Modelling at Watershed Level in Indonesia: A Review." *E3S Web of Conferences* 125 (201 9). https://doi.org/10.1051/e3sconf/201912501008.

Tarigan, Suria, Kerstin Wiegand, Sunarti, and Bejo Slamet. 2018. "Minimum Forest Cover Required for Sustainable Water Flow Regulation of a Watershed: A Case Study in Jambi Province, Indonesia." *Hydrology and Earth System Sciences* 22 (1): 581–94. https://doi.org/10.5194/hess-22-581-2018.

Tarmizi, a.M., and Mohd Tayeb. 2006. "Nutrient Demands of Tenera Oil Palm Planted on Inland Soils of Malaysia." *Journal of Oil Palm Research* 18 (June): 204–9.

Ulanowski, T. A., and B. A. Branfireun. 2013. "Small-Scale Variability in Peatland Pore-Water Biogeochemistry, Hudson Bay Lowland, Canada." *Science of the Total Environment* 454–455: 211–18. https://doi.org/10.1016/j.scitotenv.2013.02.087.

Vija P. Singh. 1994. "Elementary Hydrology Vp Singh.Pdf."

Vijiandran, J. R., M. H.A. Husni, C. B.S. Teh, A. R. Zaharah, and A. Xaviar. 2017a. "Nutrient Losses through Runoff from Several Types of Fertilisers under Mature Oil Palm." *Malaysian Journal of Soil Science* 21 (December): 113–21.

———. 2017b. "Nutrient Losses through Runoff from Several Types of Fertilisers under Mature Oil Palm." *Malaysian Journal of Soil Science* 21: 113–21.

Watanabe, Tetsuhiro, Yosuke Hasenaka, Suwondo, Supiandi Sabiham, and Shinya Funakawa. 2013. "Mineral Nutrient Distributions in Tropical Peat Soil of Riau Indonesia with Special Reference to Peat Thickness." *ﾍﾟﾄﾞｼﾞｽﾞﾄﾞ - Japanese Society of Pedology* 57 (2): 64–71.

Whitfield, Paul H., André St-Hilaire, and Garth Van Der Kamp. 2009. "Improving Hydrological Predictions in Peatlands." *Canadian Water Resources Journal* 34 (4): 467–78. https://doi.org/10.4296/cwrj3404467.

Wicke, Birka, Veronika Dornburg, Martin Junginger, and André Faaij. 2008. "Different Palm Oil Production Systems for Energy Purposes and Their Greenhouse Gas Implications." *Biomass and Bioenergy* 32 (12): 1322–37. https://doi.org/10.1016/j.biombioe.2008.04.001.

Wicke, Birka, Richard Sikkema, Veronika Dornburg, and André Faaij. 2011. "Exploring Land Use Changes and the Role of Palm Oil Production in Indonesia and Malaysia." *Land Use Policy* 28 (1): 193–206. https://doi.org/10.1016/j.landusepol.2010.06.001.

Wikantika, Ketut. 2018. "Remote Sensing Analysis In RUSLE Erosion Estimation" 4 (1): 34–45. https://doi.org/10.31227/osf.io/8q3dr.

Wischmeier, W., & Smith, D. (1965). Rainfall-erosion losses from cropland east of the Rocky Mountains, guide for selection of practices for soil and water conservation. Agriculture

Wüst, Raphael A.J., and R. Marc Bustin. 2004. "Late Pleistocene and Holocene Development of the Interior Peat-Accumulating Basin of Tropical Tasek Bera, Peninsular Malaysia." *Palaeogeography, Palaeoclimatology, Palaeoecology* 211 (3–4): 241–70. https://doi.org/10.1016/j.palaeo.2004.05.009.

Yang, Rujun, Han Su, Shenglu Qu, and Xuchen Wang. 2017. "Capacity of Humic Substances to Complex with Iron at Different Salinities in the Yangtze River Estuary and East China Sea." *Scientific Reports*, no. October 2016: 1–9. https://doi.org/10.1038/s41598-017-01533-6.

Yupi, H M, T Inoue, J Bathgate, and R Putra. 2016. "Concentrations , Loads and Yields of Organic Carbon from Two Tropical Peat Swamp Forest Streams in Riau Province , Sumatra , Indonesia." *Mires and Peat* 18 (August): 1–15. https://doi.org/10.19189/MaP.2015.OMB.181.

WAHYU ISKANDAR

Born in 1989
Department of Soil Science and Land Resource
Faculty of Agriculture-IPB University, Bogor Indonesia
wahyuiskandar@apps,ipb.ac.id; whyiskandar@gmail.com

EDUCATION

Ph.D. program (expected in 2021) in Agriculture

Kyoto University: Laboratory of Soil Science Division of Environmental Science and Technology, Faculty of Agriculture

Proposed thesis: Mineral elements transport across mineral–peat landforms under oil palm plantation in Indonesia

Master program (Degree obtained in 2017)

Kyoto University: Laboratory of Soil Science Division of Environmental Science and Technology, Faculty of Agriculture

Thesis: Mineral Nutrient Distributions in Tropical Peat of Riau, Indonesia

Bachelor Program (Degree obtained in 2015)

IPB University: Laboratory of Forest Hydrology and Watershed Management, Department of Forest Management, Faculty of Forestry

Thesis: Erosion Hazard Vulnerability and Soil Fertility Status in Forest Plantation Concession Area of IUPHHK HT-PT Korintiga Hutani, Central Kalimantan

EMPLOYMENT

University staff 2020–now

At Department of Soil Science and Land Resource Faculty of Agriculture-IPB University, Bogor Indonesia

Field Coordinator 2017–2018

JICA Partnership Program (JPP) Kyoto University and Riau University, Universitas Riau, Badan Restorasi Gambut (BRG), and Government of Bengkalis, Riau (November 2017 to September 2018) “Restoration of Peatland Ecology and Livelihood Improvement through Rewetting and Revegetation toward the Prevention of Peat Fire”

Field surveyor 2013–2014

Sub-consultant at PT. ERM Indonesia: The Mega Geothermal Project at Sarula Operation Limited (SOL) in Sarula, Tarutung, North Sumatra

PUBLICATIONS

Iskandar W, Watanabe T, Anwar S, Sabiham S, Funakawa S. (In preparation). Erosion rate and mineral elements loss in mineral upland under oil palm plantation.

Iskandar W, Watanabe T, Anwar S, Sabiham S, Funakawa S. (In preparation). Mineral element flow in an integrated peat-mineral land ecosystem in Riau-Indonesia.

Iskandar W, Watanabe T, Marwanto S, Sabiham S, Funakawa S. (2020). Landform affects the distribution of mineral nutrients in the tropical peats: a case study in a peatland of Siak, Indonesia. Soil Science and Plant Nutrition - Taylor and Francis

DOI: 10.1080/00380768.2020.1783965

Marwanto S, Watanabe T, **Iskandar W**, Sabiham S, Funakawa S. (2018). Effects of seasonal rainfall and water table movement on the soil solution composition of tropical peatland. Soil Science and Plant Nutrition - Taylor and Francis

DOI: 10.1080/00380768.2018.1436940

SCHOLARSHIPS

MEXT SCHOLARSHIP (Ph.D. program at Kyoto University)	2018– 2021
LPDP SCHOLARSHIP (Master program at Kyoto University)	2015–2020
PPA and Pemda Jabar (Bachelor Program at IPB University)	2009–2012